Russian Original Vol. 33, No. 1, July, 1972

January, 1973

SATEAZ 33(1) 631-714 (1972)

SOVIET ATOMIC ENERGY

АТОМНАЯ ЭНЕРГИЯ
(ATOMNAYA ÉNERGIYA)

TRANSLATED FROM RUSSIAN

CONSULTANTS BUREAU, NEW YORK

SOVIET ATOMIC ENERGY

Soviet Atomic Energy is a cover-to-cover translation of *Atomnaya Énergiya*, a publication of the Academy of Sciences of the USSR.

An arrangement with Mezhdunarodnaya Kniga, the Soviet book export agency, makes available both advance copies of the Russian journal and original glossy photographs and artwork. This serves to decrease the necessary time lag between publication of the original and publication of the translation and helps to improve the quality of the latter. The translation began with the first issue of the Russian journal.

Consultants Bureau journals appear about six months after the publication of the original Russian issue. For bibliographic accuracy, the English issue published by Consultants Bureau carries the same number and date as the original Russian from which it was translated. For example, a Russian issue published in December will appear in a Consultants Bureau English translation about the following June, but the translation issue will carry the December date. When ordering any volume or particular issue of a Consultants Bureau journal, please specify the date and, where applicable, the volume and issue numbers of the original Russian. The material you will receive will be a translation of that Russian volume or issue.

Subscription
$75.00 per volume (6 issues)
2 volumes per year
(Add $5 for orders outside the United States and Canada.)

Single Issue: $30
Single Article: $15

CONSULTANTS BUREAU, NEW YORK AND LONDON

c/b
227 West 17th Street
New York, New York 10011

Davis House
8 Scrubs Lane
Harlesden, NW10 6SE
England

Published monthly. Second-class postage paid at Jamaica, New York 11431.

SOVIET ATOMIC ENERGY

A translation of *Atomnaya Énergiya*

January, 1973

Volume 33, Number 1 July, 1972

CONTENTS

CONTENTS

(continued)

The Russian press date (podpisano k pechati) of this issue was 6/27/1972. Publication therefore did not occur prior to this date, but must be assumed to have taken place reasonably soon thereafter.

NEUTRON MATTER*

N. A. Vlasov

UDC 539.125.5

Chadwick [1] discovered the neutron thirteen years after the first artificial splitting of a nucleus, by Rutherford. Thereafter events moved at a quickened pace in nuclear physics. Chadwick's paper in 1932 was the culmination of a series of investigations: in 1930 Bothe and Becker [2] discovered a mysterious beryllium radiation; a year later Joliot and Curie [3] observed recoil atoms of unexpectedly high energy; and then Chadwick's measurements of the recoil atoms showed that the radiation consisted of neutral particles with a mass near the proton's – the neutron had been discovered. The name had actually been coined 10 years earlier by Rutherford and collaborators for a conjectured combination of a proton and an electron. In 1934 Joliot and Curie [4] discovered artifical radioactivity.

These two extremely important discoveries placed new and fruitful methods of investigation in the hands of atomic physicists. As early as 1934, Fermi [5] observed the first effects of uranium fission by neutrons, although four years and a multitude of experiments in different laboratories intervened before the realization dawned that this was fission and not ordinary, simpler reactions.

At once thoughts and searches in nuclear laboratories were directed toward the realization of chain reactions and technological exploitation of atomic energy. Three years after the discovery of fission, Fermi and American scientists constructed the first atomic reactor. In 1946, a year after the war, Kurchatov and his collaborators started up a reactor in the USSR. The initial fundamental experiments led on to the construction of industrial reactors; first for the production of explosive materials, later for peaceful technological purposes. And today, 40 years after the discovery of the neutron, nuclear energy is on a par with other forms of energy. The total power of atomic power stations in 1971 exceeded 20 GW – 300 times more than the power of the V. I. Lenin Dnepr Hydroelectric Power Plant – and it is increasing faster than the power of other power stations. It is estimated [6] that atomic power stations in the capitalist countries will provide 96 GW in 1975, 277 GW in 1980, and 570 GW in 1985.

Many physical laboratories and technical undertakings are equipped with experimental reactors and other neutron-producing plant. A great variety of scientific and technical problems are solved by the method of neutron physics and spectrometry. One of the most important directions of neutron investigations [7, 8] is concerned with a fundamental problem of nuclear energy – the breeding of nuclear fuel in fast reactors. Sukhoruchkin [9] has only recently completed a series of investigations and a thorough review aimed at improving the fission and radiative capture cross sections of active materials [9] in the range of energies characteristic of fast reactors.

But the most interesting problems of modern neutron physics are to be found where this subject merges with the physics of elementary particles and astrophysics – in the problem of the structure of the neutron itself and of neutron matter, the material of which neutron stars are composed. It is to these problems that we turn our attention in the present paper.

Structure of the Neutron

Even before the discovery of the neutron, in 1930, it was conjectured that the partner of the proton in the deuteron must have a magnetic moment, the difference between the proton's magnetic moment and the deuteron's being about two nuclear magnetons. In 1940, Alvarez and Bloch [10] measured the neutron's magnetic moment and the conjecture was confirmed: $\mu_n = -1.935$ nm. Now it follows from the laws of

*To mark the 40th anniversary of the discovery of the neutron.

Translated from Atomnaya Energiya, Vol. 33, No. 1, pp. 539-546, July, 1972. Original article submitted April 14, 1972.

electrodynamics that a magnetic moment is produced by electric currents; accordingly, the neutron must have some internal electromagnetic structure. Extensive series of experiments on scattering of fast electrons by protons and deuterons have been undertaken to lay bare this structure. Even at a low electron energy, 0.2-0.3 GeV, Hofstadter [11] found that when the momentum transfer q is large, an electron is scattered from a proton more weakly than from a point charge and from a neutron more weakly than from a point magnetic moment; the proton and the neutron have finite extensions. The proton charge and the neutron magnetic moment are distributed over a volume of radius $\sim 0.8 \times 10^{-13}$ cm. Searches for this distribution led Hofstadter to construct a model – inspired by theoretical notions – of alluring simplicity: the proton and the neutron each have a positive central charge; the proton's peripheral charge is positive, the neutron's negative; thus, the proton's total charge is positive, the neutron's vanishes. The picture is that of a pion or heavier meson – positive in a proton, negative in a neutron – revolving about a center in the nucleon.

Subsequent experiments did not confirm the model; reality is more complicated. Wilson et al.'s elastic scattering experiments [12] with electrons of energies up to 7 GeV showed that the proton charge distribution, e_p, the proton magnetic moment, μ_p, and the neutron magnetic moment, μ_n, can be represented by the same form factor:

$$1/(1+q^2/0.72^2),$$

where q, the momentum transferred to the scattered electron, is expressed in reciprocal fermis; all three must be distributed almost uniformly over a volume with radius 0.8×10^{-13} cm. The charge, e_n, of the neutron was found to vanish everywhere; at a scale $\sim 10^{-14}$ cm no spatial separation of positive and negative charges was found; the neutron is uniformly neutral over its whole volume.

These experiments gave rise to a new conception: the neutron is an almost uniformly magnetized cloud; the proton, an almost uniformly charged and magnetized cloud. This marks a return in some respects to the pre-Rutherford atom with its cloud-like distribution of the charge over a large volume. But this notion too is shown to be inadequate by the Stanford linear accelerator experiments [13] on the scattering of electrons with energies up to 20 GeV.

The cross section for the elastic scattering of electrons at these high energies does not decrease in the manner one would expect for a uniform distribution of the charge and the magnetic moment over a volume ($\sim q^{-2}$) but continues to decrease smoothly and rather fast ($\sim q^{-4}$) with increasing momentum transfer. The most striking feature of the inelastic scattering is discrete energy losses in the form of resonant lines in the scattered electron spectrum (Fig. 1). The lines can be ascribed to the excitation of the nucleon to the levels known from many experiments as baryon resonances. The cross sections for scattering accompanied by the formation of an excited nucleon decrease with increasing q in the same way as the elastic cross section – the nucleon structure is essentially the same in the excited states and in the ground state.

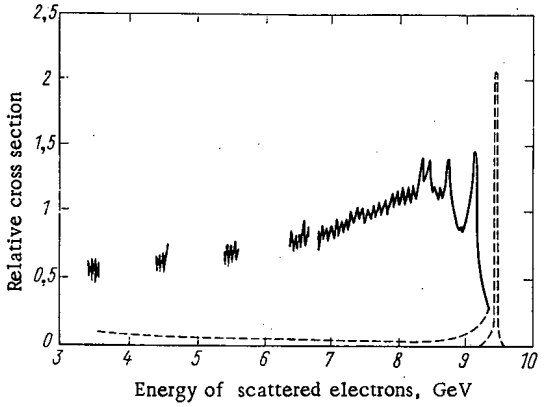

Fig. 1. Spectrum of electrons scattered by protons through 6°. The initial energy is 10 GeV. The dashed peak is the elastic scattering (reduced tenfold); the dashed tail, the correction for the effect of bremsstrahlung.

Surprisingly, the inelastic scattering cross section behaves quite differently. Figure 2 shows the cross sections for elastic and inelastic scattering as functions of q^2. The ratio of the observed cross sections to the cross section for scattering by a single point charge is plotted along the ordinate. The cross section for elastic scattering at $q^2 = 3$ (GeV/c)^2 is 1000 times smaller than for a point charge; the cross section for the inelastic scattering in which products with total rest energy W = 3.5 GeV are formed is almost independent of q^2, the behavior of the cross sections being similar at other large values of W.

A weak dependence (almost independence) of the cross section on q^2 in the scattering is characteristic of a point charge. Inelastic scattering is obviously more complicated than elastic scattering, but there is no question but that a very strong electromagnetic interaction of a point electron with another charge or magnetic moment is possible only over a very short distance and if

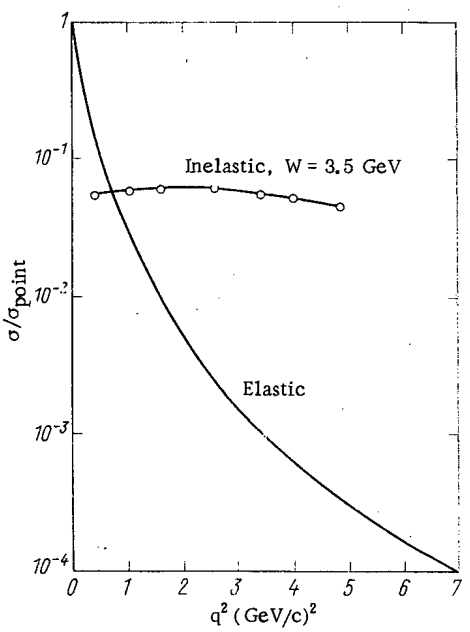

Fig. 2. Cross sections for elastic and inelastic scattering of electrons by protons as a function of q^2. The inelastic scattering corresponds to the formation of a particle (or complex) with rest energy W = 3.5 GeV.

the target is concentrated in a region of comparable dimensions.

All the experiments on the scattering of fast electrons by nucleons show that the nucleon diameter is about 0.8×10^{-13} cm but that within such a region there are structural elements with charge and magnetic moment concentrated in an extremely small volume with radius $<10^{-14}$ cm; the theoreticians call them partons – parts of a nucleon [14].

The parton model has been widely discussed [15], it being universally assumed that there are several partons – not less than three or four – in a nucleon and that they are small. The most varied assumptions are made about the mass and number of partons and their binding energy in the nucleon; they may be the quarks predicted by the classification of strongly interacting particles.

When the exciting problem of the structure of the neutron has been solved, our understanding of the laws of nature will have been raised to a higher plane.

Fast-electron experiments have penetrated "into the depths of space," to distances 10^{-15} cm. On this scale nucleons are almost uniformly charged and magnetized, and partons are almost point-like. However, the neutron as a whole could have a much more differentiated distribution of charges; it could exhibit an electric dipole moment $e\delta$ (e the elementary charge, and δ the distance between the centers of the positive and the negative charge). As long as time reversal was unquestioned, it could be assumed that $\delta = 0$. Time inversion reverses an axial vector but does not affect a polar vector; the neutron undoubtedly has a spin (axial vector), so that the existence of a nonvanishing electric dipole moment, $\delta \neq 0$ (polar vector), would make it into a time-irreversible particle. The discovery of CP noninvariance in K^0-meson decays undermined confidence in T invariance, and a nonvanishing electric dipole moment of the neutron came to be taken seriously. Interesting experiments with slow neutrons showed that $\delta < 10^{-22}$ cm [16]. Essentially, the experiments attempted to reveal a shift of the neutron magnetic resonance in parallel H and E fields when the latter, a strong electric field, is reversed. The neutron energy should change by $2Ee\delta$, but no shift was detected [17].

It must be borne in mind that the electric field interacts not only with a static dipole but also with the induced electric dipole of the neutron, the strength of which depends on the strength of the coupling of the carriers of opposite electric charge in the neutron. An increase in the accuracy of the measurement of the electric dipole moment remains desirable and new experiments are still being devised. One possibility is to observe ultracold neutrons [17], which can be kept and observed for a long time in the measuring instrument.

Methods for producing and keeping ultracold neutrons have been put forward by Zel'dovich [18] and Vladimirskii [19]; a start on implementing these ideas has been made at Dubna [20]; the continuation of these experiments is described in [21].

Neutrons in a Gravitational Field

Eötvös [22] and Dicke's [23] experiments – they showed that inertial and gravitational mass are equivalent to within 10^{-11} for elements with a different number of protons and neutrons in their nuclei (and Braginskii and Panov [23] have recently improved Dicke's result by an order of magnitude) – removed any doubt whether neutrons behaved differently in a gravitational field from other material particles in nature. This led Vladimirskii [19] to foresee the interesting possibility that ultracold neutrons "poured into an open vessel" would be retained in it by the force of gravity.

Direct measurements of the falling of neutrons in a gravitational field [24] have confirmed the assumed universal value of the acceleration of a neutron, albeit with poor accuracy ($\sim 10^{-3}$).

The effect of a gravitational field on neutrons has been exploited in an interesting manner. In 1962, Meier-Leibnitz [25] proposed a gravitational refractometer for measuring the scattering lengths of slow neutrons. Such a device was subsequently constructed in Munich; it measures the limiting angle of total reflection of neutrons from a horizontal plane, the angle of incidence on the mirror being varied by the earth's gravity field. Over the 100-meter path from the source to the mirror the neutron falls further in the gravity field, the smaller is its horizontal velocity; the gravitational field is an active element of the refractometer.

The device is not only an entirely original idea; it is very accurate. It has been used to obtain some results with record precision. These include the constants of the np and the nd interaction, which are important in nuclear physics. Recent measurements [26] for the np scattering lengths give $a_{np}^{s} = -23.719 \pm 0.013$ F for the singlet and $a_{np}^{t} = 5.414 \pm 0.005$ F for the triplet length; for the nd scattering lengths, $a_{nd}^{d} = 0.65 \pm 0.04$ F for the doublet and $a_{nd}^{q} = 6.35 \pm 0.02$ F for the quartet scattering lengths [27].

The strong gravitational fields in stars strongly affect the state of the matter in the stars and, in particular, the relative role of neutrons. During their evolution, the majority of stars pass through neutronization of their matter, when the protons are transformed into neutrons. The thermonuclear burning of hydrogen to helium and the subsequent burning of this helium to carbon and other elements are the first stages of neutronization. The gravitational contraction of a star condenses its matter; the limiting Fermi energy of a degenerate electron gas is raised and β^- decay accompanied by the formation of low-energy electrons ceases to be possible; nuclei with ever greater neutron excesses become stable; finally, the neutrons themselves become stable when the Fermi boundary passes the limit of the neutron β spectrum at ~ 0.8 MeV (at densities $\rho > 10^8$ g/cm^3).

At a very high density ($\rho > 10^{11}$ g/cm^3) a stable state of a star is possible only if the gravitational contraction is resisted by the kinetic pressure of the degenerate neutron gas. A neutron state of matter at high density was predicted very soon after the discovery of the neutron. The discovery of pulsars in 1968 showed that neutron stars in which the matter density exceeds 10^{15} g/cm^3 do exist. The power of the pulsar radiation, the repetition frequency of the pulses, and the stability of this frequency – all can be explained if a pulsar is a star of about a solar mass that rotates once "in the blinking of an eye." But if the star rotates at 30 rps (1800 rpm) – as in the Crab Nebula pulsar – it must have a high density and strong gravitational field at the surface to withstand centrifugal disintegration. Models of neutron stars constructed before the discovery of pulsars predicted a radius ~ 10 km; the flywheel effect at this radius does not lead to centrifugal disintegration at 1800 rpm but the margin is not large; if the radius is 100 km, the centrifugal acceleration at the equator is nearly equal to the gravitational acceleration.

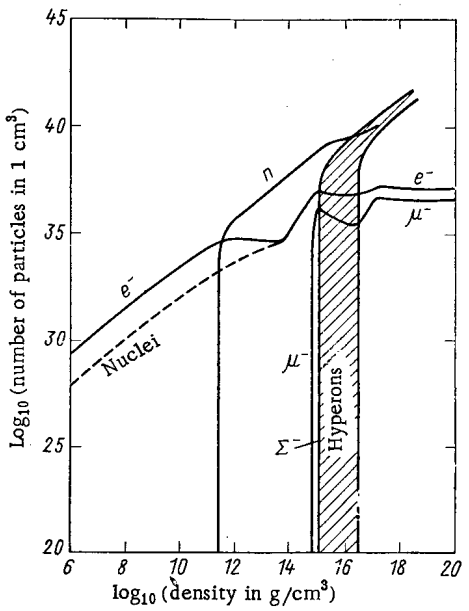

Fig. 3. Composition of dense matter as a function of the density.

Three years of pulsar observations and theoretical analysis of pulsar properties have removed all doubts; neutron stars exist, as predicted. Another pre-pulsar prediction – neutron stars should be formed in the explosion of supernovas – has been fulfilled by the discovery of pulsars at the sites of historical supernovas. The detailed working out of neutron-star models continues.

Figure 3 gives a general idea of the composition of the matter in a neutron star [28]. At the low densities near the surfaces, the principal components are the electron gas and the nuclei of the atoms. The mass of the nuclei and their neutron excess increase with the density, i.e., with depth; at a density $\sim 10^{11}$ g/cm^3 the Fermi limit of the electron spectrum is ~ 20 MeV, and the most abundant nuclei are those like Sr^{120}, which have more than 30 extra neutrons compared with Sr^{88}, the most common isotope on the Earth; at densities greater than 3×10^{11} g/cm^3 the principal component is free neutrons with an admixture ($\sim$1%) of protons and electrons; excited nucleons and hyperons make their appearance at densities $> 10^{15}$ g/cm^3.

The main features predicted by neutron-star models are: a solid crust of nuclei forming a solid crystalline lattice; a

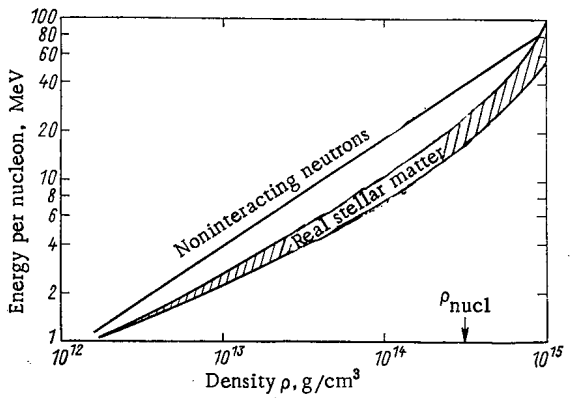

Fig. 4. Energy of neutron-star matter as a function of the density. The width of the strip for real matter reflects the spread of calculated predictions.

gaseous (or liquid) mantle composed of neutrons with an admixture of protons and electrons; and a core consisting of hyperons, excited nucleons, and other particles. The thicknesses of the layers depend on the mass of the star; the larger the mass, the thinner the crust and the thicker the core and mantle. These qualitative characteristics of the model are not in doubt, being based on well-known properties of neutrons and nuclei; but many quantitative characteristics are not known reliably and depend strongly on the assumed properties of matter at high density. One of the important and undetermined quantities is the limiting mass of a star. At a high mass, the kinetic pressure of the degenerate neutron gas or, quite generally, any state of matter is insufficient to withstand the gravitational pressure; the star collapses, forming a hitherto unobserved object – a collapsar, or black hole. The critical mass at which a star is still stable is uncertain – the estimates vary from 0.5 to $2M_\odot$, where $M_\odot = 2 \times 10^{33}$ g is the solar mass – because the composition of the matter and the pressure or energy per nucleon depend on the inadequately known interaction of nucleons.

Figure 4, which is taken from [29], shows the energy per nucleon as a function of the matter density of a neutron star. The upper curve, which is almost straight, corresponds to a degenerate gas of noninteracting neutrons; but neutrons are subject to nuclear forces of attraction at sub-nuclear densities and repulsion at higher densities; if there is an admixture of protons, the forces of attraction are even more important and the energy in the real gas is less than in an ideal gas (at the nuclear energy, $\rho_{nuc} = 3 \times 10^{14}$ g/cm^3, the energy of a real gas is approximately half that of an ideal gas). The width of the hatched strip corresponds approximately to the uncertainty of present calculations of the matter state of neutron stars.

Since the strong interaction of nucleons has a pronounced influence on the state of matter (the composition and energy), the results of calculations depend on the assumptions made about the interaction potentials. At densities $> 10^{15}$ g/cm^3 the even less-known properties of hyperon matter become decisive; the difficulties are compounded – the higher the mass of the neutron star, the more important is its hyperon core and the greater is the dependence of its limiting mass on the state of matter at super-nuclear densities [30].

The investigation of neutron stars is interesting because it casts light on the properties of matter in a wide density range, including the state of pure neutron matter, whose role in nature is fairly important. It follows from the curve of Fig. 4 that pure neutron matter does not form bound states; its energy is always positive and increases monotonically with increasing density. But the quantitative conclusions of such calculations are not sufficiently accurate; an improvement depends on further investigations of neutron and nuclear physics and the physics of elementary particles. One line of development is the production and study of nuclei with large neutron excesses in subterranean explosions [31] or in nuclear reactions [32].

A neutron star clearly contains a vast multitude of atomic nuclei, including neutron-excess nuclei, that are unstable under terrestrial conditions and cannot be obtained in laboratories. It has been conjectured that the matter of neutron stars contains super-heavy nuclei with $Z > 100$. Eruptions leading to the ejection of matter could serve as one of the mechanisms of nucleosynthesis of interstellar matter and also be a source of super-heavy nuclei.

It follows from considerations about the conditions under which neutron stars are formed and from observations of pulsar radiation that there are very strong magnetic fields, $\sim 10^{12}$ Oe, at the surface of such stars. In a field of this strength, the structure of atoms, molecules, and crystals is quite different from the usual structure under terrestrial conditions [33].

A neutron star is an extraordinarily rich laboratory; we cannot control it, but its life is stormy, and much information is available, even more than from the Sun in some respects; radio telescopes register a very slow monotonic increase in the repetition period P of pulsars ($\partial P/\partial t/P \approx 10^{-10} - 10^{-15}$), on which sudden discontinuities ($\Delta P/P$) of $\sim 10^{-9} - 10^{-6}$ are superimposed; a fairly detailed theory of "starquakes" has been developed to explain them [34]; the jumps in the period are attributed to abrupt changes in the moment of inertia of the star caused by seismic deformations of the solid crust; the relaxation after the jumps suggests

that the neutron component of the mantle is superfluid and the proton component superconducting. Of course, the models of neutron stars and pulsars are far from perfect, but the progress that has been made already in the three years since their discovery promises eventual success. Neutron stars have given birth to new branches of physics; the physics of superdense matter, the physics of superhigh gravitational and electromagnetic fields, the physics of relativistic plasmas, etc.

The new phenomena observed in pulsars and neutron stars are varied and interesting; their study has greatly extended the scope of modern science.

I should like to thank T. K. Chizhov for a discussion.

LITERATURE CITED

1. J. Chadwick, Nature, 129, 312 (1932).
2. W. Bothe and H. Becker, Z. Phys., 66, 289 (1930).
3. I. Curie and F. Joliot, Compt. Rend., 193, 1412 (1931); 194, 273 (1932).
4. I. Curie and F. Joliot, Compt. Rend., 198, 254 (1934).
5. E. Fermi, Nature, 133, 757, 898 (1934).
6. Electrical Rev., 189, 773 (1971).
7. A. I. Leipunskii, Usp. Fiz. Nauk, 95, 15 (1968).
8. G. Siborg and D. Bloom, Ibid., 106, 85 (1972).
9. S. N. Sukhoruchkin, At. Energ., 30, 76 (1971); 31, 245 (1971).
10. L. Alvarez and F. Bloch, Phys. Rev., 57, 111 (1940).
11. R. Hofstadter et al., Phys. Rev., 139B, 459 (1975).
12. R. Wilson et al., Phys. Rev. Lett., 13, 631 (1964).
13. E. Bloom et al., Ibid., 23, 930 (1969); M. Breidenbach et al., Ibid., 23, 935 (1969); G. Kendal and V. Panovskii, Usp. Fiz. Nauk, 106, 315 (1972).
14. R. Feynman, Phys. Rev. Lett., 23, 1416 (1969); H. Nieh and J. M. Wang, Ibid., 26, 1139 (1971).
15. K. Wilson, Ibid., 27, 690 (1971); J. Kuti and V. Weisskopf, Phys. Rev., D4, 3418 (1971); S. Drell, Usp. Fiz. Nauk, 106, 331 (1972).
16. P. Miller et al., Phys. Rev. Lett., 19, 381 (1967); C. Shull and R. Nathaus, Ibid., 19, 384 (1967).
17. F. L. Shapiro, Usp. Fiz. Nauk, 95, 145 (1968).
18. Ya. B. Zel'dovich, Zh. Eksp. Teor. Fiz., 36, 1952 (1959).
19. V. V. Vladimirskii, Zh. Eksp. Teor. Fiz., 39, 1062 (1960).
20. V. I. Lushchikov et al., Preprint JINR R3-4127 [in Russian], Dubna (1968).
21. L. Groshev et al., Phys. Lett., 34B, 293 (1971).
22. R. Eötvös et al., Ann. Phys., 68, 11 (1922).
23. R Dicke et al., Ann. Phys., 26, 442 (1964); V. B. Braginskii and V. N. Panov, Zh. Éksp. Teor. Fiz., 61, 873 (1971); Usp. Fiz. Nauk., 105, 779 (1971); R. Dicke, Gravitation and the Universe [Russian translation], Mir (1972).
24. I. Dabbs et al., Phys. Rev., B139, 756 (1965).
25. H. Meier–Leibnitz, Z. Angew. Phys., 14, 738 (1962).
26. L. Koestler and W. Nistler, Phys. Rev. Lett., 27, 956 (1971).
27. W. Dilg et al., Phys. Lett., B36, 208 (1971).
28. S. Tsuruta and A. Cameron, Canad. J. Phys., 44, 1895 (1966).
29. H. Bethe, Ann. Rev. Nucl. Sci., 21, 93 (1971); G. Baym et al., Nucl. Phys., A175, 225 (1971).
30. Ya. B. Zel'dovich and I. D. Novikov, Theory of Gravitation and the Evolution of Stars [in Russian], Nauka, Moscow (1971).
31. B. Diven, Ann. Rev. Nucl. Sci., 20, 79 (1970); At. Tekh. za Rubezhom, No. 1, 31 (1972).
32. G. Rudstam, Ark. Fis., 36, 9 (1967).
33. B. B. Kadomtsev, Zh. Éksp. Teor. Fiz., 58, 1765 (1970); Usp. Fiz. Nauk, 104, 335 (1971); R. Mueller et al., Phys. Rev. Lett., 26, 1136 (1971); M. Ruderman, Ibid., 27, 1306 (1971).
34. G. Baym et al., Nature, 224, 674 (1969); 229, 872 (1970); M. Ruderman, Nature, 225, 619 (1970).

ARTICLES

EVALUATING THE RELIABILITY OF THE BELOYARSK ATOMIC POWER STATION'S PUMPS ON THE BASIS OF OPERATING DATA

I. Ya. Emel'yanov, G. A. Shasharin, G. A. Kireev, A. I. Klemin, E. F. Polyakov, M. M. Strigulin, and E. A. Shiverskii

UDC 621.311.2:621.039:621.68

The characteristics of atomic power plant operation make it difficult to apply the methods generally used for evaluating the reliability of individual items of equipment (for example, pumps) on the basis of operating data. The main difficulty lies in the following. The high operational reliability of most items of equipment at an atomic power station is kept up by regular preventive maintenance. Because of this, it is relatively seldom that an item of equipment breaks down. By "breakdown" we mean a failure of the operating capacity of the equipment such that it must be immediately shut down and emergency repairs must be made. Obviously, if we evaluate the reliability of a particular item of equipment merely on the basis of its breakdown statistics, we obtain its reliability characteristics for the specific operating regime under consideration (for example, for a given frequency and kind of preventive maintenance*). If the regime of operation changes, the reliability indicators will also change.

As a rule, breakdowns seldom occur; therefore, if we want to obtain a more complete and more exact evaluation of equipment reliability, we cannot confine our basic data to breakdown statistics alone but must also take into consideration the statistics on malfunctions occurring in the operation of the equipment. By

*This frequency is often determined empirically. The choice of an optimal frequency for preventive maintenance requires an engineering–economic analysis, and the initial data taken for this analysis should be the reliability indicators of the equipment; the determination of these is the subject of this article.

TABLE 1

Designation of pump	Station unit	Type of pump	Number of pumps of the indicated	Drive power, kW	Head, kg/cm^2	Capacity, m^3/h	Speed, rpm	Temperature of pumped medium, °C
Main circulation pump (MCP)	I	TsÉN-133	3	520	10.0	650*	3000†	310
		TsÉN-133/3	1					
	II	TsÉN-133/3	4	750	15.6	650*	3000†	310
Electrical feed pump (EFP)	I	5Ts10	3	2000	158.0	270	2970	160
	II	PÉ-500-180-2	4	4000	180.0	500	2985	160
Reactor control system cooling pump (RCP)	I	TsÉNOR-133	2	55	6.0	100	3000	60
	II	TsÉNOR-133/3	2	65	7.0	125	3000*	60
Shielding system cooling pump (SCP)	I	TsÉNOR-133	2	19.5	6.5	12	3000*	60
	II	TsÉNOR-133/3	2	19.5	6.5	12	3000*	60

*Output expressed in tons/h.
†Synchronous speed.

Translated from Atomnaya Energiya, Vol. 33, No. 1, pp. 547-551, July, 1972. Original article submitted August 12, 1971; revision submitted February 2, 1972.

TABLE 2

Indicator	Unit I					Unit II				
	MCP, first period	MCP, second period	EFP	RCP	SCP	MCP	EFP, first period	EFP, second period	RCP	SCP
$\omega_b \times 10^4$, 1/h	3,3	2,48	6,8	0,82	0,58	0,44	15,7	9,7	2,74	1,56
$I^*_{b,95;\ \omega_b \times 10^4}$, 1/h	2,1 4,6	1,50 3,88	4,96 9,3	0,36 1,6	0,16 1,49	0,15 1,0	10,9 21,2	5,8 15,4	1,29 5,17	0,28 4,9
$\omega_m \times 10^4$, 1/h	0,8	2,19	12,0	1,37	1,34	2,97	14,7	8,2	0,78	1,56
$I^*_{b,95;\ \omega_m \times 10^4}$, 1/h	0,34 1,55	1,35 3,38	9,6 14,8	0,76 2,34	0,63 2,53	2,13 4,0	10,2 20,0	4,6 13,6	0,14 2,44	0,28 4,9
$\omega_c \times 10^4$, 1/h	4,1	4,6	18,8	2,19	1,92	3,41	30,4	17,2	3,52	3,12
$I^*_{b,95;\ \omega_c \times 10^4}$, 1/h	2,9 5,8	3,53 6,05	15,8 22,1	1,35 3,38	1,05 3,25	2,45 4,61	20,3 30,7	12,0 24,0	1,84 5,96	1,07 7,10
T_b, h	3000	4040	1450	12 200	17 250	22 700	638	1060	3650	6401
T_r, h	20	20	11	8,3	10	13,8	21	21	11,4	17,5
K_p	0,993	0,996	0,992	0,999	0,999	0,999	0,968	0,980	0,997	0,997
S†, man-hours	20	20	23	—	—	53	91	91	—	—

*The upper and lower values on this line represent, respectively, the upper and lower confidence limits between which the true value of the parameter ω will lie with a probability $\alpha = 0.95$.

†Labor needed for emergency repairs.

"malfunction" we will mean a defect which leaves the main operating parameters of the equipment undisturbed for some length of time (without any need for immediate shutdown) and which will be corrected during the next routine maintenance or the next emergency repair.

Malfunctions may be discovered either at repair time or during the process of operation, from the accompanying signs (for example, increased intensity of vibration, a change in the noise, a rise in the heating temperature, etc.), and, as a rule, it is difficult to determine exactly the moment at which the malfunction began. However, it may be assumed with satisfactory reliability that malfunctions arise during an operating-time interval Δt preceding the next repair. Since the length of this interval is usually small in comparison with the service life of the equipment, we may assume without any special loss of accuracy in our reliability evaluation that the times at which malfunctions occur are uniformly distributed over the time interval Δt.

Thus, in analyzing the operational reliability of equipment, especially pumps, at an atomic power station, it is convenient to consider the frequencies of the three types of events: the frequency of breakdowns, the frequency of malfunctions, and the combined frequency. Obviously, the first of these can be used for judging the reliability of a pump under a specific regime and the specific type of maintenance adopted at the atomic power station during the operating period under consideration. The combined frequency, in turn, is more conservative and less affected by differences in the type of maintenance. Since malfunctions may be regarded as potential sources of breakdown, the combined frequency enables us to judge where the lower limit of equipment reliability lies. The parameters of the combined frequency are used in calculating the average operating time of the equipment per breakdown or malfunction, in estimating the necessary amount of replacement parts and supplies, in choosing the frequency of scheduled preventive maintenance, etc.

Collection of the Statistical Information

As the subject for our reliability study, we selected the main pumps of the Beloyarsk atomic power station (Table 1). These are all high-speed pumps; the feed pumps are typical high-power pumps, while the others are special hermetically sealed pumps, in which the rotor of the electric motor turns in the pumped medium together with the rotor of the pump and is separated from the stator of the electric motor by a thin hermetically sealed Nichrome wall. The bearings of these pumps are lubricated and cooled with pre-cooled pumped water. The rotating parts of the bearings are made of high-strength alloys, and the bushings are made of special plastics.

For unit I we collected statistical data on pump operation for the period 1965-1970, and for unit II for 1968-1970, i.e., for practically the entire period of power operation of the units through 1970. Our sources of information were the operational and repair logs, the defect logs, statements of the operating times of the main pumps, and other records. We determined the following data: 1) the operating time between two

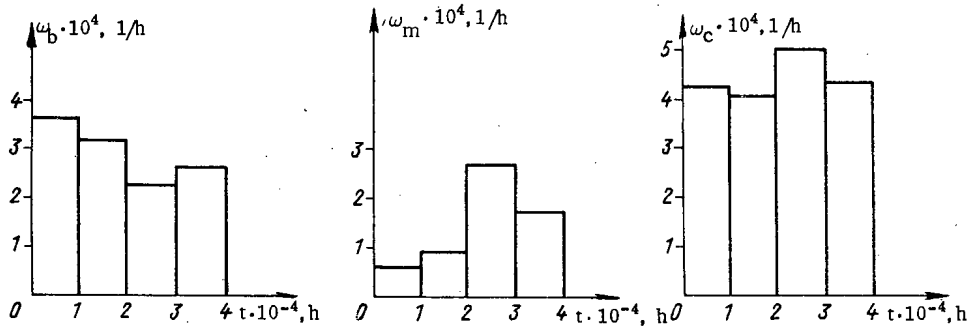

Fig. 1. Histograms of the parameters of breakdown frequency ω_b, malfunction frequency ω_m, and combined frequency ω_c for the MCP of unit I.

successive startups and shutdowns of the equipment, with an indication of the reason for the shutdown (breakdown, routine or major repair; transfer of the pump to reserve status; scheduled or emergency shutdown of the unit); 2) the nature of the breakdown; 3) the duration and degree of difficulty of the repair; 4) the nature of the repair (emergency or routine), with an indication of the malfunctions discovered and the parts replaced.

Processing of the Statistical Data

Determining the Pattern of Distribution of Operating Time between Breakdowns. In order to apply the existing methods of determining the pattern of distribution of breakdown-free operating time, we must have a sufficiently large amount of statistical data. Such data were accumulated for the MCP of unit I and the EFP of units I and II.

The histograms in Fig. 1 indicate the time variation of the frequency parameters (average numbers of events per unit time [1]) for breakdowns, for malfunctions, and for the combined sequence, as observed on the MCP of unit I. It can be seen from the figure that the parameter for the breakdown sequence decreases with time. This is attributable to the modernization of the MCP of unit I, which consisted of redesigning the attachment assembly of the Nichrome wall used for hermetically separating the rotor cavity from the stator, and redesigning the bearing assembly, the materials of the operating bearings being replaced with more reliable materials.

Because of this, the entire unit I MCP operating interval under consideration was divided into two periods: before and after the modernization. The reliability indicators for the unit I MCP were calculated separately for each period.

A similar subdivision into two periods was applied to the unit II EFP, in which we can also clearly see the effect of modernization on the pumps; in this case the modernization consisted of changing the design of the impeller in order to reduce the stresses acting on it, as well as in improving the stuffing-box seal and the discharge chamber.

For the other pumps the entire period of operation was considered as a single interval.

The histograms in Fig. 2 indicate the empirical distribution of probabilities for different operating-time values between breakdowns for the first and second periods of operation for the MCP of unit I. From the shape of the histograms, it may be assumed that the distribution law is exponential. The correctness of this hypothesis was verified by using the Pearson χ^2 criterion. The experimental and theoretical (exponential) distribution curves were found to be in good agreement (probability $P = 1 - F(\chi^2) = 0.3$, whereas $P = 0.05$ is sufficient). For the EFP of unit I and unit II we also found confirmation of the exponential distribution of operating time between breakdowns at a high level of significance ($P = 0.3$ and $P = 0.9$, respectively).

Determination of Quantitative Reliability Indicators. The principal reliability indicators for the repaired equipments in accordance with All-Union State Standard 13377-67 [1] is the breakdown frequency parameter $\omega(t)$, which is the average number of breakdowns per unit time at about time t.

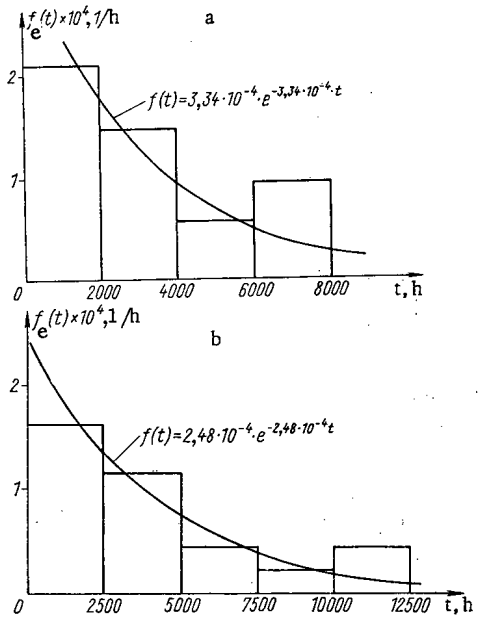

Fig. 2. Patterns of distribution of operating time between breakdowns for first (a) and second (b) periods of operation of the MCP of unit I.

The breakdown sequence parameter is found by the formula

$$\omega_b t = \frac{\sum_{i=1}^{N} m_{bi}(t+\Delta t) - \sum_{i=1}^{N} m_{bi}(t)}{N\Delta t}, \quad (1)$$

where N is the number of pumps of the same type and assignment; $m_{bi}t$ is the number of breakdowns of the i-th pump occurring up to operating time t.

When the distribution of operating times between breakdowns is exponential, i.e., when for the time interval t under consideration we have $\omega_b(t) = \omega_b = \text{const}$, formula (1) becomes considerably simpler:

$$\omega_b = \frac{m_{b\Sigma}}{T_\Sigma}, \quad (2)$$

where $m_{b\Sigma}$ is the total number of breakdowns for all pumps over the period t; T_Σ is the total operating time of the pumps.

In an analogous manner, we can calculate the parameter for the malfunction frequency and the parameter for the combined frequency:

$$\omega_m = \frac{m_{m\Sigma}}{T_\Sigma}; \quad \omega_c = \frac{m_{b\Sigma} + m_{m\Sigma}}{T_\Sigma} = \omega_0 + \omega_m, \quad (3)$$

where $m_{m\Sigma}$ is the number of malfunctions in pumps of the same type over the operating period under consideration.

Knowing the frequency parameter ω and assuming that the distribution of operating times between events is exponential, we can easily calculate [2] the probability that no event of a given type will occur during a given time t (for example, that there will be no breakdown): $P(t) = e^{-\omega t}$, or that there will be exactly m events:

$$P_m(t) = \frac{(\omega t)^m}{m!} e^{-\omega t}. \quad (4)$$

The average operating time between events of a given type (for example, between breakdowns, between malfunctions, etc.) will be

$$I = \frac{1}{\omega}. \quad (5)$$

The accuracy with which the frequency parameters ω_b, ω_m, and ω_c are determined can be estimated if we find confidence intervals for these quantities, i.e., if we find the intervals within which, with a given confidence probability α, the true values ω_b^{tr}, ω_m^{tr}, and ω_c^{tr} will lie. In accordance with [3], such intervals will have the values:

$$I_{\alpha,\omega} = \left(\omega_{lower} = \frac{\omega}{r_1}; \quad \omega_{upper} = \frac{\omega}{r_2}\right), \quad (6)$$

where r_1 and r_2 are coefficients which depend on the amount of initial statistical data, i.e., on the number m_Σ [see formulas (2), (3)] and the quantity α.

The average time for restarting a pump after an emergency shutdown was calculated by the formula

$$T_r = \frac{1}{m_{b\Sigma}} \sum_{i=1}^{m_{b\Sigma}} t_i, \quad (7)$$

where t_i is the time required for correcting the i-th breakdown (the duration of the i-th emergency repair). Knowing the average operating time per breakdown, $T_b = 1/\omega_b$, and the value of T_r, we can calculate the coefficient of preparedness of the pump, which is equal to the probability that the pump will be repaired and ready to operate at a given instant of time between the times of scheduled maintenance: $K_p = I_b/(I_b + I_r)$.

The reliability indicators of the pumps, calculated by the above formulas, are shown in Table 2.

Analysis of the Causes of Pump Breakdowns and Malfunctions. An analysis of pump operation showed that the weakest design components were the bearing assemblies, stator jackets, and mountings in the MCP, and the stuffing-box seals, bearing assemblies, and joints in the EFP. Failure of these components causes more than half of the breakdowns on these pumps.

CONCLUSIONS

1. Operational reliability analyses were conducted and quantitative parameters were obtained for the first time for the main pumps of the Beloyarsk atomic power station. The method used in collecting and processing the statistical data can be applied to evaluating the reliability of most items of equipment at an atomic power station.

2. It was shown that an assumption of exponential curves for the distribution of operating times between successive breakdowns of the MCP of unit I and the EFP of units I and II is consistent with the statistical data. There is reason to suppose that the exponential law also applies to other types of pumps. The collection and analysis of further statistical information will make it possible to confirm this conclusion.

3. A quantitative estimate of the reliability of the equipment makes it possible to compare objectively the reliability of different types of equipment and also to evaluate the effect produced by modernization of such equipment. This can be illustrated by the following examples:

a) modernization of the MCP of unit I (see above) increased the reliability of these pumps and, in particular, reduced the parameter of the breakdown sequence by a factor of

$$\frac{\omega_{\text{MCP I, 1p}}}{\omega_{\text{MCP II 2p}}} = \frac{3{,}3 \cdot 10^{-4}}{2{,}48 \cdot 10^{-4}} = 1.33 \text{ times;}$$

b) the reliability of the MCP of unit II (TsEN-133/3) is higher than the reliability of the MCP of unit I (TsEN-133) by a factor of

$$\frac{\omega_{\text{MCP I, 2p}}}{\omega_{\text{MCP II}}} = \frac{2{,}48 \cdot 10^{-4}}{0{,}44 \cdot 10^{-4}} = 5.65 \text{ times;}$$

this is attributable mainly to the change in the design of the stator arrangement in the electric motor in such a way that the stresses on the Nichrome jacket (which may be the cause of defects in the jacket) are reduced, and is also attributable to the replacement of the ventilator by a more reliable one;

c) the reliability of the feed pumps of unit II (PE-500-180-2, Sumskii Pump Works) is lower than the reliability of the older pumps (5Ts10) by a factor of

$$\frac{\omega_{\text{EFP II, 2p}}}{\omega_{\text{EFP I}}} = \frac{9{,}7 \cdot 10^{-4}}{6{,}8 \cdot 10^{-4}} = 1.42 \text{ times,}$$

which is attributable chiefly to improper design of the first impeller and defects in manufacture;

d) modernization increased the reliability of the unit II feed pumps by a factor of

$$\frac{\omega_{\text{EFP II, 1p}}}{\omega_{\text{EFP II, 2p}}} = \frac{15{,}7 \cdot 10^{-4}}{9{,}7 \cdot 10^{-4}} = 1.62 \text{ times.}$$

4) The results obtained, and, in particular, the pump reliability indicators, can be used:

a) in correcting the frequency and extent of scheduled preventive maintenance of the pumps (as a result of an engineering–economic analysis);

b) for improving the design of pumps and their component assemblies.

c) for calculating the necessary reserve equipment;

d) when combined with data on the reliability of other equipment, in estimating the overall reliability of the Beloyarsk atomic power station, as well as in predicting the reliability of newly planned atomic power stations.

In conclusion, we should like to point out that statistical data on the reliability of equipment at atomic power stations should be collected on a continuous basis. For this purpose, and also to make sure that the statistical information is complete and reliable, a unified centralized system for recording and collecting such data must be introduced.

LITERATURE CITED

1. All-Union State Standard 13377-67. Reliability in Engineering [in Russian].
2. A. I. Klemin and M. M. Strigulin, Some Problems of Reliability in Nuclear Reactors [in Russian], Atomizdat, Moscow (1968).
3. Ya. B. Shor and F. I. Kuz'min, Tables for Reliability Analysis and Control [in Russian], Sovetskoe Radio, Moscow (1968).

CHLORINATION PRODUCTS OF PLUTONIUM DIOXIDE IN MELTS OF ALKALI METAL CHLORIDES

M. P. Vorobei, O. V. Skiba,
N. B. Blokhin, and A. G. Rykov

UDC 541.661.621.039.59

In the reprocessing of irradiated oxide nuclear fuel, as well as in the production and refinement of metallic plutonium, the electrochemical method, utilizing alkali-metal chlorides as the solvent salts, is finding use [1-6]. Consequently, it is important to know in what valence states plutonium passes into the melt during the chlorination of PuO_2, as well as the influence on the valence states of plutonium on the temperature, its concentration in the melt, and the nature and physicochemical properties of the solvent salt.

It was shown in [7, 8] that in melts of the eutectics LiCl – KCl and LiCl – CsCl, depending on the experimental conditions, plutonium can have a valence of (III), (IV), or (VI). The pentavalent state is unstable and arises during the reduction of Pu(VI) to Pu(IV). This work is devoted to an investigation of the valence states of plutonium formed in the chlorination of PuO_2 in melts of lithium, sodium, potassium, rubidium, and cesium chlorides, the eutectic LiCl–KCl, and an equimolar mixture of NaCl and KCl in a broad range of temperatures and concentrations.

EXPERIMENTAL SECTION

The investigation was conducted by a spectrophotometric method. The samples were prepared for analysis by chlorination of PuO_2 in the melt of alkali-metal chlorides, followed by their rapid freezing in an atmosphere of chlorine. A weighed sample of the melt, containing ~ 5 mg plutonium, was dissolved in 2.5 ml of 2 M HCl. The absorption spectra of plutonium solutions were measured on a Hitachi EPS-2U recording spectrophotometer in the wavelength range 340-1000 nm in a 1 cm quartz cuvette. The samples analyzed for Pu(V), were dissolved in 2.5 ml of a solution of HCl, containing 1 M NH_4Cl at pH = 1.5. The plutonium concentration in the tri-, tetra-, and hexavalent states was determined according to the maxima of the absorption bands at the wavelengths, 470, 600, and 830 nm, considering the background absorption. The achievable accuracy, as a rule, was no poorer than 5%. The total content of plutonium in the samples was determined by a radiometric method. The chlorination of PuO_2 was conducted in quartz test tubes 180-200 mm long and 14-16 mm in diameter, both in an atmosphere of air and under isolated conditions. A weighed sample of PuO_2 was immersed in the melt and purged with dry gaseous chlorine until the sample dissolved entirely. The chlorine was produced by electrolysis of molten lead chloride at 550°C and freed of traces of moisture.

In the work we used sodium, potassium, rubidium, and cesium chlorides, cp and analytical grade, which were preliminarily melted, the melt purged with dry gaseous chlorine, and then vacuum treated for 15-20 min. Anhydrous LiCl was prepared according to the method proposed in [9]. The purity of PuO_2 was 99.7%.

The possibility of using the method cited above to study the valence states of plutonium in a melt was verified by spectrophotometric investigations of samples prepared under conditions analogous to those described in [8]. The results obtained (see Table 1) are in good agreement with the data of [8].

RESULTS AND DISCUSSION

LiCl. The solubility of PuO_2 in LiCl melts purged with chlorine in the temperature interval 650-800°C is low, 0.002-0.01% by weight. Plutonium exists in the melt in the oxidation state [Pu(III)].

Translated from Atomnaya Energiya, Vol. 33, No. 1, pp. 553-556, July, 1972. Original article submitted August 16, 1971.

TABLE 1

Salt solvent of eutectic composition	Temperature of experiment, °C	Gas purged through	Initial state of plutonium in melt	Plutonium concentration in melt, % by weight	Valence states of plutonium in melt after purging of gas, %			Note
					III	IV	VI	
LiCl – KCl	400	Cl_2	$PuCl_3$	0.15	10	90	–	Data of [8]
LiCl – KCl	400	$Cl_2 + O_2$*	$PuCl_3$	0.15	–	–	100	" "
LiCl – CsCl	400	Cl_2	$PuCl_3$	0.13	10	90	–	" "
LiCl – CsCl	400	$Cl_2 + O_2$	$PuCl_3$	0.13	–	–	100	" "
LiCl – KCl	400	Cl_2	$PuCl_3$	0.15	8	92	–	Our data
LiCl – KCl	400	$Cl_2 + O_2$	$PuCl_3$	0.14	–	–	100	" "
LiCl – KCl	400	Cl_2	$PuCl_3$	2.25	11	89	–	" "
LiCl – KCl	400	$Cl_2 + O_2$	$PuCl_3$	2.25	–	–	100	PuO_2 precipitated to the bottom of the test tube; residual plutonium content in the melt 0.18%
LiCl – CsCl	400	Cl_2	$PuCl_3$	0.21	5	95	–	
LiCl – CsCl	400	$Cl_2 + O_2$	$PuCl_3$	0.20	–	–	100	

*The oxygen content in the gas mixture was 33% by volume.

Eutectic LiCl – KCl (59 mole % LiCl). The solubility of PuO_2 in this eutectic depends substantially on the temperature and is negligible in the interval 350-550°C, while the product of the chlorination of PuO_2 under these conditions is Pu(VI). The concentration of Pu(VI) in the melt ranges from 0.04 to 0.08% by weight. When the temperature is raised to 850°C, the solubility of PuO_2 increases, while the stability of Pu(VI) decreases, and under these conditions, after 6-8 h of chlorination, melts containing 5-10% by weight plutonium with a ratio of the valence states Pu (III): Pu (IV) $\approx$ 1 : 3 can be obtained. One of the causes of the increase in the solubility of PuO_2 in a melt with increasing temperature is apparently the substantial increase in the solubility of chlorine in this case [10].

NaCl. The solubility of PuO_2 in a melt of NaCl in the temperature interval 800-950°C is approximately comparable with its solubility in a melt of the eutectic LiCl – KCl under the same conditions. The maximum concentrations of plutonium that could be obtained after chlorination for 6-8 h in the indicated temperature interval are 8-10% by weight. In this case the ratio of the valence states Pu(III): Pu(IV) in the melt is equal to ~ 3:1 and increases somewhat with increasing temperature and concentration of plutonium.

Equimolar Mixture of NaCl – KCl. In this melt, in the temperature interval 700-850°C, the solubility of PuO_2 increases appreciably in comparison with its solubility in the systems considered above. After 6-8 h of chlorination at the indicated temperatures, melts were obtained containing 10-20% by weight plutonium at a ratio Pu(III): Pu(IV) $\approx$ 1:2. Changes in the plutonium concentration in the melt and in the time of chlorination do not significantly influence the ratio of the valence states.

We should note that melts of the systems under consideration containing more than 0.5% by weight plutonium are unstable at the temperatures 650-900°C in air and decompose, liberating PuO_2. The residual concentrations of plutonium in a melt of an equimolar mixture of NaCl – KCl are approximately 0.2-0.4% by weight, while in melts of the remaining systems they are 0.1-0.01% by weight. The purging of air or oxygen through the melts leads to an even more profound decomposition of them, and the plutonium remaining in the melt is in the tetravalent state.

KCl. Melts of KCl in the interval 800-950°C are characterized by high solubility of plutonium, which ranges from 25 to 26% by weight. In 6-8 h of chlorination at 800-820°C, melts with 20-25% by weight plutonium were obtained at a ratio of the valence states Pu (III) : Pu (IV) $\approx$ 1 : 1.

With increasing plutonium concentration in the melt and increasing time of chlorination, the fraction of Pu (VI) increases. Melts of KCl containing up to 20% by weight plutonium are stable in air at 700-800°C, while when they are purged with a chlorine – oxygen mixture (10% by volume O_2), they decompose, liberating PuO_2. The residual concentrations of Pu (IV) in the melt are 1-1.5% by weight.

RbCl. The solubility of PuO_2 in a melt of this salt in the temperature interval 750-850°C is 25-28% by weight. After chlorination of PuO_2 for 6-8 h at the temperature 725-750°C, the concentration of Pu (IV) in the melt reached 24-26% by weight.

At 750-800°C and concentrations up to 6-8%, plutonium exists in a melt in the tetra- and hexavalent states. The ratio of these states depends on the temperature and concentration. At 750°C and concentrations 0.1-0.5% by weight, the relative content of Pu (VI) reaches 25-35%, but decreases with increasing time of chlorination and plutonium concentration.

CsCl. A melt of CsCl at the temperatures 650-850°C is distinguished by the maximum solubility of PuO_2 in comparison with the systems considered, reaching 30-35% by weight. After 6-8 h of chlorination at 650-700°C, melts containing up to 30% by weight plutonium in the oxidation state [Pu (IV)] were obtained. At concentrations of 0.1-10% by weight and 650-700°C, plutonium exists in the tetra- and hexavalent states in the melt. The ratio between these states depends on the plutonium concentration, the temperature, and the time of chlorination. In the concentration region down to 0.1% by weight at 650°C, all the plutonium in the melt is in the hexavalent state, while for the rest this system is analogous to the system with RbCl.

Melts of RbCl and CsCl, containing up to 25% by weight plutonium, are stable in air at 600-750°C, while purging with a mixture of $Cl_2 - O_2$ (10% by volume O_2) decomposes them, liberating PuO_2. The residual plutonium concentration in the melt is 1-2% by weight, and plutonium is in the hexavalent state.

In melts of these salts, containing 10-30% by weight plutonium and existing in equilibrium with PuO_2, in the temperature region up to 750°C, in all cases together with Pu (IV), Pu (VI) was detected, with a concentration not exceeding 5%. In all the samples with RbCl and CsCl containing up to 5% by weight plutonium, Pu (V) was absent.

On the basis of the experimental data obtained, a number of generalizations and conclusions can be drawn. The solubility of PuO_2 in all the systems studied, as well as the ratio and stability of the valence forms of plutonium in the melt, are influenced by the nature of the salt solvent, the solubility of chlorine in the system, the temperature of chlorination and the plutonium concentration, as well as the partial pressure of the chlorine above the melt. The increase in the solubility of PuO_2 in the series of alkali metal chlorides from lithium to cesium is apparently due to the increase in the solubility of chlorine in melts from LiCl to CsCl, as well as the increase in the stability of plutonium products in chloride melts in this direction [10], which can be explained by an increase in the complex-forming abilities of the alkali metal cations in the series from lithium to cesium. The increase in the polarizing strength of the cations in the series from cesium to lithium and, consequently, in the strength of the bond along the line $Me^+ - Cl^-$, evidently also has a definite influence on the solubility of PuO_2 in the systems cited [11, 12]. The anomalously low solubility of PuO_2 in a melt of LiCl at 650-800°C and a eutectic of LiCl – KCl at 350-550°C can evidently be explained by the rather low solubility of chlorine in these systems [10].

We should note that when the limiting solubilities of PuO_2 in the systems studied within the temperature intervals cited are reached, attempts to obtain melts with a high concentration of plutonium by increasing the temperature and time of chlorination did not give positive results. In this case PuO_2 dissolved parallel with the formation of plutonium-containing sublimates, which condensed on the cold parts of the apparatus. The plutonium content in the melt was practically unchanged until the PuO_2 dissolved entirely, and then decreased somewhat, which was due to the low thermal stability and high vapor pressure of plutonium products in the melt under the indicated conditions. The sublimates formed in the chlorination of PuO_2 are loose yellow-colored powders, readily soluble in water. In the system with NaCl, their color changes from yellow to dark brown. The relative amounts of the sublimates and their plutonium content increase with increasing plutonium concentration in the melt, rate of purging of chlorine through the melt, and the temperature of chlorination. In systems with KCl, RbCl, and CsCl the plutonium content in the sublimates formed from melts with 20-25% by weight plutonium at 700-800°C was 5-8% by weight. In the region of low plutonium concentrations (up to 5% by weight) and temperatures of 650-800°C, small amounts of sublimates are formed in the systems, while the plutonium content in them varied from 1 to 3% by weight. Spectrophotometric analysis of the sublimates showed that plutonium exists in them in the tetravalent state. Exceptions are the sublimates from the system with NaCl, in which Pu (III) is present together with Pu (IV).

A characteristic peculiarity of all the systems studied is the formation of melts containing Pu (IV) in the chlorination of PuO_2. The stability of this valence form gradually increases in the series of chlorides from sodium to cesium. In systems with NaCl, KCl, and equimolar mixture of NaCl and KCl, as well as with a eutectic of LiCl – KCl, Pu (III) exists at equilibrium with Pu (IV), and its stability increases from KCl to NaCl. Pu (VI) appears in appreciable amounts only in melts of RbCl and CsCl. Its stability in a melt of CsCl is somewhat higher than in a melt of RbCl and decreases appreciably with increasing temperature and plutonium concentration in the melt. On the basis of the experimental data obtained it can be assumed that in melts of the systems studied, during the chlorination of PuO_2, the following reactions take place:

$$PuO_2 + Cl_2 \rightleftarrows PuO_2^{++} + 2Cl^-;$$
$$PuO_2^{++} + Cl_2 \rightleftarrows Pu^{4+} + 2Cl^- + O_2;$$
$$Pu^{4+} + Cl^- \rightleftarrows Pu^{3+} + 1/2Cl_2.$$

It has been noted that an increase in the temperature of melts containing plutonium in the tri- and tetravalent states, within the range 650-900°C, led in all cases to an increase in the content of Pu (III), and was more substantial, the lower the concentration of plutonium in the melt, while slow cooling of the melts to room temperature in an atmosphere of chlorine correspondingly increased the content of Pu (IV), and more substantially the higher the plutonium concentration in the melt. This permits us to state that reaction (3) is of an equilibrium nature, while the stability of Pu (IV) increases with decreasing temperature and increasing plutonium concentration in the melt.

For reaction (3) the equilibrium constant was calculated at the temperature 750°C according to the results of spectrometric measurements in the region of dilute solutions for the system with an equimolar mixture of NaCl – KCl:

$$K_p = \frac{[Pu^{3+}][Cl]^{1/2}}{[Pu^{4+}][Cl^-]}; \quad K_p = 1.8 \pm 0.3 \times 10^{-3} \text{ (liter/mole)}^{1/2}.$$

Let us note that the removal of chlorine from melts containing Pu (III) and Pu (IV), as well as from melts containing Pu (IV) and Pu (VI), led in all cases to reduction of all of the Pu (IV) to Pu (III), while in systems with RbCl and CsCl it led to the appearance of greenish-brown precipitates. X-ray diffraction study of the precipitates in the system with CsCl indicated that they consists of two phases: PuO_2 and 10-20% by weight of the PuOCl phase, and in the system with RbCl of one phase (PuO_2). This permits us to assume that in a melt of CsCl reaction (2) proceeds by several pathways, and in particular, with incomplete stripping of oxygen from the plutonyl cation, as a result of which evidently its oxygen-containing form can exists at equilibrium with the oxygen-free form of Pu (IV) under definite conditions; when chlorine is removed from the melt, the oxygen-containing form is reduced to the oxy-cation of Pu (III).

LITERATURE CITED

1. G. Benediet et al., Report HW-SA-1936, U. S. A. (1962).
2. L. Mullins et al., Report LAMS-2441, U. S. A. (1960).
3. M. Brodsky and G. Carleson, Report ANL-FGF-318, U. S. A. (1961).
4. M. Brodsky and G. Carleson, J. Inorg. Nucl. Chem., 24, 1675 (1962).
5. M. Brodsky and G. Carleson, J. Nucl. Sci. Abstr., 17, 2938 (1963).
6. B. Bond et al., Report HW-SA-3527, U. S. A. (1964).
7. D. Gruen and R. McBeth, Ann. N. Y. Acad. Sci., 79, 941 (1960).
8. J. Swanson, J. Phys. Chem., 68, 438 (1964).
9. H. Laitinen et al., J. Electrochem. Soc., 104, 516 (1956).
10. K. D. Muzhzhavlev et al., "Tsvetnye Metally," No. 10, 46 (1970).
11. Yu. V. Baimakov and M. M. Vekhtyukov, Electrolysis of Molten Salts [in Russian], Metallurgiya, Moscow (1966), p. 24.
12. L. Pauling, The Nature of the Chemical Bond [Russian translation], Goskhimizdat, Moscow (1947).

BIOGEOCHEMICAL PROSPECTING FOR URANIUM DEPOSITS

A. L. Kovalevskii

UDC 550.84:553.495

The bases for the biogeochemical method of prospecting are the theory concerning the regularities in the accumulation in plants of the element-indicators of deposits (phytogeochemistry of indicator elements) and the theory concerning the litho- and hydrochemical aureoles dispersed in the zone of hypergenesis. The investigation of the geochemistry of indicator elements of ore deposits in the zone of hypergenesis was begun considerably earlier than the investigation of their phytogeochemistry. Therefore, at first biogeochemical methods were based only on empirical data on the increased concentration of ore elements in plants growing over the deposit. It was established in subsequent special experiments that a similar increase of the concentration in plants was not observed for all chemical elements and types of plants, nor for all types of ore deposits. These phenomena were successfully explained only after recent investigations of the regularities in the accumulation of chemical elements in plants growing on ore deposits.

Regularities in the Accumulation in Plants of Element-Indicators of Uranium. The study of the regularities in the accumulation of uranium and radium in plants established the fact that the low effectiveness

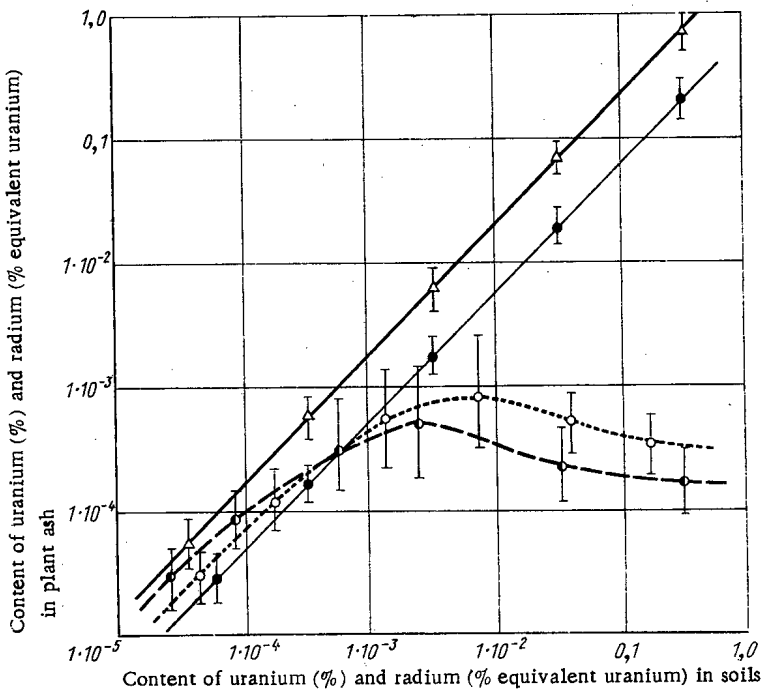

Fig. 1. Typical relationships between uranium concentrations (○—in herbaceous plants, ◐—in trees) and radium (●—in herbaceous plants, △—in trees) in soils and plants (standard deviations indicated by the vertical lines).

Translated from Atomnaya Energiya, Vol. 33, No. 1, pp. 557-562, July, 1972. Original article submitted July 26, 1971.

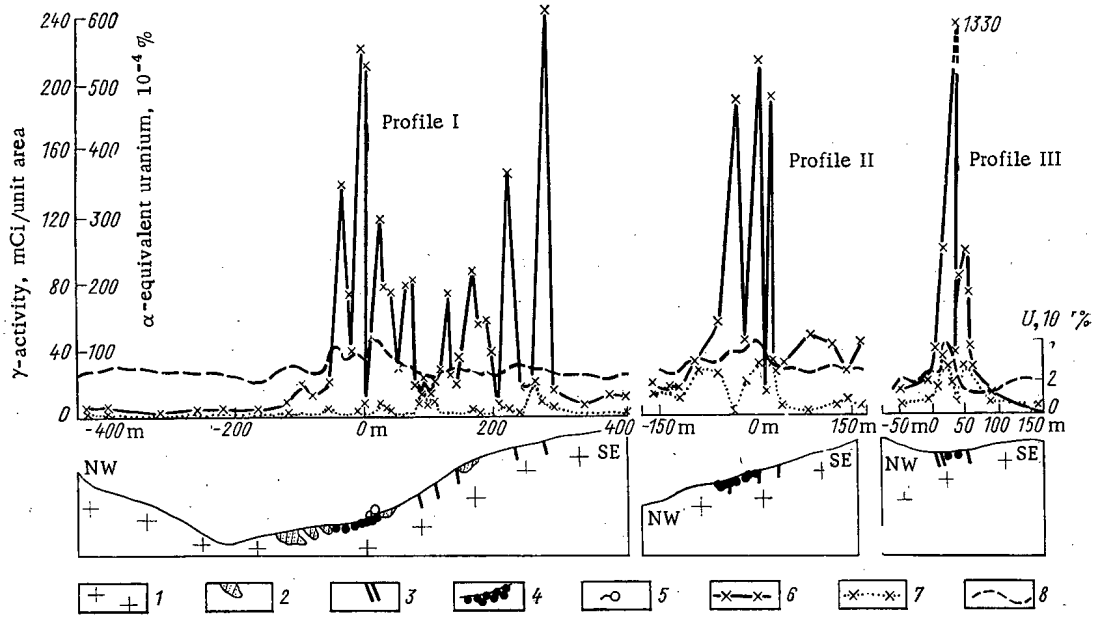

Fig. 2. Comparative effectiveness of biogeochemical and radiometric prospecting methods in an unfrozen region of the Siberian forests: 1) granites; 2) xenolites; 3) uranium ore bodies; 4) aureoles of ore bodies; 5) radioactive springs; 6) α-activity of the ash of birch branches; 7) uranium content of the ash of birch branches; 8) γ-activity on the surface of the ground.

of uranium phytometry, causing a low degree of contrast for uranium biogeochemical anomalies, and the high geological effectiveness of the indication of uranium by radium in plants (radium phytometry) are explained by the presence in plants of physiological barriers with respect to increased concentrations of uranium in soils and the absence of similar barriers with respect to radium [1, 2].

At the present time, according to a unification done by us of our own and published data, the presence of physiological barriers is established for 34 chemical elements. According to the barrier to absorption in higher plants, the chemical elements are divided into four groups: those barriered in the presence of normal contents in soils; those barriered in the presence of soil concentrations exceeding the normal by 3-30 times; those barriered in the presence of soil concentrations exceeding the normal by 30-300 times; and those not barriered in the presence of the limit of high natural concentrations in soils, exceeding the normal by 30-300 times and more (Table 1). For the majority of plant species, uranium should be referred to the first group, but for several species (with anomalous concentrations of uranium) it should be referred to the second group. Radium in all examined plant species is referred to the fourth (barrierless) group of chemical elements. As a result of further study of this question of physiological barriers, the considerable specificity of the barriers was established for various plant species, individuals, organs, cells, and cell organelles. This makes possible the utilization in many practical cases of "barrierless" objects for biogeochemical sampling (element-indicators, species and organs of plants) and thus completely or partly to exclude the negative influence of physiological barriers in plants on the results of biogeochemical surveys.

The presence of physiological barriers with respect to increased concentrations of uranium in soils is established for practically all studied plant species growing over uranium ore bodies. Therefore, the content of uranium in plants does not exceed a certain limiting concentration (Fig. 1), which is usually close to its background content in plants. Only in specific species and individuals may the uranium concentration be 3-30 times and more higher than background, which fact is apparently related to a localized enrichment of particular parts of these plants. The nature of the absorption of uranium by plants indicated above determines as a rule the low contrast of uranium biogeochemical anomalies, which are poorly reproduced on repeated sampling. This compels one to reject uranium as a basic biogeochemical indicator of uranium mineralization and to consider it as a secondary indicator. It has been established by the conducted investigations that the most suitable materials for uranium sampling are "old" organs of wood and shrub plants,

TABLE 1

Group	Chemical elements
Barriered in the presence of normal contents in soils	N, P, K, Ca, Mg, Al, Si, Fe, Mn, F, I, Cu, U
Barriered in the presence of increased contents in soils exceeding the normal by 3-30 times	Li, Rb, Cs, Cu, Sr, Ba, Zn, Y, La, Ce, Ge, Sn, S, Cr, Mo, W, U, F, Br, Co, Ni
Barriered in the presence of high soil concentrations exceeding the normal by 30-300 times and more	Na, Ag, Au, Zn, Hg, B, Ge, Sn, Pb, As, Sb, Bi, S, Se, Mo, W, F, Cl, Co, Ni
Barrierless in the presence of high soil concentrations exceeding the normal by 30-300 times and more	Na, S, Cl, Au, Cd, Ra, B, Pb, As, Mo, Se, Re

in which its content is very high and practically constant with time. In plants, the relative concentration of uranium is ordered as follows: ordinary pine trees, rhododendron, leaves of mountain ash trees, and other species (Table 2). Herbaceous plants are more expediently sampled at the end of the vegetative period and in the fall–winter–spring period of relative inactivity, since at these times the limits of uranium concentration in their above-ground parts is increased 5-20 times as compared with the spring–summer period.

In contrast to uranium, all studied plants do not have physiological barriers with respect to radium for all soil concentrations observed over uranium deposits (see Fig. 1). This makes radium in plants a reliable indicator of uranium mineralization and permits one to use it as a basic biogeochemical indicator of uranium.

The results of studies of the regularities of radium absorption in plants allows us to recommend for sampling a rather large group of plant species, accumulating this element under similar conditions in approximately the same quantities. If necessary, a correction may be made according to the plant species. For trees and shrubbery it is practical to sample 2 to 8 year old cuttings of branches or stalks in which the radium content is constant. The best time to sample herbaceous plants is the fall–winter–spring period of relative inactivity when the plant contains the highest concentrations of radium, constant with time.

Of great significance are data on the stability of the relative radium contents in various species of plants growing in regions of the USSR and over the earth as a whole. They may be utilized for grouping the species according to their concentrating power and for the introduction of corrections appropriate to the species by the sampling of plants with an essentially different concentrating power for radium. Analogous data on the stability of the relative contents in other regions of the earth were obtained for zinc. This suggests the possibility that the relative content of chemical elements in plant species may be considered as one of their essential features. Having data on the relative radium contents in various plant species growing in particular conditions does not permit one to distinguish the plant concentrator of this element (see Table 2).

Of considerable interest is the dependence of the rate of radium absorption by plants on the type of uranium mineralization and the form in which radium is found in soils. The data obtained permit one to recommend the determination of radium primarily when scanning those objects in which uranium and radium in the root zone of hypergenesis penetrate into the structure of secondary uranium minerals or are absorbed by clay and organic material. In these cases the radium is intensively absorbed by plants. As a consequence of the low accessibility of radium occurring in primary minerals (particularly those such as monazite, davidite, brannerite, and uranothorite) or connected with uranium-bearing brown iron ores, prospecting for this type of uranium mineral according to radium in plants is significantly less effective. The dependence of the rate of absorption by plants of chemical elements on the form of their occurrence in rocks and ores has been established also for zinc, boron, gold [3], and other elements that are necessarily investigated by interpretation of the results of biogeochemical mapping.

The study of regularities in absorption by plants of nonradioactive elements (see Table 2) has shown that for the correct choice of objects (species and organs of plants) these elements may be used as secondary biogeochemical indicators of uranium mineralization. The 12 examined nonradioactive element-indicators are divided into two groups. Molybdenum, zinc, cadmium, copper, nickel, cobalt, selenium, and vanadium, elements of low-petalled or neutral distribution in the above-ground organs of plants, are accumulated primarily in old organs. Lead, arsenic, silver, and bismuth, elements of low-petalled distribution, are accumulated to the highest concentrations in young organs (in leaves and green stalks). In connection with this, if it is necessary to use as element-indicators of uranium a whole complex of nonradioactive elements or elements of the second group, it is recommended that one carry out a simultaneous selection

TABLE 2

Element-indicator	Typical contents in plant ash		Highest plant-concentrators		Type of distribution in above-ground plant organs
	in the presence of background contents in soils	in anomalies	in the presence of background contents in soils	in anomalies	
Radium (α-activity in %equivalent U)	10^{-11}—10^{-10} ($0,3$—$3\cdot10^{-3}$)	10^{-9}—10^{-7} (3—$300\cdot10^{-3}$)	None	None	Acropetalled
Uranium	10^{-5}	10^{-4} (up to 10^{-2})	Not known	Pine tree, rhododendron, leaf of mountain-ash, and others	"
Lead*	$0,5$—$5\cdot10^{-3}$	10^{-3}—10^{-1} (up to 1—10)	None	Larch, lepagyrea, and others	Basipetalled
Molybdenum	$0,1$—$1\cdot10^{-3}$	10^{-3}—10^{-1}	"	Ledum, alder, reed-grass, and others	Basipetalled in pres. of background, acropetalled in anom.
Arsenic	$0,1$—$1\cdot10^{-3}$	10^{-3}—10^{-1}	"	Pseudotsuga	Basipellated
Silver	10^{-5}	10^{-4}—10^{-2}	"	Rhododendron	"
Zinc	2—$50\cdot10^{-2}$	10^{-1}—5,0 (up to 20)	Rare forms of birch	Rare forms of birch	Neutral in the presence of background contents, acropetalled in anomalies
Cadmium*	10^{-5}	10^{-4}—10^{-2}	Aspen	Aspen	Neutral
Copper	3—$30\cdot10^{-3}$	10^{-2}—10^{-1}	None	Gypsophila Patrena	Neutral in the presence of background contents, basipetalled in anomalies
Nickel	1—$5\cdot10^{-3}$	10^{-3}—10^{-2} (up to 10—14)	"	Borageineous plants	Neutral
Cobalt	$0,2$—$2\cdot10^{-3}$	10^{-3}—10^{-2} (up to 0,1)	"	Not known	"
Bismuth	10^{-7}—10^{-6}	10^{-4}—10^{-2} (up to 0,1)	"	Astragalus and others	Basipetalled
Selenium*	$0,1$—$1\cdot10^{-4}$	10^{-4}—10^{-1} (up to 10)	Alyssum flax, reed-grass, common wormwood, etc.	Astragalus	Neutral
Vanadium	1—$5\cdot10^{-4}$	10^{-3}—10^{-2} (up to 0,2)	None	Not known	Basipetalled in the presence of background contents, acropetalled in anomalies

*Elements whose loss during ashing at high temperatures may exceed 50%.

of mixed samples of old and young organs of trees and shrubs. For all 12 elements, the preliminary characteristics of their relative absorption by various plant species growing in identical or similar conditions have been obtained. For element-indicators, various forms of which differ in their concentrating property only in the presence of high soil contents, those forms are selected which are anomalous concentrators of the appropriate elements (see Table 2).

Recommended Methods. Plant specimens are sampled according to a previously marked network, oriented transversely with respect to the anticipated strike of ore bodies, ore-bearing structures, and ore lithochemical aureoles. Its thickness is determined by the scale of mapping and the anticipated width of the lithochemical aureoles of the ore bodies at the mean depth of penetration of roots in the loose blanket. For detailed mappings (scale 1:2000 to 1:5000), a grid of sampling points along the profile of up to 5-10 m between points is recommended with the goal of exposure, tracking, and mapping of the narrow ore bodies (Fig. 2).

For large samples, the dominant forms are noted which absorb the basic element-indicators in approximately identical quantities and also are anomalous concentrators. In all cases, it is recommended that one give preference to perennial plants with deeply penetrating root systems. In the absence at the point of observation of the above-indicated plants, those which are available are sampled. For trees and shrubs, it is practical to carry out a simultaneous selection of mixed samples: 1) 0.2-0.5 kg of moist material in order in order to obtain 1-2 g of the ash of old organs (2-8 year old cuttings of branches, bark, or wood) of any orientation on the plant and 2) 0.1-0.2 kg in order to obtain 0.5-1.0 g of the ash of young organs (leaves, cones, green shoots) for the determination of lead, arsenic, silver, and bismuth, element-indicators of the low-petalled distribution in plants growing on ore aureoles. Herbaceous plants should be sampled mainly in the fall—winter—spring period; in their number may be included dead plants and "rags" of vegetation, maintaining the principle of standardization of sampled material.

The ashing of plant samples should be done in perforated crucibles with a capacity of 0.5-2 liters in special ovens or on woodpiles. The mass determinations of radium in plants are carried out with the help of a radiometric α-pulse method on cerium probes (RAL-1 or "Alpha-1") not less than 10 to 15 days after their ashing, when the quantity of radon and its decay daughters in the ash will be nearly that quantity in equilibrium with the radium. Nonradioactive element-indicators of uranium are determined with the help of spectral analysis. All samples with anomalous α-activity or concentration of only one of the nonradioactive element-indicators of uranium mineralization after conducting control analyses are subjected to uranium determination by the pearl-luminescence method and a complete spectral analysis repeated four times. For a small quantity of samples with anomalous α-activity (two to five samples for each indicated biogeochemical anomaly), radium and radiothorium are determined with the help of radiochemical analysis for radon and thoron. In the results obtained from the analyses, in appropriate cases corrections are introduced for the loss of certain element-indicators during storage and the ashing of the samples, and also depending on the species of plant and the sampling time for the young organs. The majority of these corrections are determined, but some of them will be evaluated as the biogeochemical prospecting work is conducted.

The interpretation of the results of biogeochemical surveys conducted to a single standard (which refers to the species and organ of plant and the time of sampling), and also of the results of geochemical, geophysical, and geological work, is utilized in the calculation of data on physiological barriers to absorption of the element-indicators of uranium, forming a complex biogeochemical anomaly. Such a method allows one to give an approximate quantitative value for the anomalous concentrations of these elements in litho- or hydrochemical aureoles of the dispersion. As objective criteria for the interpretation of biogeochemical anomalies, it is recommended that one use the following: 1) the intensity of α-anomalies; 2) data on their uranium or thorium nature (on the basis of radiochemical analyses and uranium determination); 3) area of the anomalies; 4) productivity (determined according to the method given by Solovov [4] for metallometric anomalies); 5) a complex of elements characterized by anomalous concentrations; 6) correlations among nonradioactive elements and between radium and nonradioactive elements in plants; 7) possible correlations among these elements in litho- and hydrochemical aureoles (determined according to data on physiological barriers, plant-soil and plant-water coefficients of element-indicators forming the biogeochemical anomalies). As a result of the interpretation of biogeochemical anomalies, they can be divided into groups of varying degrees of promise, including those that show promise of a primary and secondary nature and those basically unpromising.

In connection with the fact that, in addition to radioactive elements in plants, the determination of a rather large complex of elements accompanying uranium mineralization is anticipated, the recommended biogeochemical prospecting technique permits the indication not only of uranium but also of other ore deposits.

Effectiveness of the Biogeochemical Method of Uranium Prospecting under Various Conditions. The effectiveness of biogeochemical prospecting is influenced by the choice of basic element-indicators, the mineralogical characteristics of the deposit, the types of zones of oxidation and crusts of weathering, the deposition depth of the uranium ores, their litho- and hydrochemical aureoles, and also their accessibility to the roots of plants.

Biogeochemical prospecting for uranium deposits is most effective when the following conditions are observed: 1) the utilization of radium and not uranium as the basic element-indicator and of uranium and the complex of nonradioactive element-indicators in plants as secondary indicators; 2) prospecting for deposits the minerals of which are readily soluble and accessible to plants (such as pitchblende, uranite, and micaceous but not monazite, brannerite, and rare-earth mineralizations); 3) prospecting for buried deposits and ore bodies overlain by relatively thin formations (of the order of 1-10 m thick, but sometimes 10-30 m and more); and 4) prospecting for objects with weakened or leached out lithochemical aureoles of dispersion near the ground surface (see Fig. 2).

The basic advantages of the biogeochemical method are as follows: its great profundity in comparison with simple prospecting methods (radiometry, uranometry, and metallometry of the ground surface, emanation surveys) and its significantly lower cost in comparison with detailed radiometric, uranometric, and metallometric surveys. Therefore, the best candidates for the wide application of biogeochemical prospecting are forested unfrozen regions in which leached out lithochemical aureoles near the ground surface are uncommon, and arid regions in which some perennial plants have very deeply penetrating root systems (up to 10-20 m, and sometimes up to 30-70 m).

In a forested unfrozen zone the biogeochemical method finds practical application in prospecting for ore bodies and deposits having sharply leached out and thinly buried (up to 5-20 m) lithochemical aureoles of dispersion. In an arid zone it finds practical application only in areas overlain by a cover which includes allochthone formations of relatively small thickness (from 1-3 m to 10-30 m, and sometimes even more). The practice of biogeochemical prospecting for uranium in the USA [5] and for polymetallic ores in Kazakhstan [6] attests to the possibility of finding deposits in the presence of a thickness of loose cover exceeding the maximum root depth by 10 to 40 m and reaching 40 to 60 m. This fact, in all likelihood, is connected with the presence of a contact between the plants and the lithochemical aureoles of ore bodies via the upper water-bearing horizon and its capillary border.

CONCLUSIONS

Biogeochemical prospecting for uranium deposits is still little used in practice and can be further refined. Such refinements should include the following:

1) Development of methods of car and aircraft biogeochemical mapping, during the conduct of which the sampling and transportation of samples of plants will be conducted by means of trucks and helicopters;
2) Development of aerial biogeochemical methods, based on determinations of radium and nonradioactive element-indicators of uranium given off from plants into the air in conjunction with their transpiration of water;
3) Development of aerial methods of radium determination in plants with the help of aerial emanation mapping, based on the registration of radon (or its decay daughters) emanated from the plants;
4) Development of faster field methods for radium determinations in plants without ashing or even without sampling;
5) Development of special high-yield automatic ovens for ashing plant samples;
6) Development of more productive methods and instrumentation for α-analysis of plant samples, with automated analysis.

LITERATURE CITED

1. A. L. Kovalevskii, Izv. Sibirsk. Otd. Akad. Nauk SSSR, No. 4, 108 (1962).
2. A. L. Kovalevskii, Natural Radioactive Elements in Siberian Plants [in Russian], Buryatskoe Kn. Izd-vo, Ulan-Ude (1966).
3. A. L. Kovalevskii, in: Mineral Petrography of the Trans-Baikal Region [in Russian], Buryatskoe Kn. Izd-vo, Ulan-Ude (1968), pp. 148-153.
4. A. P. Solovov, The Theory and Practice of Metallometric Surveys [in Russian], Izd-vo Akad. Nauk Kaz. SSR, Alma-Ata (1959).
5. H. Cannon, U.S. Geol. Surv. Bull., No. 1176 (1964).
6. V. O. Getmanchuk et al., in: Biogeochemical Prospecting for Ore Deposits [in Russian], Buryatskii Filial Sibirsk. Otd. Akad. Nauk SSSR, Ulan-Ude (1969), pp. 59-65.

COMPARISON OF γ-RAY AND NEUTRON PERSONNEL DOSIMETERS AT CRITICAL ASSEMBLIES

I. B. Keirim-Markus, S. N. Kraitor,
V. V. Kuz'min, G. M. Obaturov,
V. I. Popov, V. V. Rybanov,
A. D. Sokolov, Yu. K. Chumbarov,
and V. A. Shalin

UDC 539.12.08

Considerable attention has been devoted recently to the development of personnel dosimeters for neutrons. The construction of mica track dosimeters for neutrons (MTD for short) employing the fissionable materials Np^{237} (MTD-Np-7), U^{238} (MTD-U-8), and U_{nat} (MTD-U_{nat}) was proposed [1]. A neutron dosimeter consisting of U^{235} and Np^{237} behind a filter of 0.1 g/cm² B^{10} (MTD-Np-B) was also proposed [2] in which the ratio of the isotopes and the filter thickness were chosen in such a way that the dosimeter efficiency reproduced kerma dependence on neutron energy. A thermoluminescent personnel dosimeter using CaS was also described [3].

This paper gives the results of comparative measurements of the personnel dosimeters mentioned. At the same time, γ-ray doses were measured with IFK-2.3 personnel dosimeters [4], and with IKS [5] and LiF [6] thermoluminescent dosimeters. In some cases, sets of tissue-equivalent, low-efficiency Geiger counters were used, which made it possible to determine the LET spectrum for the neutron and γ radiation [7], as well as sets of threshold detectors containing fissile isotopes and silicate glass in order to determine the neutron spectrum and dose composition [8].

Dosimeter irradiation was performed at the location of critical assemblies (type BR-1 with beryllium and copper reflectors [9]), and of an assembly with a graphite reflector, at 4-5 points located at different distances R from the center of the core.

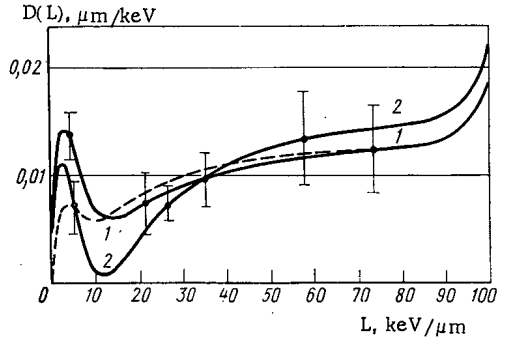

Fig. 1. LET spectra of neutron kerma for assembly 1. Curve 1 and dashed curve are measurements at location 1; curve 2 shows measurements at location 4 (the dashed curve shows measurements with greater statistical accuracy).

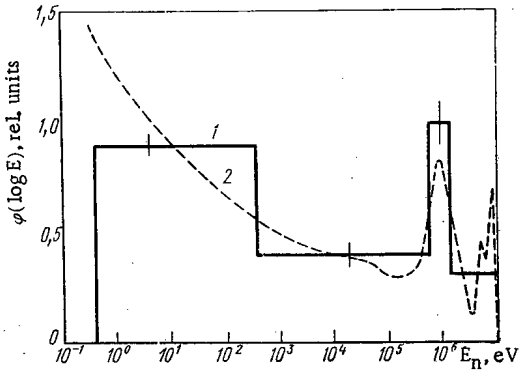

Fig. 2. Neutron spectrum at assembly 2: 1) experimental; 2) calculated.

Translated from Atomnaya Energiya, Vol. 33, No. 1, pp. 563-566, July, 1972. Original article submitted August 20, 1971.

TABLE 1

Assembly	Location	R, cm	Neutron kerma, rad						γ-Ray exposure dose, R		
			thermal	0.4 eV–MeV	1.5–10 MeV	0.4 eV–10 MeV	25 keV–10 MeV	25 keV–10 MeV	IFK	IFK	LiF
			$MTD-U_{nat}$	MTD-Np-7	MTD-U-8	MTD-Np-B	CaS	TEGC			
1	1	55	0,372	17,0	10,7	18,5	16,4	14,8	6,44	7,3	6,4
	2	55	0,332	18,3	10,9	19,7	17,2	15,6	6,4	6,24	6,2
	3	108	0,174	5,54	4,44	7,2	3,52	5,4	2,54	2,7	2,6
	4	145	0,148	3,10	—	3,9	1,72	—	2,00	1,64	2,00
	5	240	0,114	2,76	2,04	1,83	—	—	1,06	1,10	1,62
2	1	86	0,64	44,6	15,55	48,0	58	24,8	7,5	7,3	8,0
	2	125	0,57	22,9	10,15	26,4	26,9	—	4,8	4,2	4,2
	3	208	0,47	9,16	3,83	11,1	11,4	—	3,0	2,9	3,5
	4	220	0,43	8,3	—	—	—	4,36	—	2,75	—
	5	281	0,42	6,28	2,72	6,80	6,42	—	2,3	2,4	—
3	1	112	7,6	1,93	1,12	—	—	—	—	33,3	—
	2	137	7,2	1,49	0,72	—	—	—	—	30,3	—
	3	219	4,0	0,64	0,31	0,65	—	—	—	14,4	—
	4	274	2,65	0,41	0,26	0,43	—	—	—	11,8	—

TABLE 2

Energy interval	Neutron flux, %	Neutron kerma	
		%	rad
1.4–10 MeV	6	39	0,97
0.56–1.4 MeV	9	40	1,00
400 eV–0.56 MeV	28	21	0,52
0.4–400 eV	57	0	0

Calculations of neutron kerma from readings of the dosimeters containing U_{nat}, U^{238}, and Np^{237} was carried out in accordance with the formulas given in [1] with the average dose sensitivity for the assemblies with beryllium (assembly 1) and copper (assembly 2) reflectors assumed to be the same as that for the Godiva assembly; for the graphite assembly (assembly 3), the dose sensitivity was assumed the same as that for fission neutrons outside a carbon shield. The average sensitivity calculated in [2] was used for the dosimeter consisting of Np^{237} and a filter of 0.1 g/cm^2 B^{10}; this was assumed to be the same for all spectra. Etching of the track detectors (mica and silicate glass) was done in hydrofluoric acid, and tracks were counted with BMI-1 and MBI-9 microscopes.

In determining neutron kerma by means of the CaS dosimeters, the gamma component, determined from the reading of an LiF dosimeter depleted in Li^6, was subtracted from the total light sum. Measurement of the light sum was made with a laboratory instrument [10]. The γ-ray doses recorded by the thermoluminescent dosimeters were measured on an IKS-A instrument [5]; those obtained with IFK-2.3 dosimeters were measured on a DFÉ-10 instrument.

The set of tissue-equivalent, low-efficiency Geiger counters (TEGC) consisted of three counters at pressures of 6, 15, and 40 mm Hg for determining the LET spectra of particles emerging from the tissue-equivalent walls of the counters and three similar counters with graphite walls for determining the contribution from proton recoils and for calculations of neutron kerma, average LET value, and quality factor [7].

The threshold detectors consisted of U^{235} + Cd, U^{235} + 1 g/cm^2 B^{10}, Np^{237}, U^{238}, and S^{32}. The spectrometric characteristics of this set have been described [8]; with it, one can determine neutron fluxes in the following energy intervals: 0.4-400 eV, 400 eV-0.56 MeV, 0.56-1.4 MeV, 1.4-2.8 MeV, and above 2.8 MeV. A method for calculating kerma from the measured neutron spectrum has been reported [11].

Calibration of the dosimetry systems used was carried out under laboratory conditions using Po-Be, Pu-Be, and Co^{60} sources; the error was no worse than 20%.

The results of comparative measurements of neutron kerma and γ-ray exposure dose are given in Table 1, which indicates that the readings of the various personnel dosimeters for neutrons and γ-rays are reasonably close and that discrepancies between them are no more than 30%. At those points where the measurements were made with sufficient statistical accuracy (neutron kerma greater than 10 rad), the

disagreement was no more than 15%. Readings of the TEGC, on the whole, were somewhat lower than the readings of the track dosimeters because the counters determine neutron kerma only for proton recoils and do not take into account heavy nuclei. The disagreement for assembly 2 is considerable (as much as 45%) and is possibly associated with inaccurate monitoring while the measurements were made.

The readings of the CaS thermoluminescent dosimeters are also somewhat low because these dosimeters are insensitive to neutrons with energies below 25 keV.

The data obtained make it possible to give the dosimetric characteristic of the radiation from the critical assemblies investigated. To begin with, the neutron dose compositions are significantly different. The fast neutron contribution to the total kerma is 60-80% for assembly 1, is only 35-40% for assembly 2 and a total of 7-12% for assembly 3, and is reduced somewhat with separation from the core because of the increase in the flux of scattered neutrons. This is also confirmed for assembly 1 by measured LET spectra (Fig. 1) which indicate an increase in the flux of charged particles with large values of linear energy transfer at large distances from the assembly. Calculated average LET values based on these spectra also point to softening of the neutron spectrum with increasing distance from the critical assembly.

The neutron spectrum φ (log E) for assembly 3, measured at 0.5 m from the core, is given by the histogram in Fig. 2. Data from the activation set was not analyzed because the irradiation level was low. As is evident, neutrons with energies below 0.56 MeV make a significant contribution to the flux, which is characteristic of fission neutrons outside carbon shielding; such a spectrum, taken from [12], is shown in Fig. 2 (curve 2). The neutron dose composition calculated from the spectrum is shown in Table 2. It is clear that the contribution of neutrons with energies above 1.4 MeV to the kerma of epithermal neutrons is 39%. This is somewhat lower than follows from the data from detectors MTD-Np-7 and MTD-U-8 (58%) and may be caused by errors in calibration with the various neutron sources and by the poor statistical accuracy of the measurements. At the same time, the kerma values determined by both methods agree within 11% since the average dose sensitivity calculated from the histogram in Fig. 2 is practically the same as that assumed in the calculation of kerma.

Softening of the neutron spectrum by the carbon reflector leads to a considerable rise in the contribution of thermal neutrons to the total kerma for assembly 3. Where the contribution is 1-5% at most for assemblies 1 and 2, it is predominant and reaches 84% for assembly 3 (see Table 1).

The ratio between kerma and γ-ray dose is greatly different for assemblies 1-3. For the assembly with a beryllium reflector, this ratio is 1.6-2.6, for the assembly with a copper reflector it is 3-6.7, and for the assembly with a graphite reflector is amounts to 0.25-0.32. Consequently, in the neighborhood of the last assembly, the determining dosimetric factor is not neutrons but γ rays because a significant portion of the fast neutrons is moderated to thermals in the carbon and the specific dose of the latter is small.

In conclusion, the authors are grateful for assistance with the experimental work extended by V. I. Golubev, A. V. Zvonarev, Yu. F. Koleganov, K. K. Koshaeva, B. G. Dubovskii, N. A. Baimugin, L. A. Geraseva, and P. G. Dushin.

LITERATURE CITED

1. G. M. Obaturov and Yu. K. Chumbarov, Collected Papers on Problems of Dosimetry and Radiometry of Ionizing Radiation [in Russian], Atomizdat, Moscow (1972).
2. I. A. Bochvar et al., Handling of Radiation Accidents, Proc. Symposium, IAEA, Vienna (1969), p. 235.
3. V. A. Kazanskaya et al., in: Nuclear Instrument Construction [in Russian], No. 13, Atomizdat, Moscow (1970), p. 213.
4. V. F. Kozlov, Photographic Dosimetry of Ionizing Radiation [in Russian], Atomizdat, Moscow (1964).
5. A. I. Bochvar et al., Pribory i Tekh. Éksperim., No. 6, 66 (1969).
6. I. Cameron, XI International Congress of Radiology, Paper N149, Rome (1965).
7. I. B. Keirim-Markus and V. I. Popov, in: Problems of Dosimetry and Radiation Protection [in Russian], No. 10, Atomizdat, Moscow (1969), p. 14.
8. K. K. Koshaeva et al., JINR Preprint P3-5421 (1970).
9. A. I. Leipunskii et al., At. Energ., 5, 277 (1958).
10. V. V. Kuz'min et al., At. Energ. 22, 482 (1967).
11. K. K. Koshaeva and S. N. Kraitor, in: Metrology of Neutron Radiation at Reactors and Accelerators [in Russian], VNIIFTRI, Moscow (1971), p. 165.
12. I. A. Bochvar et al., Neutron Monitoring, Proc. Symposium, IAEA, Vienna (1967), p. 459.

INSTABILITY OF AXIAL OSCILLATIONS IN AN ELECTRON RING ACCELERATOR

P. R. Zenkevich, D. G. Koshkarev, and É. A. Perel'shtein

UDC 621.384.639

The stability of a system of two annular beams consisting of two different types of particles has recently received close attention because of the development of the method of collective ion acceleration [1]. The possibilities of the method (the energy gain per unit length and the number of ions which can be accelerated) are governed by the ring parameters, which must be maintained during the acceleration.

In a stability analysis it is customary to distinguish between azimuthal and transverse (axial and radial) branches of coherent oscillations. In this paper we examine the stability of electron–ion rings with respect to axial "wriggles" without any change in the shape of the transverse cross section; i.e., we examine the axial dipole instability (or "snake"), which is one of the most dangerous of the transverse oscillations.

In previous studies [2-4] of this problem, the intrinsic fields were neglected; in particular, no account was taken of the effect of the field radiated by the oscillating electron ring on the electron motion (the electron–electron interaction). The question therefore arose of whether the energy loss of the ring due to coherent radiation could suppress the instability of the two-beam system. A negative answer was found to this question in [5] for the particular case of a single-component electron ring in a resonator.

Here we will take up the problem of the dipole oscillations of an electron ring under different conditions (in free space and in a waveguide with cuts). It turns out that under these conditions the intrinsic field leads to a coherent instability.

Momentum dispersion, which supresses this instability, can be reduced by external-field Bennett focusing. Analysis of the oscillations of electron–ion rings has shown that the effects due to the coherent-radiation field do not suppress dipole resonances.

Dipole Oscillations of an Electron Ring in Free Space. We consider an electron ring with a circular cross section; R is the radius of the central orbit of the ring, a is the radius of the transverse cross section, the z axis is perpendicular to the median plane passing through the central orbit, r is the distance from the ring axis, and φ is the azimuthal angle. Then the equation for $\overline{z}_e$, the deviation of the local center of gravity of the beam from the median plane, is

$$\frac{d^2\overline{z}_e}{dt^2}+\Omega_e^2\overline{z}_e=\frac{e}{m\gamma}[E_z-\beta H_r], \tag{1}$$

where $d/dt = \partial/\partial t + \Omega\,\partial/\partial\varphi$; Ω is the electron-revolution frequency, Ω_e^2 is the frequency for free electron oscillations in the axial direction, E_z and H_r are the fields due to the nonequilibrium increments in the charges and currents, and $\gamma = [1-\beta^2]^{-1/2}$.

To analyze Eq. (1), we write Ω_e^2 as

$$\Omega_e^2=\lambda^2\Omega^2+\Omega_c^2, \tag{2}$$

where $\lambda\Omega$ is the frequency of oscillations due to the external focusing field, and Ω_c^2 is the correction due to the intrinsic field of the steady-state beam.

Substituting $\overline{z}_e = z_0 \exp[i(n\varphi-\omega t)]$, into Eq. (1), we find a dispersion relation for the oscillations of the electron beam:

Translated from Atomnaya Energiya, Vol. 33, No. 1, pp. 567-572, July, 1972. Original article submitted August 20, 1971; revision submitted December 14, 1971.

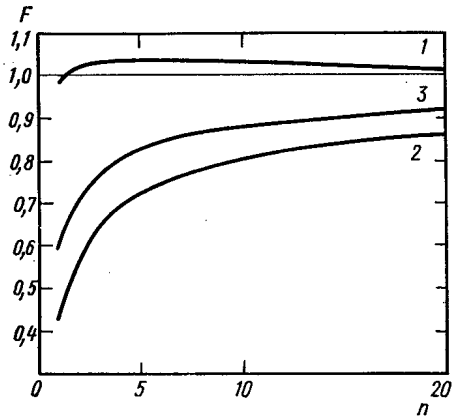

Fig. 1. Dependences of the function F, divided by their asymptotic values, on n. 1) $0.9\,n^{-2/3}F_1$; 2) $2.5\,n^{-1/3}F_2$; 3) $1.41\,n^{-2/3}F_3$.

$$\lambda^2-(x-n)^2=U_n+iV_n,$$

$$\text{where } U_n=\frac{\Omega_c^2}{\Omega^2}-\mathrm{Re}\,\frac{1}{\Omega^2 z_0}\cdot\frac{e(E_z-\beta H_z)}{m\gamma}; \tag{3}$$

$$V_n=\mathrm{Im}\frac{1}{\Omega^2 z_0}\cdot\frac{e(E_z-\beta H_r)}{m\gamma};\quad x=\frac{\omega}{\Omega}. \tag{4}$$

The "quasistatic"* component U_n on the right side of dispersion relation (3) arises because of the field components which are $\pi/2$ out of phase with respect to $\overline{z_e}$; the radiation component V_n, in phase with $\overline{z_e}$ is due to coherent radiation.

It is shown in the Appendix that for an electron beam in free space we can write

$$U_n\approx\frac{\nu_e}{\gamma}(0.6+\ln 4n)\quad\text{for}\quad n\ll\frac{R}{a}; \tag{5}$$

$$V_n=\frac{\nu_e}{\gamma}[F_1-2F_2(x-n)]\approx\frac{\nu_e}{\gamma}[1.1n^{2/3}-0.8n^{1/3}(x-n)], \tag{6}$$

where $\nu_e = N_e r_e/2\pi R$, r_e is the classical radius of the electron, and N_e is the total number of electrons in the ring.

The solution of Eq. (3) is

$$x=n+i\frac{\nu_e}{\gamma}F_2\pm\sqrt{\lambda^2-U_n-i\frac{\nu_e}{\gamma}F_1}. \tag{7}$$

Taking into account Landau damping, we find the threshold dispersion for the axial coherent instability:

$$\left|\frac{\Delta(n\Omega-\Omega_e)}{\Omega}\right|\geqslant\mathrm{Im}x. \tag{8}$$

Let us compare this threshold value with that for the azimuthal radiation instability in free space [6]:

$$\frac{\Delta(n\Omega)}{\Omega}\geqslant\sqrt{\frac{\nu_e}{\gamma}}n^{1/3}\left|\frac{\partial(\ln\Omega)}{\partial(\ln p)}\right|, \tag{9}$$

where p is the azimuthal momentum of the electrons.

If the external focusing is chosen to satisfy the condition for stability of one-particle oscillations of the electrons ($\lambda^2 > \nu_e \ln 8R/a$), we have $\lambda^2 > U_n$, and the required dispersion is given by (9). If, on the other hand, we have $\lambda = 0$, condition (8) becomes more stringent than (9).

During the acceleration of electron–ion rings, however, it is very difficult to achieve efficient external focusing in the axial direction. The only real focusing methods are apparently self-focusing of the electrons by means of image forces or focusing by ions.

Dipole Oscillations of an Electron Beam in a Waveguide with Longitudinal Cuts. We consider the waveguide with longitudinal cuts (a "squirrel cage") which has been proposed for the self-focusing of an electron beam [7]. The walls of such a waveguide constitute a diffraction grating transparent to E waves but opaque to H waves. In a squirrel cage the H waves propagate as in free space; small-n E waves are not excited, since the condition $R/b \approx 0.6$–0.8, where b is the waveguide radius, must be satisfied for self-focusing to occur. In calculating U_n we can thus assume that the forces acting on the beam are the sum of forces acting in free space and the image forces. Calculating these image forces in the quasistatic approximation, we find near the wall (for $b-R/b \ll 1$) that U_n is given approximately by

$$U_n\approx\frac{\nu_e}{\gamma}\left[0.6+\ln(4n)-\frac{n^2}{2}\ln\frac{4R}{b-R}\right]. \tag{10}$$

For V_n (see the Appendix) we have

$$V_n\approx\frac{\nu_e}{\gamma}F_3(x,\ n)\approx\frac{\nu_e}{\gamma}0.7n^{2/3}. \tag{11}$$

The term proportional to n^2 in Eq. (10) describes quasistatic focusing which appears during wriggles of the electon ring parallel to the reflecting surface.

From Eq. (10) we see that for quasistatic focusing of the most dangerous mode, n = 1, the wall must be approached very closely ($R/b > 0.95$). If this condition does not hold, it follows from Eqs. (7), (10), and

*Here "quasistatic" is a relative term, since U_n is also affected by the radiation field.

(11) with $\lambda = 0$ that the instability increment in the squirrel cage receives contributions from both quasistatic and radiation terms.

Dipole Oscillations in Electron–Ion Rings. When ions are present, we must supplement Eq. (1) with an equation describing the oscillations of the local center of gravity of the ions [2-4]:

$$\frac{d^2\bar{z}_i}{dt^2} + \Omega_i^2 \bar{z}_i = \Omega_i^2 \bar{z}_e, \tag{12}$$

where Ω_i is the frequency at which the ions oscillate in the field of the electrons. Assuming $\bar{z}_i$ and $\bar{z}_e$ to be proportional to $\exp[i(n\varphi - \omega t)]$, we find the dispersion relation

$$(Q_i^2 - x^2)[Q_e^2 - (x-n)^2 - U_n - iV_n] = Q_i^2 Q_i^2, \tag{13}$$

where $Q_i = \Omega_i/\Omega$ is the betatron oscillation frequency of the ions, Q_i^2 is the square of the betatron frequency of the electronic oscillations in the field of the ions, and $Q_e^2 = \lambda^2 + Q_i^2$.

In analyzing Eq. (13) it is convenient to treat separately the effects due to U_n and V_n. Assuming $V_n = 0$, we find from Eq. (13) a dispersion relation for the oscillations for electron–ion rings in quasistatic fields:

$$(Q_i^2 - x^2)[\tilde{Q}_e^2 - (x-n)^2] = \varphi(x) = Q_i^2 Q_i^2, \tag{14}$$

where $\tilde{Q}_e^2 = Q_e^2 - U_n$. This equation has the same form as the standard dispersion relation associated with electron–ion oscillations. Analysis of Eq. (14) shows that with $U_n < 0$ the instability regions found in [4] expand. We can neglect the effect of the quasistatic components of the electron–electron forces if there is a sufficient number of ions and if

$$Q_e^2 \gg \frac{\nu_e}{\gamma}. \tag{15}$$

If we add a radiation term to Eq. (14), the entire working range of frequencies Q_e and Q_i (for free space and for a squirrel cage) becomes an instability region. The increment for this radiation instability can be evaluated on the basis of perturbation theory. Letting x_0 be the root of Eq. (14), we find that Δx, the correction to x_0 due to the radiation field, is

$$\Delta x \approx \frac{iV(x_0, n)(Q_i^2 - x_0^2)}{\left(\frac{d\varphi}{dx}\right)_{x=x_0}}.$$

This expression holds under the condition $|\Delta x/x_0| \ll 1$, i.e., sufficiently far from the boundaries of the stability region corresponding to Eq. (14). Analysis of (16) shows that when there is a slight coupling of electron–ion oscillations, the ions reduce the increment for the radiation instability. In this region the ions can be thought of as causing an external focusing, and the instability increment can be evaluated from Eq. (7) after λ is replaced by Q_e.

Oscillations within the instability region for the resonant coupling of electron–ion oscillations remain unstable when coherent radiation is taken into account, although the increments change slightly. At the center of the resonant band for the electron–ion instability (at $n - Q_e = Q_i$) the resultant increment is approximately equal to the sum of the radiation-instability and resonant-coupling increments found separately.

We have neglected Landau damping; however, in the region of most interest here, the region of stability with respect to resonant coupling, the radiation instability of the beam can be suppressed by choosing an electron-beam dispersion above the threshold [see (8)].

We note in conclusion that the mechanism for the radiation instability is apparently related to energy transfer from azimuthal motion to axial motion due to the magnetic field produced by the azimuthal components of the nonsteady-state current. This instability arises at frequencies near $(n - Q_e)\,\Omega$, which correspond to waves displaying the anomalous Doppler effect. At the center of the resonant band for the two-beam instability the radiation-instability increment consists of the increment corresponding to resonant coupling of electron–ion oscillations, since the maximum increment for the two-beam instability also corresponds to natural frequencies near $(n - Q)\,\Omega$.

The authors thank A. B. Kuznetsov and L. A. Yudin for useful comments.

APPENDIX

We consider the force exerted on the center of gravity of the electron beam due to the nonequilibrium charge and currents which arise during dipole oscillations. Since this force depends weakly on the

steady-state distribution, we adopt the simplest model, that of a beam having an infinitesimally small radial dimension and a constant surface charge density. We assume that during the dipole oscillations the beam shifts as a unit without any change in the density distribution (this is a valid assumption if the oscillation wavelength is much greater than the transverse beam dimension and if the frequency dispersion of the oscillations of particles is slight). Then using this model, we find the following expressions for ρ and j, the nonequilibrium increments in the particle density and current:

$$\left.\begin{aligned}\rho &= \frac{eN_e z_0}{4\pi ar}\left[\delta(z-a)-\delta(z+a)\right]\\ &\quad\times\delta(r-R)\exp\left[i(n\varphi-\omega t)\right];\\ \dot{\gamma}_\varphi &= \Omega r\rho;\ \dot{\gamma}_z = i(\omega-n\Omega)\int\rho\,dz.\end{aligned}\right\} \tag{A-1}$$

We first consider the case in which the beam is in a cylindrical waveguide of radius b. In such a waveguide the radiation field is a superposition of the quasistatic field and the E and H waves. Expanding the charge and currents in terms of the orthonormal functions for an empty waveguide [8], we find the following expressions for the field components at z = 0:

$$\left.\begin{aligned}E_z^{\mathrm{I}} &= -\frac{eN_e z_0}{a}\sum_{s=1}^{\infty}A_{sn}I_n^2(k_sR)\,e^{-k_sa};\\ H_r^{\mathrm{I}} &= 0;\end{aligned}\right\} \tag{A-2}$$

$$E_z^{\mathrm{II}} = -\frac{eN_e z_0}{a}\sum_{s=1}^{\infty}A_{sn}I_n^2(k_sR)\left[e^{i\sqrt{\frac{\omega^2}{c^2}-k_s^2}a}-e^{-k_sa}-\frac{\omega(\omega-n\Omega)}{c^2\left(\frac{\omega}{c^2}-k_s^2\right)}e^{i\sqrt{\frac{\omega^2}{c^2}-k_s^2}a}\right]; \tag{A-3}$$

$$H_r^{\mathrm{II}} = \frac{eN_e z_0}{a}\sum_{s=1}^{\infty}A_{sn}I_n^2(k_sR)\,\frac{\frac{\omega}{c}n}{k_s^2R}\left[e^{i\sqrt{\frac{\omega^2}{c^2}-k_s^2}a}-\frac{\omega(\omega-n\Omega)}{c^2\left(\frac{\omega^2}{c^2}-k_s^2\right)}e^{i\sqrt{\frac{\omega^2}{c^2}-k_s^2}a}\right]; \tag{A-4}$$

$$\left.\begin{aligned}H_r^{\mathrm{III}} &= -\frac{eN_e z_0}{a}\beta\sum_{p=1}^{\infty}B_{pn}(I_n')^2(k_pR)\,e^{i\sqrt{\frac{\omega^2}{c^2}-k_s^2}a};\\ E_z^{\mathrm{III}} &= 0;\\ A_{sn} &= 2b^{-2}I_{n+1}^{-2}(k_sb);\ B_{pn} = 2b^{-2}\frac{I_n^{-2}(k_pb)}{1-\frac{n^2}{(k_pb)^2}}.\end{aligned}\right\} \tag{A-5}$$

Here I_n and I_n' are a Bessel function and its derivative, respectively, $I_n(k_sb) = I_n'(k_pb) = 0$, $\beta = \Omega R/c$, superscript "I" corresponds to the quasistatic field, "II" corresponds to E waves, "III" corresponds to H waves, and the factor $\exp[i(n\varphi-\omega t)]$ is omitted.

The expressions for fields in free space can be found from Eqs. (A-2)-(A-4) by going to the limit $b\to\infty$ and using

$$\sum_s A_{sn} = \sum_p B_{np} \to \int_0^{\infty} k\,dk. \tag{A-6}$$

Substituting Eqs. (A-2)-(A-4) into Eq. (1), and using the standard method to evaluate the integrals [9], we find with an account of Eq. (A-6) the following expressions for U_n and V_n in free space:

$$U_n \approx \frac{\nu_e}{\gamma}\left\{0.6+\ln 4n-\left(\frac{n\alpha}{2}\right)^2\ln\frac{8}{\alpha}+\frac{\alpha^2}{4}\left[\frac{n^2}{2}+\left(n^2-\frac{1}{4}\right)(0.6+\ln 4n)-\frac{(n-1)(3n+1)}{2}\right]\right\}; \tag{A-7}$$

$$V_n = \frac{\nu_e}{\gamma}\left[F_1(x,\,n)-2F_2(x,\,n)(x-n)\right], \tag{A-8}$$

where

$$F_1(x,\,n) = 2\pi xn^2\int_0^1 dt\sqrt{1-t^2}\left[\frac{1-t^2}{t^2}I_n^2(\beta xt)+\frac{\beta^2x^2}{n^2}(I_n')^2(\beta xt)\right] = 2\pi xn^2\left\{\frac{1+3\beta^2\left(\frac{x}{n}\right)^2}{8\beta^2x^2}\left[I_{2n}(2\beta x)-I\right]\right. \tag{A-9}$$

$$\left.+\frac{1-\beta^2\frac{x^2}{n^2}}{2}I+\frac{1-\beta^2\left(\frac{x}{n}\right)^2}{4\beta x}I_{2n}'(2\beta x)\right\};$$

$$F_2(x,\,n) = 2\pi x^2\int_0^1 t\sqrt{1-t^2}\,I_n^2(\beta xt)\,dt = \frac{\pi^2}{\beta^2}\left[\frac{\beta x}{2}I_{2n}'(2\beta x)-\frac{I_{2n}(2\beta x)}{4}+\left(\beta^2x^2-n^2+\frac{1}{4}\right)I\right], \tag{A-10}$$

where

$$\alpha = \frac{a}{R}\ ;\ I = \int_0^1 I_{2n}(2\beta x u)\, du.$$

In the ultrarelativistic case and for large n, for which we have

$$\max(1;\ 2Q_e) \ll n^{1/3} \ll \gamma,$$

Eqs. (A-9) and (A-10) can be replaced by their asymptotic limits

$$F_1 \approx 1.1 n^{2/3};\quad F_2 = 0.4 n^{1/3}. \tag{A-11}$$

Figure 1 shows computer-calculated functions F_1 and F_2 divided by their asymptotic values (for $\beta = 1$, and $x = n$).

For separate case of the radiation field due to H waves (this case corresponds to motion in a waveguide with longitudinal cuts) we find

$$V_n = \frac{\nu_e}{\gamma} F_3(x,\ n) = \frac{\nu_e}{\gamma} 2\pi\beta^2 n^3 \int_0^1 t\sqrt{1-t^2}\, I_n^2(nt)\, dt. \tag{A-12}$$

Figure 1 also shows the function F_3, divided by its asymptotic value ($0.7n^{2/3}$).

LITERATURE CITED

1. V. Veksler et al., Collective Linear Acceleration of Ions. Proceedings of the VI International Conference on High Energy Accelerators, Cambridge, 1967, p. 289.
2. G. I. Budker, At. Énerg., 5, 9 (1956).
3. B. V. Chirikov, At. Énerg., 19, 239 (1965).
4. D. Koshkarev and P. Zenkevich, Particle Accelerators, 3, 1 (1972).
5. I. N. Ivanov and V. G. Makhan'kov, JINR Preprint P9-3475-2, Joint Institute for Nuclear Research, Dubna (1967).
6. A. G. Bonch-Osmolovskii, É. A. Perel'shtein, and V. N. Tsytovich, Proceedings of the VII International Conference on Charged-Particle Accelerators [in Russian], Vol. II, Erevan (1970), p. 574.
7. G. V. Dobilov et al., JINR Preprint P9-4737 Joint Institute for Nuclear Research, Dubna (1969).
8. P. M. Morse and H. Feshbach, Methods of Theoretical Physics, McGraw-Hill, New York (1953).
9. D. Ivanenko and A. Sokolov, Classical Theory of Fields [in Russian], Gostekhizdat, Moscow (1951).

WEAK SHOCK WAVES IN BOILING WATER AND GAS – LIQUID SUSPENSIONS

Yu. P. Neshchimenko and L. Ya. Suvorov

UDC 532.529

The working element of a boiling thermal reactor is a two-phase mixture in which nonstationary processes like shock waves can occur. Reported here are results of modeling the propagation of weak shock waves in boiling water, water with steam and air bubbles, water with air or helium bubbles, and also in glycerin with air bubbles.

Measurements were made on the velocity of the shock wave and density jump as functions of the shock strength and the initial density and composition of the mixture. The structure of the shock transition was studied. The dispersed vapor–gas–liquid mixture was regarded as continuous and moving with uniform velocity. The equation for the adiabatic curve of the shock wave is written approximately as

$$V_0 - V = xV_{01}\frac{p - p_0}{p} + y(V_{02} - V_3),$$

where x and y are the parts by mass of gas and vapor in the mixture; V_{01}, V_{02}, and V_3 are the specific volumes of gas, vapor and liquid in the original mixture; and V and p are the specific volume and pressure behind the shock front respectively.

This equation is a generalization of the equation* for the case of phase transitions. Under the action of the shock wave condensation of the vapor bubbles and fractionation of the gas bubbles occur. The width of the wave in boiling water depends on the condensation rate of the steam. The structure of the shock front in a gas–liquid suspension depends on the mechanical and thermal interactions of the components. The rate of heat exchange depended in an essential way on the properties of the gas. Properties of the liquid component had only a slight influence on the shock wave parameters.

When a shock wave is reflected from a gas–mixture interface, after impinging on it from the gas side, the interface can be regarded as undeformed. Corrections for the compressibility of the mixture and the scattering of the wave from the rough interface did not fall outside the limits of accuracy of the measurements. When a shock wave, propagating in a mixture, is reflected from a rigid wall the pressure jump across its front is approximately doubled.

*I. Campbell and A. S. Pitcher, Proc. Roy. Soc., A243, No. 1235, 534 (1958).

Translated from Atomnaya Energiya, Vol. 33, No. 1, p. 573, July, 1972. Original article submitted November 1, 1971.

DISTRIBUTION OF RADIOACTIVE CERIUM BETWEEN THE VAPOR AND LIQUID PHASES UPON EVAPORATION OF WATER SOLUTIONS

A. D. Chistyakov and V. F. Bagretsov

UDC 541.123;621.039.714

At atomic electric power stations in the USSR, the purification of decontamination solutions is achieved by evaporation. In view of this, there is a practical interest in the determination of possible limitations of the evaporation technique with respect to the purity of the vapor product. In the limit, the attainable vapor purity (with the absence of dropping removal) is determined by the coefficients of the physical–chemical distribution (K_p) of the substances between the vapor and liquid phases. The values of K_p depend on the nature of the substance, the composition of the solution which is evaporated, and the temperature. In the present paper, the dependence of K_p Ce (III) on the concentration of hydroxyl ions at the boiling temperature of water solutions (p = 1 atm) is considered. According to the data in [1], the distribution coefficient for cerium with few system parameters must be determined by the expression

$$K_p = K_M \beta, \tag{1}$$

where K_M is the thermodynamic molar coefficient for the distribution of $Ce(OH)_3$; β is the fraction of $Ce(OH)_3$ molecules out of the whole concentration of cerium in the solution which is evaporated.

In alkaline solutions with the absence of strong complexing, one must be concerned with only two forms of actually dissolved cerium: $Ce(OH)_3$ and $Ce(OH)_2^{+1}$. Therefore, the values of β can be calculated from the dissociation constant for the reversible reaction:

$$Ce(OH)_3 \rightleftharpoons Ce(OH)_2^{+1} + OH^{-1};$$

$$K_d = \frac{[Ce(OH)_2^{+1}][OH^{-1}]\gamma_{\pm(1-1)}^2}{[Ce(OH)_3]} = \frac{\alpha [OH^{-1}]\gamma_{\pm(1-1)}^2}{\beta}, \tag{2}$$

where α is the fraction of $Ce(OH)_2^{+1}$ ions in the solution which is evaporated; $\gamma_{\pm(1-1)}$ is the average coefficient of activity for the $Ce(OH)_2^{+1}$ and OH^{-1} ions. Since $(\alpha + \beta) = 1$, then it follows from Eq. (2) that

$$\beta = \frac{[OH^{-1}]\gamma_{\pm(1-1)}^2}{K_d + [OH^{-1}]\gamma_{\pm(1-1)}^2}$$

and consequently

$$K_p = K_M \frac{[OH^{-1}]\gamma_{\pm(1-1)}^2}{K_d + [OH^{-1}]\gamma_{\pm(1-1)}^2}.$$

The values for K_d and K_M can be found by solving the system of two equations based on Eq. (4) when evaluated for two series of experimental values for K_p and $[OH^{-1}]$. For this purpose, experiments were set up with a distribution of Ce^{144} in a Ce (III)–NaCl–NaOH–H_2O system. The technique has been discussed in [2]. The experiments showed that an increase in the concentration of NaOH (the concentration of NaCl equals 0.66 M) from 0.002 up to 1 N leads to an increase in K_p Ce^{144} from 7.7×10^{-7} up to 4.2×10^{-5}, i.e. approximately 55 times. The calculated value of K_d is equal to 0.054, the value of K_M equals 4.8×10^{-5}.

The analysis of Eq. (4) shows that, for the determination of the minimum values of K_p for cerium (and other rare-earth elements), a feasible evaporation results in an acid state. In this case, the coefficients of purity for the vapors of rare-earth elements can attain magnitudes greater than 10^8.

LITERATURE CITED

1. O. I. Martynova, Zh. Fiz. Khimii., 38, 1065 (1964).
2. A. D. Chistyakov, Zh. Fiz. Khimii., 46, 275 (1972).

Translated from Atomnaya Energiya, Vol. 33, No. 1, pp. 573-574, July, 1972. Original article submitted May 6, 1971.

DISTRIBUTION OF NUCLEAR FISSION NEUTRONS IN A QUASIHOMOGENEOUS MEDIUM CONTAINING URANIUM*

Yu. B. Davydov and A. T. Markov

UDC 550.8:553.495

Nuclear fission neutron logging is a new method for the identification of uranium in pores [1, 2]. In this paper, the solution of the straightforward problem of the theory of nuclear fission neutron logging is considered for the case when the perturbing influence of the pores can be neglected.

The problem is formulated in the following manner. The homogeneous medium is specified by an arbitrary one-dimensional mineralization $q = q(Z)$, where $q(Z)$ is the uranium content by weight in the medium. Let us assume that a change in the chemical composition of the medium resulting from the uranium mineralization does not affect its physical properties determining the neutron transport. In a pore passing through the quasihomogeneous medium under consideration, there is placed a point source of neutrons. It is required to find the distribution of the nuclear fission neutron flux along the axis of the pore.

To solve the problem, the diffusion approximation from neutron transport theory was utilized. The solution was obtained by construction of the flux function for a plane source of nuclear fission neutrons with subsequent integration over the entire space of the source distribution.

The results were utilized for the numerical calculation of the nuclear fission neutron flux in a uranium-containing carbonate medium with a different porosity and a different degree of salinization of the water filling the pores.

An inversion effect was established for the nuclear neutron flux which is analogous to the inversion effect for the neutron flux of the source. Its practical utilization lies in the fact that by trial and error the lengths of the probe can reduce essentially the dependence of the results of the logging on the water-content of the rocks. The calculations show that the length of the inversion probe for the delayed nuclear fission neutrons differs little from the length of the inversion probe for the source neutrons.

Analysis of the data obtained permits one to conclude that, in the general case, there is observed an essential dependence of the recorded effect on the type of probe, its length, the output of the active region, and the chemical composition of the medium. The results of the calculation can be utilized with the development of the logging technique and methods for a quantitative estimate of the uranium content, permitting one to take into account the influence of the factors indicated.

LITERATURE CITED

1. S. Amiel and M. Peisakh, At. Énerg., 14, 535 (1963).
2. S. A. Igumnov, Izv. Vuzov. Gornyi Zh., 2, 3 (1966).

THE YIELD OF CAPTURE GAMMA RAYS FROM A LAYER OF IRON STRUCK OBLIQUELY BY NEUTRONS†

S. F. Degtyarev, N. N. Repin,
V. A. Sakovich, V. M. Sakharov,
A. P. Suvorov, and V. V. Tarasov

UDC 621.039.538

By measurements and calculations of the spatial and energy distribution of neutrons in a shielding barrier made of iron, boron carbide, and polyethylene, struck obliquely by a broad unidirectional beam of

*Translated from Atomnaya Energiya, Vol. 33, No. 1, p. 574, July, 1972. Original article submitted August 2, 1971; revision submitted December 2, 1971.

†Translated from Atomnaya Energiya, Vol. 33, No. 1, p. 575, July, 1972. Original article submitted November 19, 1971; abstract submitted February 24, 1972.

neutrons from the spectrum of a reactor [1], it was shown that increasing the angle of incidence of the neutrons to 60° leads to a decrease of the density of capture gamma-ray sources by a factor of 1.5-2 at the same depth in the shielding in the direction of the incident neutrons.

In connection with this, the present study was conducted to investigate by computational and experimental methods the yield of capture gamma rays from a layer of iron in the shielding barrier. The angular distribution of the flux of capture radiation energy beyond an iron layer having a thickness of $t/\cos\theta_0$, which took on values of 28 and 40 cm, was calculated for neutron incidence angles of $\theta_0 = 0$, 45°, and 60°. The calculation was carried out by numerically integrating with respect to the depth of the shielding the angular distributions of gamma rays from a plane isotropic source of neutrons beyond the shielding barrier [2].

Measurements of the spectral–angular distribution of capture gamma rays beyond a barrier of iron, boron carbide, and polyethylene were carried out for an iron-layer thickness of 28 cm, using a spectrometer with a 40 × 40 mm stilbene crystal and neutron discrimination based on the shape of the pulse [3].

The angular distribution of the capture gamma-ray energy flux for energies of more than 3 MeV, obtained by computation and experiment, is shown in Fig. 1. As can be seen, the results are in good agreement.

Thus, when the angle of incidence of the neutrons is increased from 0 to 60°, the total capture gamma-ray energy flux is reduced by a factor of approximately 1.5. The angular distribution of the energy flux beyond the iron layer consists mainly of unscattered gamma rays and is practically isotropic in the observed range of neutron angles of incidence. It was also found that the shape of the capture gamma-ray spectra is almost completely independent of the angle of incidence of the neutrons and of the angle at which the gamma quanta leave the shielding barrier.

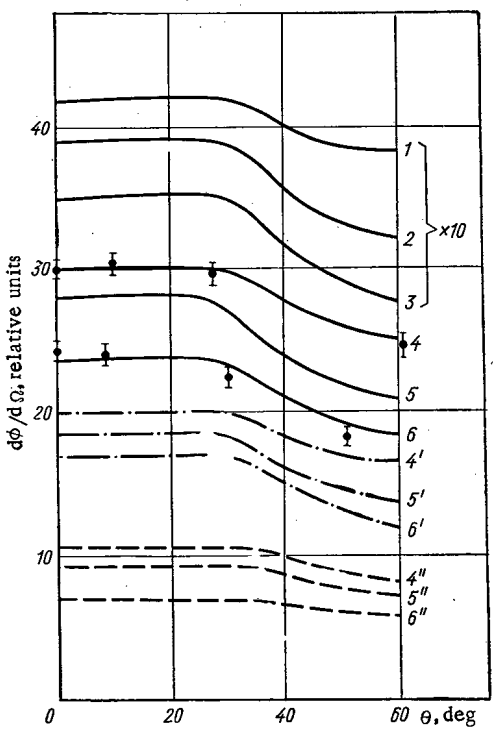

Fig. 1. Angular distribution of capture gamma-ray flux over the surface of an iron barrier 40 cm thick for angles of incidence of 0, 45°, and 60° (Curves 1, 2, and 3, respectively) and a thickness of 28 cm for the same angles of incidence (curves 4, 5, and 6, respectively). –·–·–) Flux of unscattered gamma quanta; ——) total flux; – – –) flux of scattered gamma quanta; ●) experimental results.

LITERATURE CITED

1. P. A. Barsov et al., in: Problems of Reactor Shielding Physics [in Russian], No. 5, Atomizdat, Moscow (1972), p. 74.
2. A. A. Viktorov et al., in: Problems of Dosimetry and Radiation Protection [in Russian], No. 9, Atomizdat, Moscow (1969), p. 50.
3. O. A. Trykov and I. V. Goryachev, Pribory i Tekh. Éksperim., 6, 63 (1967).

RESPONSE OF COAXIAL CABLE WITH POLYETHYLENE FILLER TO PULSED RADIATION

V. M. Gorbachev, N. A. Uvarov,
G. A. Gurov, and V. N. Kudrya

UDC 621.315.212.019.39

Electrical signals appearing in coaxial uncharged cable subjected to bombardment by pulsed neutron radiation and γ-radiation, an effect reported on several occasions in the literature [1-4], were investigated. The parameters of the high-intensity neutron pulse and γ-ray pulse were as follows: average neutron energy $\overline{E}_n \approx 1.4$ MeV, average γ-photon energy $\overline{E}_\gamma \approx 1.25$ MeV, flux density of neutrons and γ-photons $I_{n,\gamma} \approx 10^{15}$ to 5.10^{16} particles/cm^2·sec, pulse width at half height $\tau_{1/2} \approx 100$ μsec.

Flat spirals of type RK-19 cable, $l = 10$ m in length, were arranged at right angles to the incident flux at different distances from the source. The signals were picked up from the core of the cable and recorded by an oscillograph. The results obtained in four successive exposures with intervals of about 24 h show (see Fig. 1) that the signal generated in the first irradiation is of positive polarity, with the maximum leading the maximum of the radiation pulse by as much as ~ 50 μsec. Positive bipolar and negative signals were recorded in the second irradiation. Negative signals were recorded in all of the subsequent pulses. One exception is the trace obtained when spirals positioned at comparatively great distances from the radiation source were irradiated. As the exposure dose builds up, the "sensitivity" $\varkappa$ of the cable to radiation, i.e., the level at which the current generated by the cable per unit intensity of radiation is picked up, drops by hundreds of times. This effect is irreversible in character if the irradiation conditions are maintained. When the orientation of the spiral is reversed (turning through 180°), the "sensitivity" is restored. The sensitivity required in the case of uncharged RK-19 cable not previously charged, over one meter length, $\varkappa \approx 10^{-22}$ A/particle/cm^2·sec.

The signals generated on the braiding of the cable when the core is grounded are of negative polarity, and no shift of the maximum was detected. By using lead and paraffin shields, we can estimate the partial contributions made by neutrons and by γ-photons.

The results obtained were analyzed within the framework of the electret model. The current in the circuit of the cable core appears to be due primarily to a change in the surface charge σ of the dielectric $i \approx d\sigma/dt$. The decrease in the current in response to the buildup of the dose is evidence of the buildup and storage of the charge belonging to an electret. The remanent polarization leads to a nonlinearity in the

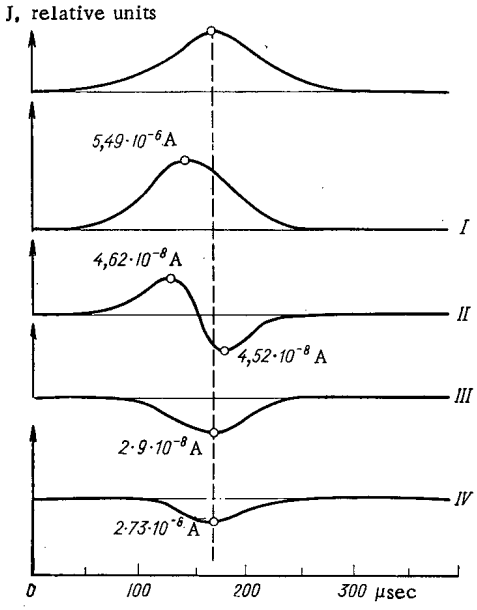

Fig. 1. Shape of electrical signals appearing in response to pulsed irradiation of cable. Scale 100 μsec. Amplitude values of current J indicated, in A. Pulse of n, γ-radiation indicated above curves.

Translated from Atomnaya Energiya, Vol. 33, No. 1, p. 576, July, 1972. Original article submitted September 13, 1971; revision submitted December 13, 1971.

reproduction of the shape of the radiation pulse. Actually, the surface charge density on the polyethylene is comparatively low, because saturation does not occur before the radiation pulse reaches its maximum. This causes the shift in the maximum of the pulse current.

Other aspects of the generation of electrical signals in cable in response to a pulse of penetrating radiation are also discussed in the paper.

LITERATURE CITED

1. H. Wichlein, Communication and Electronics, No. 64, 473 (1963).
2. S. Harrison et al., IEEE Trans. Nucl. Sci., NS-10, No. 5 (1963).
3. R. M. Zaidel', Zh. Priklad. Mekhan. i Tekh. Fiz., No. 3, 66 (1968).
4. V. V. Zubov, et al., Vysokomolekulyarnye Soedineniya, 9, 2746 (1967).

MEASUREMENTS OF α FOR U^{235} AND Pu^{239} AT 2 keV

V. G. Dvukhsherstnov, Yu. A. Kazanskii, and V. M. Furmanov

UDC 539.1.083

Measurements of α, the ratio of the radiative capture to fission cross sections, have been made for U^{235} and Pu^{239} using a single-crystal scintillation spectrometer with discrimination between neutron and gamma pulses by luminescence time. A beam of 2 keV neutrons was obtained by passing the neutron leakage spectrum of the Obninsk power station uranium–graphite reactor through scandium and titanium filters 219 and 6.7 g/cm^2 thick respectively. The background measurements were made with the beam shuttered by a supplementary manganese filter 4.5 g/cm^2 thick. With the 8g U^{235} sample the total fraction of various backgrounds relative to the effect for 2 keV neutrons was about 100% for gamma rays and ~ 30% for neutrons; with the 10 g Pu^{239} sample it was about 70% for gamma rays and ~ 45% for neutrons.

TABLE 1. Values of α for 2±0.35 keV Neutrons

Sample	Sample thickness, nuclei /barn	Obninsk (our data)	ITÉF (1970)	Harwell (1970)
Pu^{239}	Extrapolation to 0	1,42	—	—
	$1{,}2\cdot10^{-3}$	—	—	0,91
	$2{,}2\cdot10^{-3}$	—	1,34	—
	$5{,}1\cdot10^{-3}$	1,35±0,09	—	—
	$1{,}5\cdot10^{-2}$	1,21±0,07	—	—
U^{235}	$4{,}1\cdot10^{-3}$	0,49±0,04	—	—
	$6{,}0\cdot10^{-3}$	0,51±0,04	—	—

The apparatus was calibrated with a thermal neutron spectrum. The results of the measurements were normalized to the value of α^{th} calculated for the thermal neutron spectrum by using estimated cross sections.

The results of the measurements for Pu^{239} agree with data of the ITEF experiment (Table 1).

Translated from Atomnaya Energiya, Vol. 33, No. 1, p. 577, July, 1972. Original article submitted September 3, 1971; abstract submitted January 13, 1972.

LETTERS TO THE EDITOR

DETERMINATION OF PARAMETERS FOR THE KINETICS OF SUBCRITICAL INSTALLATIONS

B. I. Kolosov, I. P. Matveenko,
V. Ya. Pupko, É. A. Stumbur,
V. A. Tarasov, and A. G. Shokod'ko

UDC 621.039.512

One of the most common methods for investigating breeder systems is the study of the effects which appear with the introduction of relatively small samples. This enables one to utilize the apparatus of first order perturbation theory in the interpretation of such experiments. As a rule, such changes are conducted in reactors near the critical stage, and the extent of the system's perturbation serves to alter its reactivity.

For highly subcritical systems where determination of the reactivity is difficult, analogous methods of investigation of their neutron–physical characteristics can be developed on the basis of the pulse neutron source procedure [1]. The basic experimentally measurable quantity characterizing the perturbation of the system is the change in the asymptotic logarithmic decrement α for prompt neutrons.

The asymptotic distribution for prompt neutrons $\Phi(\bar{r}, \bar{v})$ in a breeder system is determined* by the equation

$$\hat{Q}_p\varphi - \hat{L}\varphi + \frac{\alpha}{v}\varphi = 0, \tag{1}$$

where

$$\hat{Q}_p\varphi \equiv (1-\beta)\chi_p \int \nu\Sigma_f(\bar{r}, \bar{v}')\,\varphi(\bar{r}, \bar{v}')\,d\bar{v}';$$

$$\hat{L}\varphi \equiv \bar{\Omega}\nabla\varphi + \Sigma_t(\bar{r}, \bar{v})\,\varphi - \int \Sigma_s(\bar{r}, \bar{v}' \to \bar{v})\,\varphi(\bar{r}, \bar{v}')\,d\bar{v}';$$

the rest is standard notation.

In particular, such experiments make possible a relatively simple determination of the parameters for the system's kinetics – the production time and the lifetime for prompt neutrons:

$$\Lambda = \frac{\left(\varphi^+, \frac{1}{v}\varphi\right)}{(\varphi^+, \hat{Q}_p\varphi)};$$

$$l = \frac{\left(\varphi^+, \frac{1}{v}\varphi\right)}{(\varphi^+, \hat{L}\varphi)},$$

where $\varphi^+(\bar{r}, \bar{v})$ is the eigenfunction of the equation conjugate to Eq. (1) [2]. These parameters are connected through the relation

$$\alpha = \frac{1}{l} - \frac{1}{\Lambda}.$$

The difference between the production time Λ and the lifetime l increases in proportion to an increase in the quantity α, i.e. a decrease in the reactor's K_{eff}; for a subcritical $\Lambda > l$.

Application of first order perturbation theory (for a quasistationary neutron distribution: this theory is developed in [3]) shows that the prompt neutron production time Λ can be measured in a relatively simple

*It is assumed, as in the majority of experiments [1], that $\alpha \gg \lambda_i$, i.e., larger than all of the decay constants of the delayed neutron sources and therefore one can neglect them.

Translated from Atomnaya Énergiya, Vol. 33, No. 1, pp. 579-580, July, 1972. Original article submitted September 9, 1971.

manner through a partial replacement of the entire volume of the active zone for the fissionable materials by an absorber with equivalent absorbing and emitting properties [4].

In general, there follows from perturbation theory:

$$\delta\alpha=\frac{(\varphi^+,\ \delta\hat{L}\varphi-\delta\hat{Q}_p\varphi)}{\left(\varphi^+,\ \frac{1}{v}\varphi\right)},$$

where $\delta\hat{L}\varphi-\delta\hat{Q}_p\varphi=-\varphi\delta\Sigma_t+\int\varphi\delta\Sigma_s\,d\bar{v}'+(1-\beta)\times\int\varphi\delta(\nu\Sigma_f)\,d\bar{v}'$. It is obvious that in the case of partial replacement, mentioned above, when $\delta\hat{L}=0$, and $\delta\hat{Q}_p=-\varepsilon\hat{Q}_p$ (where ε is the fraction of fissionable material replaced by the equivalent absorbent), we have

$$\delta\alpha=\frac{(\varphi^+,\ \hat{Q}_p\varphi)}{\left(\varphi^+,\ \frac{1}{v}\varphi\right)}\varepsilon=\frac{\varepsilon}{\Lambda}.$$

However, in practice, in an experiment, it is convenient to make a complete substitution of the fissionable material by an absorbent ($\varepsilon=1$) in a small volume of the active zone ΔV_i. This results in a change in the logarithmic decrement of the prompt neutron flux $\Delta\alpha_i$ for all of the system which is observed in the experiment. The addition of the effects from similar processes throughout the volume of the active zone enables one to determine the production time:

$$\Lambda=\frac{1}{\sum\Delta\alpha_i}.$$

The lifetime l can be obtained from Eq. (4).

One should mention that, provided the experiment is extremely simple, one measures the minimum value of the logarithmic decrement for prompt neutrons, which is determined in such a manner that the parameter Λ characterizes the asymptotic (in time) neutron distribution, although, in principle, the method enables one to find the analogous quantities for the higher harmonics.

Experimental verification of this method was carried out in a heterogeneous uranium–water installation [5]. A hexagonal lattice of high concentration fuel elements, spaced at 3.2 cm intervals, was placed in a Plexiglas tank filled with water. The tank had the shape of a rectangular prism and was a critical reactor without a reflector. A decrease in K_{eff} was achieved because of successive discharges of an even number of symmetrically spaced fuel elements commencing at two opposite external boundaries of the system. Constructed in this manner, the subcritical systems have fixed external dimensions, but variable (along one of the axes) dimensions for the active zone and the water reflector.

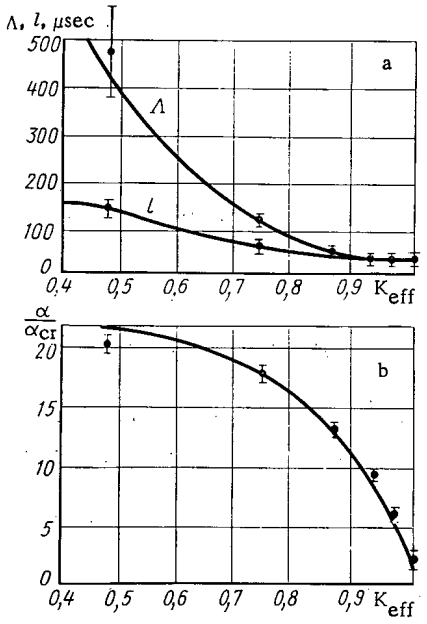

Fig. 1. Dependence of the parameter for the kinetics on K_{eff}. ——) Calculation; ●) experimental results.

The logarithmic decrements for prompt neutrons were measured by using an impulse neutron source with the aid of the apparatus and technique for the processing of experimental data analogous to that described previously [5].

For the experiments there were prepared absorbents from powdered boron carbide (mixed with Al_2O_3), which, with respect to absorption cross section (for V = 2200 m/sec) and geometrical extent correspond to the fuel composition. In subcritical installations the effect of the perturbation was determined with the replacement of one of the fuel elements by an absorber, and the number of observation points was determined by the symmetry and number of fuel elements in the system. Since replacement of the whole fuel element in the given reactor resulted in a relatively large perturbation, the effect in a critical system was measured for short specimens (up to 0.1 of the length of a fuel element), so subsequently a corresponding correction was introduced into the results of the experiments.

For consideration of the inequivalence of the substitution through absorption and scattering cross section, specific calculations* in the 18-group of the P_1-approximation were performed

*The calculations were performed by R. M. Strutinskii.

(allowing for the homogeneity in the thermal group), showing that for a given heterogeneous system the correction in this effect is insignificant (~3.5%).

The results of the experiments and the calculated relations obtained by the "Spectrum" program [6] are presented in Fig. 1. The experimental results agree with the calculated data and indicate that, for the study of a system, the parameter Λ (see graph a) varies over a broad range (from ~30 up to ~500 μsec). One should mention that an extremely large increase in the production time corresponds to a reduction in the relation $\alpha/\alpha_{cr} = f(K_{eff})$ (see graph b), i.e., transition to the case of a "thick" reflector [7]. In addition, the lifetime of the prompt neutrons approaches the value of the lifetime of the thermal neutrons in the reflector (its maximum value for the given installation is 170 μsec).

The authors are grateful to Yu. E. Egorov for help with the experiments and to R. M. Strutinskii for conducting the calculations.

LITERATURE CITED

1. Pulsed Neutron Research, IAEA, Vienna (1965).
2. B. Davison, Neutron Transport Theory, Clarendon Press, Oxford (1957).
3. E. Pendlebury, Proc. Phys. Soc. A, 68, 474 (1955).
4. V. Ya. Pupko, Preprint FEI-103 (1967).
5. E. A. Stumbur et al., At. Énerg., 25, 13 (1968).
6. B. I. Kolosov, Preprint FEI-166 (1969).
7. E. I. Stumbur et al., At. Énerg., 27, 215 (1969).

DETERMINATION OF MIGRATION AREA

I. V. Sergeev and Yu. A. Platovskikh

UDC 621.039.51.12

The usual definition of the migration area $M^2 = L^2 + \tau$ can be utilized to find the k_{eff} of a bare reactor in the case where fission takes place only in the thermal region. The present article shows how the migration area can be determined when fission occurs in the epithermal region.

We write the static equation for the neutron density $N(r, v)$ in the form

$$HN = k_{eff}^{-1} \chi(v) \int_0^\infty \nu v' \Sigma_f N(r, v')\, dv', \tag{1}$$

where the operator H describes scattering, absorption, and diffusion of neutrons; $\chi(v)$ is the fission spectrum. By using Green's function $G(r, v; r_0, v_0)$, satisfying the equation $HG = \delta(v - v_0)\,\delta(r - r_0)$, we then restate Eq. (1) in the form

$$N(r, v) = k_{eff}^{-1} \int_0^\infty dv' \int_0^\infty dv_0 \int dr_0 \chi(v_0)\, \nu v' \Sigma_f(v')\, N(r_0, v')\, G(r, v; r_0, v_0).$$

Hence, after multiplying both sides of the equation by $\nu v \Sigma_f$, and integrating with respect to v, we end up with an integral equation for the fission density

$$\begin{aligned} m(r) &= \int_1^\infty \nu \Sigma_f N(r, v)\, dv; \\ m(r) &= k_{eff}^{-1} \int dr_0 m(r_0) K(r, r_0), \end{aligned} \tag{2}$$

where $K(r, r_0) = \int_0^\infty dv \int_0^\infty dv_0 \nu v \Sigma_f \varkappa(v_0)\, G(r, v; r_0, v_0)$ is the number of fission events occurring at the point r per single neutron generated with the spectrum $\varkappa(v_0)$ at the point r_0. Expanding $m(r_0)$ into a Taylor series and retaining only the first three terms of the expansion, and also assuming $K(r, r_0) = K(|r - r_0|)$, we obtain a differential equation for m(r):

$$m(r) = k_{eff}^{-1} k_\infty (1 + M^2 \nabla^2) m(r), \tag{3}$$

where $k_\infty = \int dr K(|r - r_0|)$;

$$M^2 = \frac{1}{6} \cdot \frac{\int dr (r - r_0)^2 K(|r - r_0|)}{\int dr K(|r - r_0|)}, \tag{4}$$

and here integration is carried out throughout all space.

In this definition, M^2 has the meaning of the mean square distance traversed by the neutron from the point where it is produced till it takes part in a fission reaction. The final result is independent of the geometry, so that further calculations will be performed in application to a plane geometry. We now write the expression for M^2 in a different form, derived from the definition (4):

$$M^2 = \left(\int_0^\infty \nu v \Sigma_f n(v)\, \tau^+(v)\, dv \right) \left(\int_0^\infty \nu v \Sigma_f n(v)\, dv \right)^{-1}, \tag{5}$$

where $\tau^+(v) = \frac{1}{2} \cdot \frac{\int_0^\infty \psi(x, v)\, x^2\, dx}{n(v)}$; $\psi(x, v) = \int_0^\infty \varkappa(v_0)\, G(v, v_0, x)\, dv_0$; $n(v) = \int_0^\infty \psi(x, v)\, dx$. The function $\tau^+(v)$ is equal to the mean square distance traversed by the neutron at velocity v. The variables $\tau^+(v)$ and n(v) refer to the same medium as Eq. (1), but without fission. We now break the interval $(0, \infty)$ up into two parts with

Translated from Atomnaya Énergiya, Vol. 33, No. 1, pp. 580-582, June, 1972. Original article submitted September 2, 1971.

respect to the velocity: from 0 to v_{lim} and from v_{lim} to ∞. We assume here that thermal neutrons fall into the first interval, while slowing-down neutrons fall into the second interval. Then, when $v \geq v_{lim}$ we have $\tau^+(v) = \tau(v)$, where $\tau(v)$ is the age in the conventional sense. In order to describe the thermal region we apply the diffusion approximation

$$-vD\frac{d^2G_1}{dx^2}+H'G_1=cG_2(v_{lim}\, v_0,\, x)\,\delta(v-v_{lim}),$$

where H' describes absorption and scattering of neutrons, and the subscripts 1 and 2 refer to intervals $(0, v_{lim})$ and (v_{lim}, ∞) respectively. Integration in the collision integral is carried out from 0 to v_{lim}. From the equation for G_1, we infer the equation for $\psi_1(x, v) = \int_0^{v_{lim}} \chi(v_0)\, G_1(v, v_0, x)\, dv_0$:

$$-vD\frac{d^2\psi_1}{dx^2}+H'\psi_1=c\psi_2(v_{lim}\, x)\,\delta(v-v_{lim}), \tag{6}$$

where $\psi_2(x, v) = \int_{v_{lim}}^{\infty} \chi(v_0)\, G_2(v, v_0, x)\, dv_0$. After taking the Fourier transform of Eq. (6) and an eigenfunction expansion of the equation $(-\varkappa^2 vD + H')\,\varphi = 0$, we get

$$\bar{\psi}_1(k, v)=c\bar{\psi}_2(k, v_{lim})\sum_n \frac{h_n^{-1}\varphi_n^+(v_{lim})\,\varphi_n(v)}{k^2+\varkappa_n^2}, \tag{7}$$

where $\bar{\psi}_1$ and $\bar{\psi}_2$ are the Fourier transforms of ψ_1 and ψ_2; k is the parameter of the Fourier transformation; $\varkappa_n$ are spatial eigenvalues; h_n are normalizing constants. The constant c can be determined from the condition that ψ_1 and ψ_2 be joined at $v = v_{lim}$. We retain only the first term in the expansion (7)

$$\bar{\psi}_1(k, v)=ch_0^{-1}\frac{\bar{\psi}_2(k, v)\,\varphi_0^+(v_{lim})\,\varphi_0(v)}{\varkappa_0^2+k^2}=\frac{\bar{\psi}_2(k, v_{lim})}{\psi_2(0, v_{lim})}\cdot\frac{\varkappa_0^2}{\varkappa_0^2+k^2}\,n_1(v), \tag{8}$$

where $n_1(v)$ is the spectrum of the thermal neutrons. Recalling that $\tau^+(v)=\frac{1}{2}[n(v)]^{-1}\frac{d^2\psi_1}{dk^2}\Big|_{k=0}$ and that $\varkappa_0 = L^{-1}$, we derive an expression for $\tau^+(v)$ in the thermal region:

$$\tau^+(v) = \tau(v_{lim}) + L^2.$$

Accordingly, we have

$$\tau^+(v) = \tau(v), \quad v \geq v_{lim};$$
$$\tau^+(v) = \tau(v_{lim}) + L^2, \quad v < v_{lim}.$$

Now, using this result in the definition of M^2 (5), we arrive at our final formula for the migration area with fission in the epithermal region taken into account:

$$M^2=F_1[\tau(v_{lim})+L^2]+F_2\bar{\tau}, \tag{9}$$

where

$$F_1=\frac{\int_0^{v_{lim}} \nu v\Sigma_f n_2(v)\,dv}{\int_0^{\infty} \nu v\Sigma_f n(v)\,dv};$$

$$F_2=\frac{\int_v^{\infty} \nu v\Sigma_f n_2(v)\,dv}{\int_0^{\infty} \nu v\Sigma_f n(v)\,dv}; \qquad \bar{\tau}=\frac{\int_v^{\infty} \nu v\Sigma_f \tau(v)\, n_2(v)\,dv}{\int_v^{\infty} \nu v\Sigma_f n_2(v)\,dv}.$$

Here F_1 and F_2 are the fractions of fission events occurring in the thermal region and in the epithermal region. It can be shown that the results obtained are valid not only in the diffusion approximation, but equally well in any other approximation. Estimates show that $\bar{\tau}$ can be three to four times less than $\tau(v_{lim})$ in a reactor with a sufficiently hard spectrum, while M^2 calculated according to Eq. (9) may be 30-40% less than $L^2 + \tau(v_{lim})$. If we are to measure M^2 in terms of the definition proposed here, we have to resort not to the resonance indicator, but rather to an indicator of the same fissionable material as will be used in the research reactor. Equation (9) can be generalized to cover the many-group approximation. A formula similar to Eq. (9) can be derived for the nonleakage probability as well. We infer from Eq. (5) the criticality condition for a bare reactor:

$$k_{eff} = k_\infty(1 - B^2M^2).$$

The rigorous expression for M^2 with the continuous spectrum of spatial eigenvalues taken into account exhibits the form

$$M^2 = \left(\sum_{n=0}^{N} \frac{p_n}{h_n \varkappa_n^4} + \int_{\varkappa_{\min}}^{\infty} \frac{p_\varkappa d\varkappa}{h_\varkappa \varkappa^4} \right) \left(\sum_{n=0}^{N} \frac{p_n}{h_n \varkappa_n^2} + \int_{\varkappa_{\min}}^{\infty} \frac{p_\varkappa d\varkappa}{h_\varkappa \varkappa^2} \right)^{-1}, \tag{10}$$

where p_n, $\varkappa = \int \theta_n$, $\varkappa\nu v\Sigma_f \, dv \int \theta_n^+$, $\varkappa\chi \, dv'$, and $\theta_n^+, \varkappa$ and $\theta_n, \varkappa$ are the adjoint and direct eigenfunctions of the discrete and continuous spectra of the equation $(-\varkappa^2 vD + H')\,\theta = 0$. Equation (10) can be derived from the expansion of the Fourier transform of $G(v, v_0, x)$ in eigenfunctions $\theta_n(v)$.

A MORE ACCURATE INTERPRETATION OF DYNAMIC EXPERIMENTS IN REACTIVITY DETERMINATIONS

B. P. Shishin

UDC 621.039.562

The accuracy in measuring the reactivity of a reactor depends largely on the accuracy in analyzing the readings Q(t) of the detector which records the time variation of the neutron density on the basis of the nonstationary reactor equation, in particular, the equation with effective parameters [1].

Our aim was to improve the accuracy in interpreting experiments on reactivity determination by taking into account the specific features of the experiments and the characteristics and location of the detector.

The equations of detector readings related to the reactor's effective parameters (the reactivity ρ, the generation time of fission neutrons Λ, and the effective share of delayed neutrons $\beta_{i\text{eff}}$) are the following [1, 2]:

$$\frac{dQ(t)}{dt}=\frac{\rho-\beta_{\text{eff}}}{\Lambda}Q(t)+\varepsilon\sum_{i}^{i}\lambda_i C_i+\varepsilon S; \tag{1}$$

$$\varepsilon\frac{dC_i(t)}{dt}=\frac{\beta_{i\text{eff}}}{\Lambda}Q(t)-\lambda_i C_i(t),\quad i=1,\ 2,\ \ldots,\ l. \tag{2}$$

The values of ρ, β_{eff}, Λ and other parameters have been determined in [1]. The sensitivity function of the detector $\varepsilon = \langle\varepsilon(x)\, n(x)\rangle$ is the integral (over the x-phase volume of the detector) of the product of the detector's sensitivity with respect to a single neutron, $\varepsilon(x)$, and the neutron density $n(x)$ in the field in which the detector is located [2]. It is assumed that $n(x, t) = n(x)\, n(t)$.

The need for two related experiments is a specific feature of experimental methods of subcriticality determination. It is not sufficient to perform one experiment, since the number of unknown parameters is larger than the number of equations used in processing the experimental results.

TABLE 1. Working Equations of Different Methods of Reactivity Determination

"Multiplication method"	"Rod dropping" and "shooting source" methods	"Pulsed source method"
$Q_1(t)=\dfrac{S_1\Lambda_1\varepsilon_1}{\Lambda_1+\sum\limits_i\dfrac{\beta_{i\text{eff}}}{\lambda_i}}\,t$	$Q_1=\varepsilon_1$	$Q_1(t)=Q_1(0)\exp(-\omega t)$
$Q_2=-\dfrac{S_2\Lambda_2\varepsilon_2}{\rho_2}$	$Q_2=-\dfrac{S_2\Lambda_2\varepsilon_2}{\rho_2-\beta_{2\text{eff}}}$	$Q_2=-\dfrac{S_2\Lambda_2\varepsilon_2}{\rho}$
$\rho_2=-\dfrac{1}{Q_2}\cdot\dfrac{dQ_1}{dt}\left(\Lambda_1+\sum\limits_i\dfrac{\beta_{i\text{eff}}}{\lambda_i}\right)F$	$\rho_2=\left(1-\dfrac{Q_1}{Q_2}F\right)\beta_{2\text{eff}}$	$\rho=\beta_{1\text{eff}}-\omega\Lambda_1$ $\rho=-\dfrac{\int_0^T Q_1(t)\,dt}{Q_2T}F\beta_{1\text{eff}}$
$F=\dfrac{S_2\Lambda_2\varepsilon_2}{S_1\Lambda_1\varepsilon_1}$	$F=\dfrac{\varepsilon_2\sum\limits_i^i\beta_i\langle n_2^+(x)\,\chi_i P n_1(x)\rangle}{\varepsilon_1\sum\limits_i\beta_i\langle n_2^+(x)\,\chi_i P n_2(x)\rangle}$	$F=\dfrac{\varepsilon_2\langle n^+(x)\,\chi P n_1(x)\rangle}{\varepsilon_1\langle n^+(x)\,\chi P n_2(x)\rangle}$

Note: The subscript 1 pertains to the parameters and detector readings in the first experiment, while the subscript 2 pertains to the second experiment.

Translated from Atomnaya Energiya, No. 7, pp. 582-584, July, 1972. Original article submitted September 23, 1971; revision submitted December 28, 1971.

In a constant-subcriticality reactor, different neutron distributions can be created by choosing the characteristics of the external neutron source. Each distribution corresponds to definite numerical values of Λ, β_{ieff}, and ε, which vary in a very small range near criticality and in a wider range for extremely subcritical reactor states. This follows from the definitions of such functionals [1, 2]. The constancy of a functional treated as the reactivity is ensured by choosing the weighting function $n^+(x)$, which is the solution of the conjugate equation in the relatively critical model, where ρ is the eigenvalue of the problem [3].

In connection with this, it is necessary to improve the theoretical basis of reactivity measurement methods. Table 1 provides the working equations of several well-known methods of reactivity determination. The equations were derived by analogy with the procedure used in [4]. Equations (1) and (2) were used as a basis, while the parameters Λ, β_{eff}, ε, and S in the related experiments were considered to be unequal. In using the "multiplication method," the first experiment is performed on a critical reactor in the presence of a steady neutron source. The detector records the linear increase in the neutron density $Q_1(t)$. The second experiment is performed on a subcritical stationary reactor for fixed positions of the source and the detector. The readings of the latter are constant in time. The differences in the values of the parameters Λ, ε, and S in the reactivity equation are accounted for by the parameter F.

In using the "rod dropping method," the detector readings Q_1 are first recorded in a critical reactor without a source. After the rods have been dropped (immediately after the rapid power decay), the reactor behaves as in the presence of a steady neutron source, which is provided by fission fragments – the emitters of delayed neutrons accumulated in the first experiment; in this case,

$$S_2 = \sum^{i} \frac{\lambda_i \langle n_2^+(x)\, \chi_i C_{i,1}(x)\rangle}{\langle n_2^+(x)\, n_2(x)\rangle} = \sum^{i} \beta_i \frac{\langle n_2^+(x)\, \chi_i P n_1(x')\rangle}{\langle n_2^+(x)\, n_2(x)\rangle},$$

where $P_n(x') = \int_x \nu\Sigma_f(x')\, n(x')\, dx'$ [1]. The brackets $\langle\,\rangle$ denote integration over the reactor's phase volume.

In using the "shooting source method," the first experiment is performed on a subcritical stationary reactor with a steady source. The second experiment involves observation of the transient processes after the source has been quickly removed from the reactor; the analysis procedure is similar to that of the preceding method.

In the case of the "pulsed source method" [4], a subcritical reactor is acted upon by short-duration fast neutron beams over a long period of time (at constant time intervals T; $\lambda_i^{-1} \gg T \gg \omega^{-1}$). Rapid decay of prompt fission neutrons occurs in the first experiment, while the second experiment is performed with a steady external source, which is provided by stored fission fragments – sources of delayed neutrons. Let us determine the corresponding effective source S_2. Fragments with the density $\sum^{i} \beta_i \int_0^T P n(x,t)\, dt$ are generated during a single fission burst in the reactor [1]. Since a steady-state process is contemplated, the same number of fragments decays during the time T. The number of neutrons emitted by the fragments per unit time per unit volume of the phase space is

$$S_2(x, t) = \frac{1}{T} \sum^{i} \beta_i \chi_i \int_0^T P n_1(x, t)\, dt.$$

The effective source is described by [1]:

$$S_2 = \frac{1}{T \langle n^+(x)\, n_2(x)\rangle} \sum_i \beta_i \langle n^+(x)\, \chi_i \int_0^T P n_1(x, t)\, dt = \frac{1}{T} \int_0^T n_1(t)\, dt \sum_i \beta_i \frac{\langle n^+(x)\, \chi_i P n_1(x)\rangle}{\langle n^+(x)\, n_2(x)\rangle}$$

$$= \frac{1}{T} \int_0^T Q_1(t)\, dt \frac{\beta_{1\,eff} \langle n^+(x)\, n_1(x)\rangle}{\varepsilon_1 \Lambda_1 \langle n^+(x)\, n_2(x)\rangle}.$$

The definition $Q(t) = \varepsilon_n(t)$ is used in the case [2]. Two reactivity equations can be written on the basis of pulse experiments. One of them is the well-known Simons – King equation, which relates ρ to the decay constant ω, while the other is based on detector readings in two experiments. For F = 1, the latter expression for ρ coincides with Sostrand's working equation. The Gozani equation is obtained from it if $Q_1(t) = Q(0) \exp(-\omega t)$ and F = 1. By eliminating the reactivity from the two equations, we readily obtain an expression for β/Λ:

$$\left(\frac{\beta}{\Lambda}\right)_1 = \frac{Q_2 T \omega}{F \int_0^T Q_1(t)\, dt - Q_2 T}.$$

By substituting expression (6) in the Simons – King equation, we follow the Garrelis and Russel procedure of reactivity determination [4]. The expressions for ρ and β/Λ contain the parameter F, which accounts for the differences between the neutron fields in related experiments.

Thus, the working reactivity equations used in the above methods are distinguished from the well-known expressions [4] by the parameter F, which contains in concise form information on the actual reactor in related experiments, the relatively critical reactor model, the specific investigation method, and the physical characteristics of the detector and its position. A similar theory can be developed for other methods of measuring ρ.

For reactor states close to criticality, $F \approx 1$, since the neutron fields in the experiments to be compared differ insignificantly from the neutron field in a critical reactor. In extremely subcritical systems, the value of F can be appreciably different from unity. Calculation of the parameter F makes it possible to increase the range of reactivities to be measured. However, this does not provide the final solution of the problem, since the calculated values of F introduce in the result errors which are difficult to estimate. Examples of successful calculations of the correction factor are given in [5, 6].

LITERATURE CITED

1. T. Gozani, Nucleonik, 5, No. 2, 55 (1963).
2. S. Chwaszczewshi, Nucleonik, 12, No. 2, 75 (1969).
3. F. Morse and G. Feschbach, Methods of Theoretical Physics [Russian translation], Vol. 1, Izd. Inostr. Lit., Moscow (1960).
4. D. R. Kipin, Physical Principles of Nuclear Reactor Kinetics [in Russian], Atomizdat, Moscow (1967).
5. M. El-Zeftawy and L. Ruby, Nucl. Sci. and Engng., 45, No. 3, 335 (1971).
6. O. Aizawa, J. of Nucl. Sci. and Technol., 6, No. 9, 498 (1969).

COMPONENT DIFFUSION IN UC-ZrC SYSTEM

G. B. Fedorov, V. N. Gusev,
E. A. Smirnov, G. I. Solov'ev,
and S. S. Yankulev

UDC 539.219.3:669.822

Only one work [1] is known to have considered the diffusion properties of UC-ZrC solid solutions. An important limitation of [1] is the use of sintered samples and also the fact that the diffusion characteristics of only uranium and carbon have been investigated. The study of component diffusion in these alloys has considerable practical and theoretical importance.

The raw materials for the alloys were uranium monocarbide and zirconium carbide. Uranium monocarbide was prepared by melting spectrally pure graphite with uranium of 99:83 wt.% in an arc furnace. By chemical analysis the carbon content was found to be 4.86 ± 0.1 wt.%. The samples were prepared by

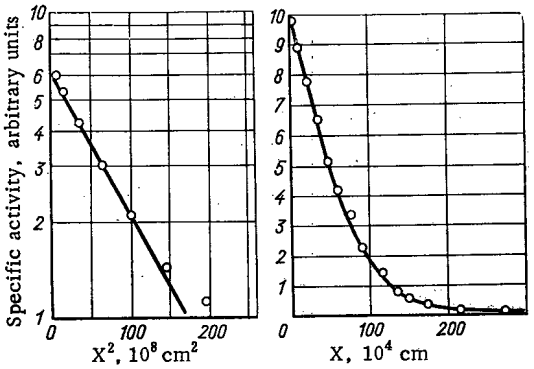

Fig. 1. Penetration curves of Zr^{95} (a) and C^{14} (b) into $U_{0.42}$, $Zr_{0.113}C_{0.465}$ at 2373°K.

TABLE 1. Coefficients and Parameters of Component Diffusion in UC-ZrC Alloys

Sample number	Alloy composition	Isotope	D*, cm²/sec·10¹¹				D_0, cm²/sec	Q, kcal/g·atom
			2173° K	2273° K	2373° K	2473° K		
1	$U_{0.497}C_{0.503}$	U^{235}	0,22	0,60	1,5	4,3	$2,7\cdot10^{-2}$	100
		Zr^{95}	0,22	0,60	1,6	4,2	$5,0\cdot10^{-2}$	103
		C^{14}	3000	5500	2600	17000	$6,5\cdot10^{-2}$	63
2	$U_{0.422}Zr_{0.113}C_{0.465}$	U^{235}	0,12	0,37	1,0	2,6	$4,6\cdot10^{-2}$	105
		Zr^{95}	0,11	0,30	0,96	2,3	$7,1\cdot10^{-2}$	107
		C^{14}	310	590	1000	2100	$9,0\cdot10^{-3}$	64
3	$U_{0.254}Zr_{0.264}C_{0.482}$	U^{235}	0,038	0,14	0,49	1,5	1,6	125
		Zr^{95}	0,065	0,25	0,66	1,9	$2,3\cdot10^{-1}$	114
		C^{14}	130	280	510	1000	$2,4\cdot10^{-2}$	72
4	$U_{0.147}Zr_{0.378}C_{0.475}$	U^{235}	0,023	0,098	0,38	1,2	9,6	135
		Zr^{95}	0,042	0,18	0,54	1,6	1,3	123
		C^{14}	17	36	68	160	$1,0\cdot10^{-2}$	78

Note: D* are component diffusion coefficients found by the radioactive tracer method; D_0 is the preexponential factor; Q is the activation energy.

Translated from Atomnaya Énergiya, Vol. 33, No. 1, pp. 584-586, July, 1972. Original article submitted September 14, 1971.

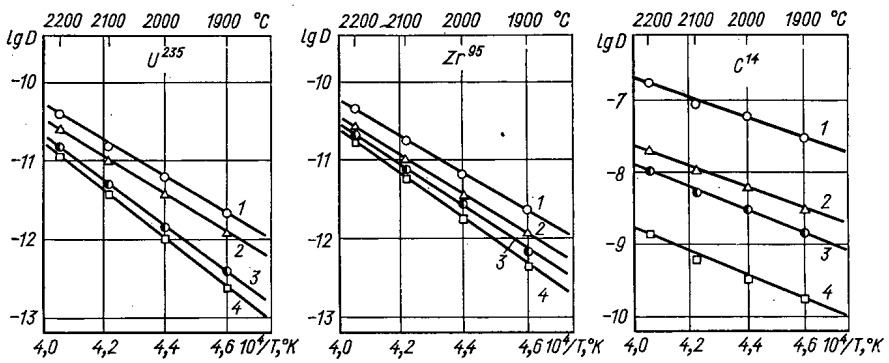

Fig. 2. Temperature dependence of diffusion coefficients of UC-ZrC components (the numbers at the curves correspond to the alloy numbers in Table 1).

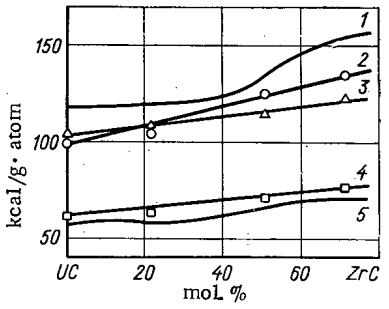

Fig. 3

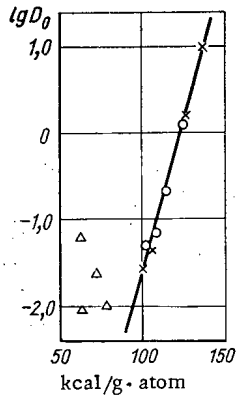

Fig. 4

Fig. 3. Concentration dependence of activation energy of UC-ZrC component diffusion: 1) uranium [1], 2) uranium, 3) zirconium, 4) carbon, 5) carbon [1].

Fig. 4. Dependence of D_0 on Q for UC-ZrC alloys: ×) uranium, ○) zirconium, △) carbon.

compressing an appropriate mixture of uranium and zirconium carbides under a pressure of 50 kgf/mm^2 and sintering the resulting moldings for 2 h at 2200°C in a vacuum oven. The sintered samples were then remelted in an arc furnace in an atmosphere of pure argon.

The resulting composition of the samples is listed in Table 1. The content of nitrogen in the alloys did not exceed 0.02 wt.%. X-ray and metallographic analysis proved all alloys to be single-phase alloys. The melted samples were homogenized by annealing for 4 h at 2200°C.

The diffusion of components was studied with the aid of the radioactive isotopes U^{235}, Zr^{95}, and C^{14}. U^{235} and Zr^{95} isotopes were deposited together on polished sample surfaces by sputtering in a vacuum of the order 10^{-6} mm Hg. The thickness of the sputtered layer did not exceed 500 Å. The C^{14} isotope was added to one of the diffusion pair samples in the course of arc melting.

The penetration depth of uranium and zirconium was 10-20μ and that of carbon up to 600μ. In the study of Zr^{95} and C^{14} diffusion in UC-ZrC alloys, direct measurement of gamma and beta activity was hampered by the presence of gamma and beta radiation of natural uranium. The gamma radioactivity of samples was thus measured using the integral discriminator technique described in [2]. The beta radiation was found from the difference in sample activity without and with a filter. The filter (aluminum foil) thickness was chosen to provide negligible absorption of uranium beta radiation and almost full absorption of carbon beta. The diffusion coefficients were calculated by the constant-source method.

The penetration curves of uranium, zirconium, and carbon in the studied materials indicate that limiting diffusion takes place in all cases (Fig. 1). The bulk diffusion coefficients (see Table 1) were calculated from the initial portions of the curves.

With increasing doping of uranium carbide with zirconium carbide the level of diffusion mobility of uranium, zirconium, and carbon atoms in UC-ZrC alloys decreases (Fig. 2) and the activation energies increase gradually (Fig. 3). The much higher diffusion mobility is probably due to the fact that the samples have a porosity of about 11-16% [1] and also to the fact that direct deposition of C^{14} on the sample surface by cementation could result in an additional concentration of carbon in the diffusion zone [1].

The results of this study indicate that zirconium carbide doping strengthens the interatomic bond in the UC-ZrC solid solution. This is also confirmed by a study of the compatibility of UC-ZrC alloys with refractory metals [3].

Some information about the nature of diffusion in carbide systems can be gained from an analysis of the dependence of the preexponential factor D_{0i} on the activation energy Q_i. The fact that the relationship $D_{0i} = A \exp(Q_i/B)$, where A and B are constants, holds indicates that the nature of both the chemical bond and the component diffusion mechanism does not change [4]. This holds for metallic elements (uranium and zirconium, Fig. 4). No such definite conclusion can be drawn for the diffusion of carbon since the different departures from the stoichiometric carbon content change the concentration of structural defects in the carbon sublattice.

LITERATURE CITED

1. N. A. Evstyukhin and G. I. Solov'ev, Metallurgy and Research of Pure Metals [in Russian], Vol. 9, Atomizdat, Moscow (1971), p. 74.
2. G. B. Fedorov, E. A. Smirnov, and F. I. Zhomov, Metallurgy and Research of Pure Metals [in Russian], Vol. 7, Atomizdat, Moscow (1968), p. 116.
3. Thermionic Conversion of Energy [in Russian], Vol. 1, Atomizdat, Moscow (1964).
4. G. B. Fedorov, Mobility of Atoms in Crystalline Lattices [in Russian], Naukova Dumka, Kiev (1965), p. 40.

DIRECT CONVERSION OF ENERGY FROM CHARGED PARTICLES WITH A TAPERED DIAPHRAGM SYSTEM

O. A. Vinogradova, S. K. Dimitrov,
A. M. Zhitlukhin, A. I. Igritskii,
V. M. Smirnov, and V. G. Tel'kovskii

UDC 621.36

The idea of direct conversion of the energy of charged particles escaping from the mirror of a thermonuclear reactor was advanced in [1]. The experimentally measured efficiency of a system with a periodic electrostatic field [2] reached 86% with the number of reflected particles being ~ 7% in this case.

In this paper, we propose a tapered diaphragm system with a steady decelerating field **E**. For the case of an ideal narrow beam entering the field at an angle $\pi-\alpha$ with respect to the direction of **E** (line OA, Fig. 1a), particles at each energy travel along their own particular parabola with the line passing through the vertices of these parabolas (the points where the particles have least energy) being the line OB, which is at an angle $\pi-\beta$ such that $\tan\beta = 2\tan\alpha$. For a very narrow beam, this means that it is sufficient to cut off the diaphragm edges along the line OB in order to obtain an efficiency $\eta = 1-\varepsilon$, where $\varepsilon = (v_x^2/v^2)\sin^2\alpha$ (v is the particle velocity at the entrance to the system and v_x is the velocity component perpendicular to the field **E**). With $\alpha = 0.1$ rad, we find $\varepsilon \approx 0.01$ and $\eta \approx 99\%$ (for a sufficiently dense arrangement of the diaphragms).

For a parallel beam of finite diameter d (see Fig. 1b), the edges of the diaphragms can be cut off along O"B close to OB. Because of the existence of the different vertex lines O'C and O"D, the intersection

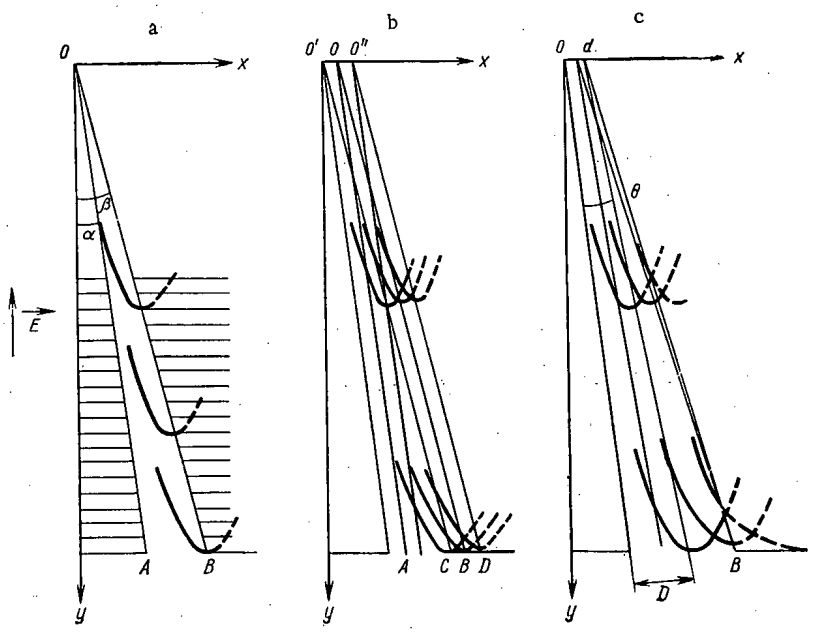

Fig. 1. Ion trajectories in a tapered diaphragm system.

Translated from Atomnaya Énergiya, Vol. 33, No. 1, pp. 586-589, July, 1972. Original article submitted June 26, 1971.

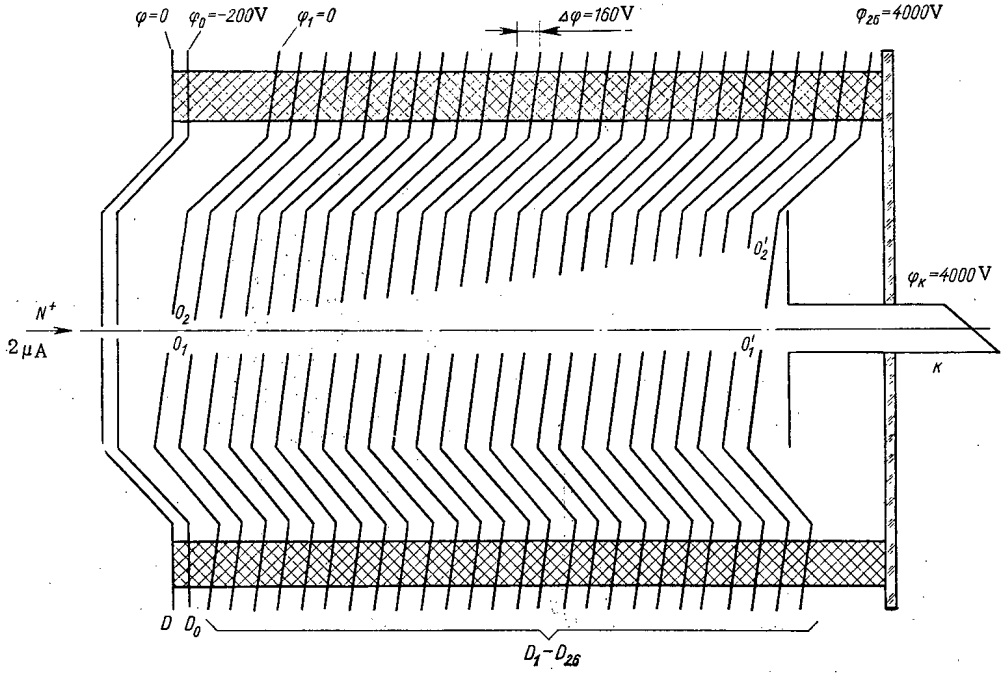

Fig. 2. Tapered diaphragm system with constant decelerating field.

of parabolas with the line O"B will be more removed from the vertex when the angle α is smaller. There is therefore an optimal angle α for which the energy of perpendicular motion $W_\perp$ is not too great while the spread in the points of intersection of the parabolas with the line O"B for a given energy is sufficiently small.

A parabola with a vertex at $y = \lambda$ and entrance angle $\pi-\alpha$ is described by the equation

$$y = x \operatorname{ctg} \alpha - \frac{x^2 \operatorname{ctg}^2 \alpha}{4\lambda}. \tag{1}$$

This equation indicates that the deviation Δy from λ of the points of intersection with the line O"B for particles having sufficiently high energy can be estimated to be, for boundary rays of the beam and small α,

$$\Delta y = \frac{d^2}{16\lambda} \operatorname{ctg}^2 \alpha, \tag{2}$$

whence we obtain for ε

$$\varepsilon \approx \frac{W_\perp + W_n}{W_\parallel} = \xi + \frac{\varkappa d^2}{16\lambda^2 \xi}, \tag{3}$$

where W_n is the energy loss resulting from the finite diameter of the beam; $W_n/W_\parallel \equiv \varkappa \Delta y/\lambda$; $\varkappa$ is a coefficient which depends on particle distribution over the beam cross section ($\varkappa \leq 1/2$ for a uniform distribution of particles over the beam cross section); $\xi \equiv W_\perp/W_\parallel = \tan^2 \alpha$.

The equation (3) indicates that ε is a minimum if the condition

$$\operatorname{tg}^2 \alpha_{opt} = \frac{d}{4\lambda} \sqrt{\varkappa} \tag{4}$$

is satisfied, with

$$\varepsilon_{min} = 2 \operatorname{tg}^2 \alpha_{opt} = \frac{d}{2\lambda} \sqrt{\varkappa}. \tag{5}$$

For example, when $d = 1$ cm, $\lambda = 17$ cm, and $\varkappa = 1/2$, we obtain $\tan \alpha_{opt} = 0.1$, $\varepsilon = 0.02$, and $\eta = 98\%$.

In the case of a diverging beam, assuming the angle of divergence θ (see Fig. 1c) is such that the final diameter D of the beam is considerably larger than d, we obtain for small α and θ and high-energy particles the estimates

$$\Delta y \approx \frac{D^2}{4\lambda} \operatorname{ctg}^2 \alpha; \qquad \operatorname{tg}^2 \alpha_{opt} = \frac{\theta \sqrt{\varkappa}}{2}; \qquad \varepsilon_{min} = \theta \sqrt{\varkappa}. \tag{6}$$

For $\theta = 0.07$ and $\varkappa = 1/2$, we obtain $\tan \alpha_{opt} = 0.16$, $\varepsilon_{min} = 0.05$, and $\eta = 95\%$. Reflection of particles with energies greater than eEd cotan $\alpha/4$ (approximately 20% of the maximum energy of the particles) is eliminated.

Thus a tapered diaphragm system with constant decelerating field possesses definite advantages for recovery from beams which are sufficiently narrow in comparison with the length of the device and not too divergent with the energy spread in the beam being 50% of the maximum ion energy.

Experimental study of conversion efficiency was carried out with a system having the geometry and potential distribution shown in Fig. 2. The diaphragm D gives an initial beam diameter d = 3 mm. An electric field which prevents entrance of electrons into the device is created by diaphragms D, D_0, and D_1. The operating diaphragms D_2-D_{25} contain slits, the respective widths of which are 5.5 and 21.1 mm in diaphragms D_2 and D_{25}.

The line $0_1 0_1'$ corresponds to the profile of the ion beam and is tilted at an angle $\theta/2 = 1°$ with respect to the axis (the half-angle divergence of the beam). The line $0_2 0_2'$ is the geometric location of the vertices of the parabolas (1) and is tilted at an angle $\gamma_1 = 6°20'$ with respect to the beam axis. The slope of the planes of the diaphragms with respect to the beam axis is $\gamma = 6°50'$, which corresponds to an angle $\alpha = 0.119$ between the electric field intensity vector E and the direction of particle flight. The diaphragm spacing is 5 mm. The diaphragm D_{26} with an opening 7.3 mm in diameter was installed to reduce distortion of the field at the exit. The initial current I^+ was measured with a Faraday cup while the decelerating field was off. Based on Eqs. (6), one finds $\varepsilon_{min} = 0.025$ and $\eta_{max} = 97.5\%$.

A high-voltage pulse $U_a = 4$ kV was applied to the anode of the source. At the source exit, a monoenergetic ion beam was obtained with an energy which varied from 1 to 4 keV. The current intensity I^+ in the beam was no more than 2 μA for N^+ ions. The beam current and the currents from the diaphragms were measured with an accuracy of 5%. The system efficiency was determined from

$$\eta = \frac{\Sigma I_i U_i + I_k U_k}{I^+ U}, \qquad (7)$$

where I_i is the current from the i-th diaphragm, U_i is the potential on the i-th diaphragm, I_k is the collector current, U_k is the collector potential, and U is the potential on the source anode.

From curves for the dependence of conversion efficiency on ion beam energy (Fig. 3), it follows that in a tapered diaphragm system ions of a given energy are incident mainly on "their" diaphragm, which ensures high conversion efficiency ($\eta_{av} = 96\%$). The absence of reflected particles was demonstrated experimentally.

In the energy range 3.8-4 keV, the conversion efficiency was measured every 20 eV (Fig. 4). In this case, a stabilized voltage from a rectifier was applied to the source anode. The source operated in a quasi-stationary mode. A pulsed, monoenergetic ion beam was produced at the source exit. At an ion energy W = 4 keV, the entire current was incident on diaphragm 25 since the collector potential $\varphi_k = 4$ keV and the particle energy $W_\parallel = W = W_\perp < 4$ keV. In this case, the efficiency $\eta = 96\%$. The conversion efficiency increases as the ion energy approaches the value of the potential on diaphragm 25, and $\eta = 97\%$ when W = 3.92 keV. Then a redistribution of currents between diaphragms 24 and 25 occurs and the efficiency falls. For

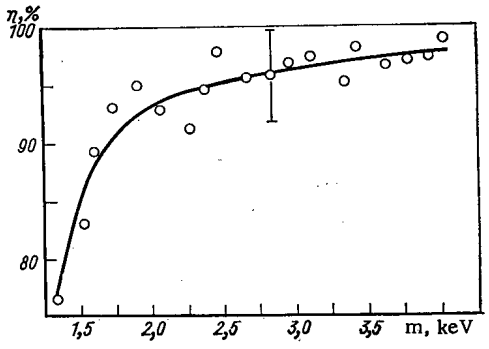

Fig. 3

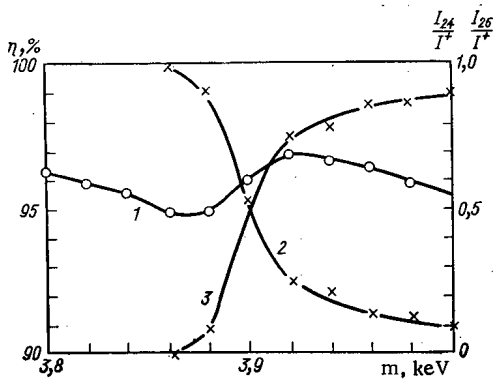

Fig. 4

Fig. 3. Conversion efficiency as a function of ion energy for a tapered diaphragm system.

Fig. 4. Energy dependence of conversion efficiency (curve 1) and currents from diaphragm 24 (curve 2) and diaphragm 25 (curve 3).

$W_{\parallel} = 3.84$ keV (the potential, Φ_{25}, on diaphragm 25 is 3.84 keV) the vertices of the parabolas (1) lie in the plane of diaphragm 25 and the current must divide equally between diaphragms 24 and 25. This was confirmed experimentally. The average conversion efficiency in the energy range 3.8-4 keV is $\eta_{av} = 96\%$ (η was measured with an accuracy of $\pm 5\%$).

From the condition $\tau \leq 1/\omega_0$ for the smallness of the space-charge effect (τ is the particle flight time through the system and ω_0 is the plasma frequency) and Eq. (5), we obtain a bound for the quantity ε resulting from space charge:

$$\varepsilon \geqslant d\,(\pi \varkappa Zej)^{1/2}\,(2AM/W_{\parallel}^3)^{1/4} = 8.0d\,(Zj)^{1/2}\,(A/W_{\parallel}^3)^{1/4}, \tag{8}$$

where A and Z are the atomic weight and charge multiplicity of the ion; M and e are the mass and charge of the proton (furthermore, $\lambda = d\sqrt{\varkappa}/2\varepsilon$, see (5)).

Thus for deuterons at the exit of an expander [1] (W = 800 keV, d = 100 cm, and $j = 4 \times 10^{-4}$ A), we have $\varepsilon \geq 0.12$ according to Eq. (8). In order to obtain $\varepsilon = 0.04$ for reactor conditions, it is necessary to improve the system; for example, one might divide the incoming ion flux into several layers of smaller width d, focus the beam beforehand to compensate for the repulsive effect of space charge, and achieve direct conversion of part of the perpendicular energy $W_{\perp}$ which is not recovered in the proposed system.

LITERATURE CITED

1. R. Post, B. N. E. S. Nuclear Fusion Reactor Conference, September, 1969, Paper 2.1, p. 88.
2. R. Moir et al., IV IAEA Conference on Plasma Physics and Controlled Nuclear Fusion Research, Wisconsin, June 17-23, 1971, CN-28/K-1.

THEORY OF THE SELF-CONSISTENT INTERPRETATION OF SPECTRA IN ACTIVATION ANALYSIS

N. V. Zinov'ev and N. M. Mukhamedshina

UDC 519.281.3:539-16.08

Successful application of large electronic computers in activation analysis is possible only for sufficiently effective algorithms. At the same time, it is quite obvious that calculational methods, exhibiting analogs of the graphical variations in the interpretation of spectra, cannot provide significant improvements in sensitivity and stability for determination of impurities. They do not confirm the expectations and the simple formalisms of the method of least squares, since they do not take into account the polyisotopic nature of the standards and the potentialities of their contamination. The main difficulty with simple formalisms of the method of least squares is the combination of a large number of extremely small components because of the likelihood that the samples and standards contain all the elements of the periodic system.

The algorithm discussed below takes into account the enumerated difficulties and, consequently, can lead to some broadening of the possibilities for instrumental activation analysis.

Let us take a system of amplitudes $\Phi(k, i)$ for the spectra of a sample. Within the limits of error, one can state that for sufficiently wide variations in the mass-time parameter i (i = 1, 2, 3, ..., R) and the number of channels k (k = 1, 2, 3, ..., n), there is satisfied the equality

$$\Phi(k, i) = \sum_{j=1\ (j\neq i)}^{R} \alpha_{ij}\Phi(k, j),$$

in which α_{ij} are linear coefficients which are determined by means of the method of least squares.

If in this sense the system of $\Phi(k, i)$ is complete, and this is possible in principle for any sample, then Eq. (1) will be satisfied for any i. One can regard the self-consistency of a specimen's spectra as a marked effect, and methods of interpretation are based upon this fact through the self-consistencies.

Let us assume now that it is necessary to determine the presence of an element whose standard provides a system of amplitudes f(k, i) for the spectra. The spectra of a sample and a standard can be represented by the expressions

$$f(k, i) = \sum_{m=1}^{q} A_m\Psi_m(k)\, C(m, i) + \varphi(k, i);$$

$$\Phi(k, i) = \sum_{m=1}^{q} B_m\Psi_m(k)\, G(m, i) + \overline{\varphi(k, i)},$$

where q is the number of significant isotope-identifiers for an element, activated with irradiation; A_m, B_m are the initial activities; $\Psi_m(k)$ is the form of the normalized spectrum of the isotope-identifier; C(m, i), G(m, i) are the mass-time coefficients of the i-th isotope; $\overline{\Phi(k, i)}$, $\Phi(k, i)$ are ensembles of mixing activities.

For the representation of the interpretation algorithm, we define the spectra

$$H(k, i) = \Phi(k, i) + \sum_{j=1}^{p} f(k, j)\, N(j, i);$$

$$Z(k, i) = \Phi(k, i) - \sum_{j=1}^{p} f(k, j)\, N(j, i).$$

Translated from Atomnaya Énergiya, Vol. 33, No. 1, pp. 589-590, July, 1972. Original article submitted August 23, 1971.

One can select the optimum values of the matrix elements N (j, i) only in a known combination of activities or by iteration methods. Therefore, without great loss to the result, one can represent them by quantities of the Kronecker symbol type.

The number p of spectra for a standard should be nearly complete in the same sense as has been discussed for Eq. (1).

The essential self-consistent interpretation of spectra justifies any of the following four statistical systems of linear equations:

$$\Phi(k, i)=\sum_{j=1}^{r_1} H(k, j)\, W_1(j, i)+L_1(k, i);$$

$$\Phi(k, i)=\sum_{j=1}^{r_2} Z(k, j)\, W_2(j, i)+L_2(k, i);$$

$$f(k, i)=\sum_{j=1}^{r_3} H(k, j)\, W_3(j, i)+L_3(k, i);$$

$$f(k, i)=\sum_{j=1}^{r_4} Z(k, j)\, W_4(j, i)+L_4(k, i).$$

Here the functionals L_s (k, i) are represented by the expressions

$$L_s(k, i)=\sum_{j=1}^{E_s} u(k, j)\, \alpha_s(j, i);$$

the matrices W_s (j, i) and α_s (j, i) form a set of linear coefficients which are determined by the method of least squares; u (k, j) are various combinations of the spectra for the standards and samples consisting of the mixing components.

The isotopic composition of u (k, j) should not be crossed with the selected forms $\Psi_m(k)$ in the spectra f (k, i). The necessity of the $L_s(k, i)$ is connected with the possibility for incompleteness of the $\{\Phi(k, i)\}$ and $\{f(k, i)\}$ systems.

Within the limits of statistical error, the coefficient coupled with the spectrum $\Psi_m(k)$ ought to equal zero. This provides a possibility for determining the ratio B_m/A_m. Since this ratio will depend on the original Eqs. (6)-(9), then the desired estimate of the contents

$$\rho_s(m, i)=\left[\frac{B_m(i)}{A_m(i)}\right]_s$$

depends on the type of expansion (s = 1, 2, 3, 4), Eqs. (6)-(9), the isotope-identifier number of the element (m = 1,2,...,q), and the spectrum number of the sample or standard (i = 1, 2, ..., R or i = 1, 2, 3 ..., p). Therefore, obtaining a series of quantities $\rho_s(m, i)$, it is necessary to average them taking account of the fact that, with fixed s and m, the set of estimates for $\rho_s(m, i)$ when i = 1, 2,..., R (or p) can be considered nearly statistically independent; a significant statistical dependence is observed with other combinations of indices among the estimates.

In Eq. (11), the statistical quasi-independent variables W_s (j, i) enter nonlinearly. Consequently, the mathematical expectation $\overline{\rho_s(m, i)}$ can differ significantly from the most probable, i.e. essential for analysis, value of the quantities $\rho_s(m, i)$ which is obtained by substitution into Eq. (11) of the estimates W_s (j, i) following from the method of least squares. Because of this same statistical variance of the estimates, one must determine the quantity

$$D^2[\rho_s(m, i)]=\int_{-\infty}^{\infty}[\rho_s(m, i)-\overline{\overline{\rho_s(m, i)}}]^2 \prod_{j=1}^{R, p} V[W_s(j, i)]\, dW_s(j, i)$$

in which the function $V[W_s(j, i)]$ is a probability density.

The integral (12) does not have an analytical representation, therefore one must utilize either numerical integration or another approximation method. The final averaging of the $\rho_s(m, i)$ with the calculated variances, which are interchangeable in the given case with the quantities $D[\rho_s(m, i)]$, is standard procedure and is not covered in the report.

Application of the program for a partial interpretation [1] provides satisfactory results [2]. But at the same time, difficulties can arise because of the interfering components with half-life periods similar to the period of the isotope-identifier. A self-consistent algorithm does not have such a disadvantage, but

the nonlinearity and the statistical dependence on the final estimate require the determination of the components which affect its efficiency.

LITERATURE CITED

1. N. V. Zinov'ev, At. Énerg., 27, 128 (1969).
2. N. V. Zinov'ev and N. M. Mukhamedshina, Zh. Analiticheskoi Khim., 26, 2127 (1971).

SPATIAL, ANGULAR, AND ENERGY DISTRIBUTIONS OF FAST NEUTRONS BEYOND THREE-LAYERED BARRIERS

V. B. Elagin and G. Sh. Pekarskii

UDC 539.125.52

Spatial, angular, and energy distributions of fast neutrons from a unidirectional point source beyond three-layered barriers of steel–plastic–steel and tungsten–aluminum oxide–tungsten were investigated in order to determine their dependence on the thickness of the individual layers.

Calculations were carried out on an M-20 computer by the Monte Carlo method for neutrons with initial energies of 14 and 2.5 MeV and for neutrons with the spectrum of a Po-Be source. Multigroup constants* were employed. The energy distribution of scattered neutrons from a source with E_0 = 14 MeV

*L. P. Abagyan et al., Group Constants for Nuclear Reactor Calculations, Atomizdat, Moscow, 1964.

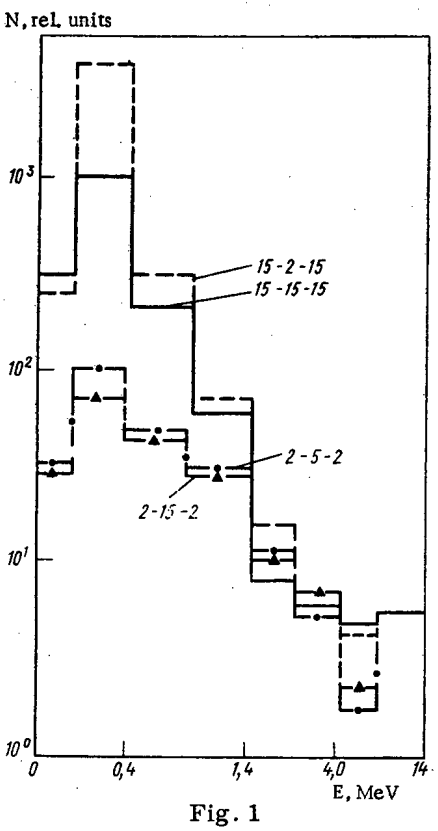

Fig. 1

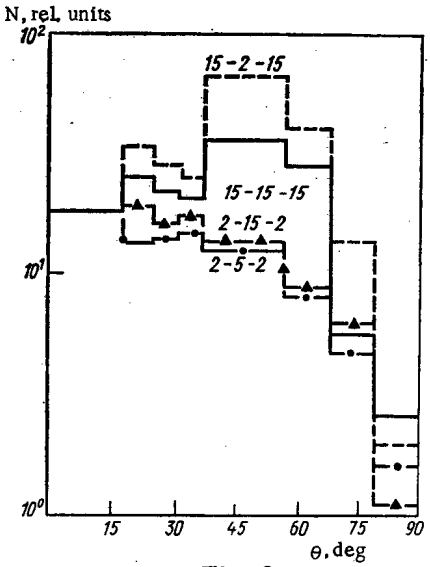

Fig. 2

Fig. 1. Energy distribution of neutrons scattered by a steel–plastic–steel barrier for E_0 = 14 MeV.

Fig. 2. Angular distribution of neutrons beyond a steel–plastic–steel barrier for E_0 = 14 MeV.

Translated from Atomnaya Énergiya, Vol. 33, No. 1, pp. 590-591, July, 1972. Original article submitted September 23, 1970.

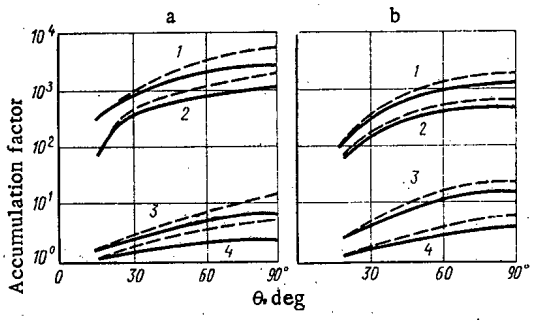

Fig. 3

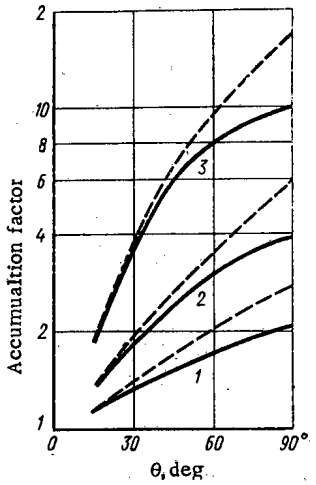

Fig. 4

Fig. 3. Dependence of the accumulation factor on the angle of the detector for steel–plastic–steel barriers with layer thicknesses (in cm): (1) 15-15-15, (2) 15-2-15, (3) 2-15-2, (4) 2-5-2. E_0 = 14 MeV (a); E_0 = 2.5 MeV (b).

Fig. 4. Dependence of the accumulation factor on the collimation angle for neutrons with the spectrum of a Po-Be source and tungsten–aluminum oxide–tungsten barriers with layer thicknesses (in cm): (1) 1-5-1, (2) 2-5-2, (3) 5-5-5.

beyond a steel–plastic–steel barrier is shown in Fig. 1. The curves are labeled with numbers giving the thicknesses of the layers of the barrier in centimeters. The results are normalized to the number of neutrons in the first energy interval and they characterize the spectrum of the neutrons passing through a unit area. The angular distribution of the neutrons is shown in Fig. 2. The results are normalized to the number of neutrons in the angular interval $0.95 < \cos\theta \leq 1.0$.

Frequency functions of neutron fluxes $\bar{J}(z, \theta, E)$ and $N(z, \theta, E)$ were used in the calculation of certain functions of the radiation field beyond the barrier. Specifically dependence of the accumulation factor of fast neutrons on the collimation angle of the detector was studied.

The results are shown in Figs. 3 and 4. The solid curves correspond to the accumulation factor for neutron currents and the dashed curves to the fluxes.

These results enable one to determine the effect of the collimator aperture on the recorded contribution of scattered neutrons and the difference in detector readings between neutron fluxes.

AUTORADIOGRAPHIC VARIANT OF ACTIVATION ANALYSIS FOR INVESTIGATING SOLUBILITY OF IMPURITIES IN SEMICONDUCTORS

G. F. Yuldashev, M. M. Usmanova, and Yu. A. Vodakov

UDC 3.543.53

The study of the quality of alloying of semiconductors in reference to different methods for growing semiconductor crystals, and determinations of the solubility of various impurities in semiconductors, are matters of considerable interest. Most of the analytical techniques available, including activation analysis, provide a general picture of the content of the analyzed component in the specimen independently of whether that component is present in the form of a solid solution or whether it is present in the form of inclusions belonging to a second phase. Random microinclusions consequently introduce a certain error into the results of an analysis undertaken with the object of ascertaining the content of the component present as a solid solution alone [1].

We set up experiments to determine the solubility of scandium, yttrium, chromium, and several rare earths in specimens of silicon carbide grown from melt solutions by the floating zone refining method [2], and of gallium in epitaxial films of silicon carbide prepared by the sublimation method.

The specimens, sealed in quartz capsules, were irradiated by a stream of neutrons of flux density $1.8 \cdot 10^{13}$ neutrons/cm^2 · sec for 10 h or 100 h, depending on the impurity element to be determined. Within 25 to 30 h after irradiation, the specimens were etched in a mixture of HF and HNO_3.

The identity of the alloying impurity and the average concentration of that impurity in the specimen were determined with the aid of a gamma-ray spectrometer with a NaI(Tl) crystal of size 40 × 40 mm.

An autoradiograph was made by exposing the specimen under investigation in close contact with a photographic emulsion, in order to investigate the distribution pattern and achieve a quantitative determination of the concentration of the impurity in different portions of the specimen. Mikrat-300 photographic film was used in this work.

The concentration of impurity was determined by comparing the photographic densities of the autoradiographs taken of the test specimen and of a standard. The sensitivity of the impurity determination was calculated on the basis of the formula

TABLE 1

Number assigned to specimen	Mean concentration of scandium (instrumental variant)		Concentration of scandium in portions of specimen yielding uniform darkening of photographic film, atom/cm^3
	wt. %	atom/cm^3	
1	$3 \cdot 10^{-2}$	$1.3 \cdot 10^{19}$	$2.9 \cdot 10^{17}$
10	$2 \cdot 10^{-2}$	$8.7 \cdot 10^{18}$	$3.0 \cdot 10^{17}$
15	$2.1 \cdot 10^{-2}$	$9.0 \cdot 10^{18}$	$2.7 \cdot 10^{17}$
19	$1.9 \cdot 10^{-3}$	$8.0 \cdot 10^{17}$	$3.0 \cdot 10^{17}$
31	$6.0 \cdot 10^{-3}$	$2.8 \cdot 10^{18}$	$3.3 \cdot 10^{17}$
71	$1.4 \cdot 10^{-2}$	$6.1 \cdot 10^{19}$	$3.1 \cdot 10^{17}$

Translated from Atomnaya Énergiya, Vol. 33, No. 1, pp. 592-593, July, 1972. Original article submitted October 12, 1971.

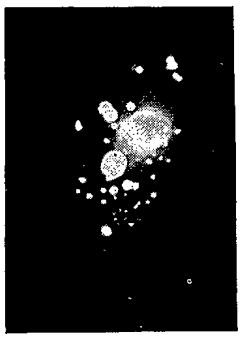

Fig. 1

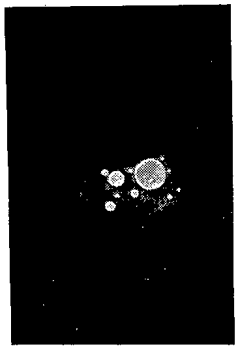

Fig. 2

Fig. 1. Typical autoradiograph of specimen of SiC grown from a melt solution (scandium) 400 μ in thickness.

Fig. 2. Autoradiograph of same SiC specimen with thickness reduced to 100 μ.

$$n = \frac{2\lambda D}{hf\sigma\Theta\,(1-e^{-\lambda t_1})\,e^{-\lambda t_2}\,(1-e^{-\lambda t_3})}\ \text{atom/cm}^2,$$

where λ is the decay constant of the isotope obtained in the activation of the impurity, in sec^{-1}; D is the minimum number of β-particles bringing about a sufficiently distinct radiograph, in units of 10^8 electrons per cm^2 [3]; h is the thickness of the specimen, in cm; f is the neutron flux, neutrons/$\text{cm}^2 \cdot \text{sec}$; σ is the activation cross section of the impurity, in cm^2; Θ is the abundance of the impurity isotope being activated, in a naturally occurring mixture of isotopes; t_1 is the activation time ($t_1 = T_{1/2} < 100$ h, and $t_1 = 100$ h when $T_{1/2} > 100$ h); t_2 is the time interval extending from the end of the irradiation exposure to the beginning of the measurements (this time is determined by the properties of the matrix; $t_2 = 45$ h in the case of a matrix containing silicon); t_3 is the exposure time for autoradiography.

It was found, as a result, that practically all of the test specimens grown from melts of chromium, scandium, yttrium, and the various rare earths, contain without exception appreciable inclusions over the entire surface area of the crystals, apparently either in the form of disseminations of pure solvents or in the form of their carbides or silicides. Figure 1 shows a typical radiograph of such specimens. This accounts also for the large spread in the concentrations arrived at via the instrumental method, e.g., for scandium in various specimens grown under identical conditions (see Table 1).

It is clear in Fig. 1 that the photographic density due to fogging of the photographic emulsion by the disseminations of impurity is quite high in the case of specimens 300 to 400 μ thick: there is overlap from distinct fogging points. Reduction in specimen thickness brought about by polishing made it possible to eliminate several points on the radiographs, with halo in the remaining points reduced somewhat (Fig. 2).

The solubility that we found (e.g., for scandium in silicon carbide grown from a melt solution) is $3 \cdot 10^{17}$ atoms/cm^3. The same method was resorted to in order to find tentative values of the solubility of chromium, yttrium, and various rare earths in silicon carbide.

LITERATURE CITED

1. V. M. Glazov and V. S. Zemskov, Physicochemical Fundamentals of the Alloying of Semiconductors [in Russian], Nauka, Moscow (1967).
2. G. F. Yuldashev et al., Report to the IV All-Union Conference on Semiconducting Silicon Carbide [in Russian], Giredmet, Moscow (1972).
3. M. E. Drits, Z. A. Sviderskaya, and É. S. Kadaner, Autoradiography in Metals Science [in Russian], Metallurgizdat, Moscow (1961).

REDUCTION IN THE OFF-DUTY OPERATION FACTOR FOR A LINEAR ACCELERATOR

D. I. Adeishvili, I. A. Grishaev,
N. I. Mocheshnikov, and A. E. Tolstoi

UDC 621.384.64:539.122

In connection with the ever increasing restrictions on the beam parameters for linear electron accelerators (LEA) and with the extension of their performance for conducting a physical experiment, the LEA-storage element system can be the means of overcoming several limitations inherent in accelerators of that type. Even earlier, attention was drawn to a stored beam-thin target system, interesting from the point of view of the possibilities for experiments of a wide variety of types and precisions [1]. There is also a design for for the construction of a ring-shaped electron beam dilator in the LEA [2].

In the present work, it is shown that with the aid of a storage element, without any intrinsic changes in its structure and design, the pulsed electron beam of a LEA is converted into a beam of γ-rays whose intensity and duration can be varied over a broad range.

The investigations were carried out on the storage device of the Institute of Physics and Technology of the Academy of Sciences of the Ukrainian SSR [3] whose injector serves the first five units of the linear accelerator at an energy of 300 MeV [4]. The main operating region for the LEA: 70 MeV electrons, 50 mA current pulse for 1.2 μsec, and 1-50 Hz injection frequency. The accelerator beam (Fig. 1) was formed by a rotation-focusing storage system, inserted in the ring, whereupon it was trapped by the inflector's pulse field and gathered in the magnetic path, along with a switched on HF-supply. The target in the form of an $\sim 35\ \mu$ ($\sim 2.5 \times 10^{-3}$ rad) thick wire could be introduced remotely into the operating region of the ring's vacuum chamber and mounted vertically with an accuracy of ± 0.5 mm relative to the equilibrium orbit of the circulating beam. The resulting interactions of the electrons with the target resulted in the production of bremsstrahlung radiation in the detection apparatus. In addition an opportunity was provided to measure the inherent life-time of the beam in the target through the synchrotron radiation by means of a photomultiplier.

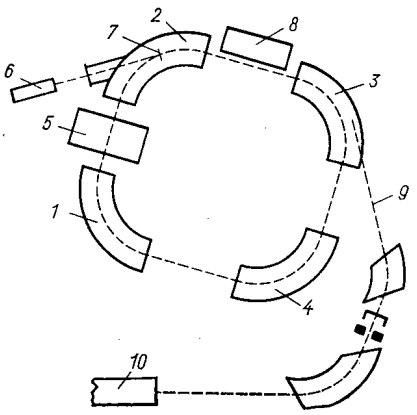

Fig. 1. Experimental arrangement: 1-4) storage quadrants; 5) high frequency gap; 6) γ-ray detector; 7) target; 8) inflector; 9) trajectory of the electron beam which is injected into the ring; 10) LEA exit.

The interaction of the circulating beam with the target can be achieved in two ways: a) during the entire time of the experiment, the target was located in the storage element's chamber at the equilibrium orbit; the injection of particles was carried out at a constant frequency in the presence of the target; b) at first there occurs a buildup of the maximum possible number of particles, after which the target is introduced until it comes in contact with the stored beam; afterwards, as all of the particles thoroughly interact, the target is removed from the chamber, and the cycle is repeated.

The first method provides an opportunity of obtaining a quasi-continuous beam of γ-quanta with an off-duty factor $\lesssim 10$ (in its dependence on the storage element, injector, and target parameters), thus the beam is "expanded" by a factor of 10^3. However, the background conditions in this case will be unfavorable because of the

Translated from Atomnaya Énergiya, Vol. 33, No. 1, pp. 593-594, July, 1972. Original article submitted October 7, 1971.

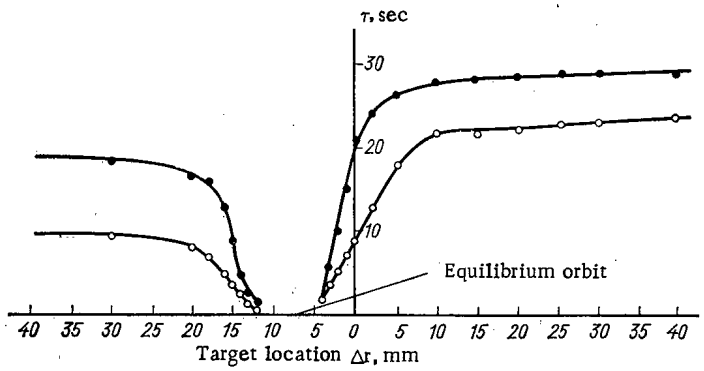

Fig. 2. Dependence of the stored electron beam's lifetime on the target's position, measured by bremsstrahlung (●) and synchrotron (○) radiation.

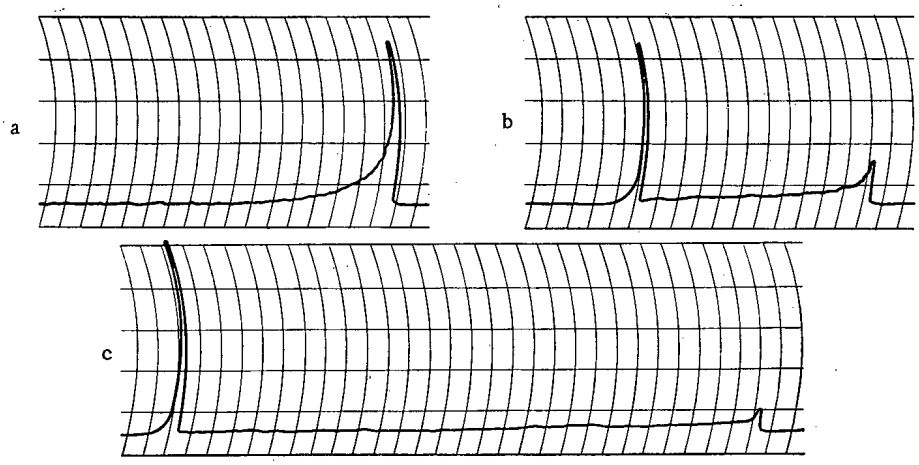

Fig. 3. Dependence of the bremsstrahlung radiation intensity on the time for different mutual orientations of the circulating beam and the target (the course of time is from right to left; the scale is 1 sec per unit: a, b, c represent the target at distances of 4, 8, and 16 mm, respectively, from the equilibrium orbit.

incomplete agreement of the accelerator's and the storage element's phase spaces, which usually occurs in an actual situation.

The second method provides a more "pure" result, because the target is introduced into the stabilized circulating electron beam when the accelerator-injector is disconnected. The experimental results obtained by using the second method are cited below.

The γ-quanta yield per electron with interaction of the beam with a target is estimated on the basis of the relationship for the scattering of particles in matter [5], taking into account the maximum permissible angle for the deflection of the particles in the chamber of the storage element under consideration ($\theta^2_{max} \approx 3.5 \times 10^{-3}$):

$$\frac{N_\gamma}{N_-} \approx \frac{\theta^2_{max} E^2_-}{E^2_s},$$

where E_- is the electron energy; E_S is a constant having a dimension of energy [5] (for example, when $E_- = 100$ MeV, the yield $N_\gamma/N_- = 8 \times 10^{-2}$).

In the first series of experimental measurements, the effects of the target are explained by the dynamics of the stored beam [6]. The measurements were carried out simultaneously on the synchrotron and the bremsstrahlung radiation. The lifetime of the circulating beam (the time for the particle intensity to be reduced

by a factor of e) was determined. The results are presented in Fig. 2. It is seen that the character of the variation in both curves is identical. The deviations in the absolute values of the bremsstrahlung and the synchrotron signals are explained by the aftereffects of the components of activity induced in the elements of the injection and measuring channels, and the decrease in the curves on the left is explained by the "cut-out" of the vertical apertures of the storage device's vacuum chamber (and the corresponding lifetime of the beam) in proportion to that introduction of the target into the chamber. The results obtained show that by varying the position of the target with respect to the equilibrium orbit one can obtain a beam of bremsstrahlung radiation of various durations.

Further investigations were carried out with an improved vacuum in the storage element's chamber (6×10^{-8} mm Hg) which ensured a lifetime of 240 sec for the stored beam without a target. In Fig. 3, there is presented the dependence of the bremsstrahlung radiation intensity on the time for different mutual orientations of the electron orbit and the target. Measurements were conducted with a circulating current of 5–8 mA which corresponds to $(6 - 9.6) \times 10^8$ electrons in the storage element and an integrated yield of $\sim 10^7$ γ-quanta. As is seen from Fig. 3, this current can be distributed over time in a desired manner. The peak on the left in the graphs is a result of a rapid discharge at the target of a part of the circulating beam which does not interact completely with the target at the end of the cycle.

The results obtained indicate the possibility of producing a continuous beam of γ-quanta by means of a LEA-storage element system. One should consider these results as preliminary because the problem of obtaining a maximum possible photon yield has not been raised. Meanwhile, increasing the number of stored particles up to 10^{11}, which is completely feasible under our conditions, can produce a photon yield up to 10^9–10^{10} per cycle.

LITERATURE CITED

1. V. G. Zelevinskii et al., Izv. AN SSSR, Seriya Fiz., 33, No. 4, 686 (1969).
2. R. Beck et al., DSS/SOC-ALLIS-32. SEFS-TD-70.65, October (1970).
3. Yu. N. Grigor'ev et al., At. Énerg., 23, No. 6, 531 (1967).
4. A. K. Walter et al., in: Proceedings of the International Conference on Accelerators (Dubna, 1963) [in Russian], Atomizdat, Moscow (1964), p. 435.
5. R. Roy and D. Reed, Interactions of Photons and Leptons with Matter, Academic Press, New York –London (1968), p. 93.
6. D. I. Adeishvili et al., Preprint FTI AN USSR, KhFTI-70-29, Khar'kov (1970).

ABSORPTION SPECTRUM OF IRRADIATED POLYMETHYLMETHACRYLATE

N. P. Kuz'menko and N. P. Dergachev

UDC 678.01:539.12.04

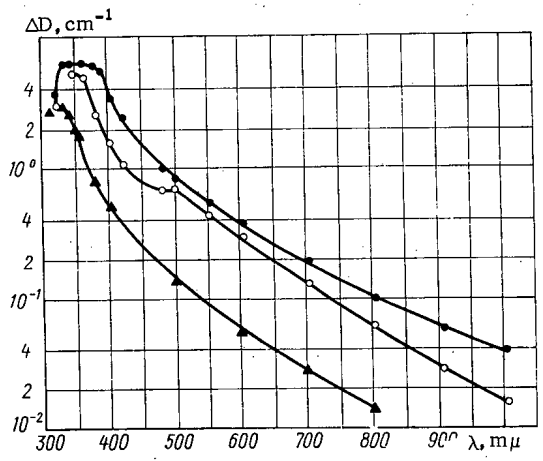

Fig. 1. Absorption spectra of polymethylmethacrylate after various irradiation doses for P = 130 R/sec. ●) I = 10^6 R; ○) I = 10^7 R; ▲) I = 10^8 R.

The absorption spectrum of polymethylmeth acrylate (type SOL) irradiated by Co^{60} γ rays was investigated and the dependence of the increase in optical density on dose received and its rate was studied. The absorption spectrum was determined in the 320-1000 mμ range using an SF-4 spectrophotometer. The error in measurement of the optical density was less than 3%. The dose rate was determined by calculation and was monitored with glass dosimeters. The relative error in the determination of the dose rate was $\lesssim 10\%$.

Observation of the changes in optical density could only be carried out up to a dose of $\sim 10^8$ R because the samples became brittle with further irradiation and cracked spontaneously. The results are shown in Figs. 1-3.

The increase in optical density was determined from the equation

$$\Delta D = D_f - D_i, \quad D = -\lg K,$$

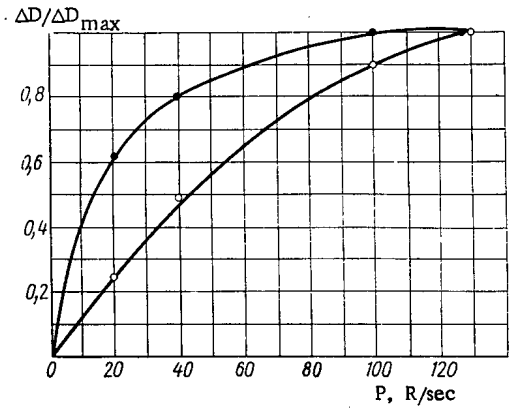

Fig. 2

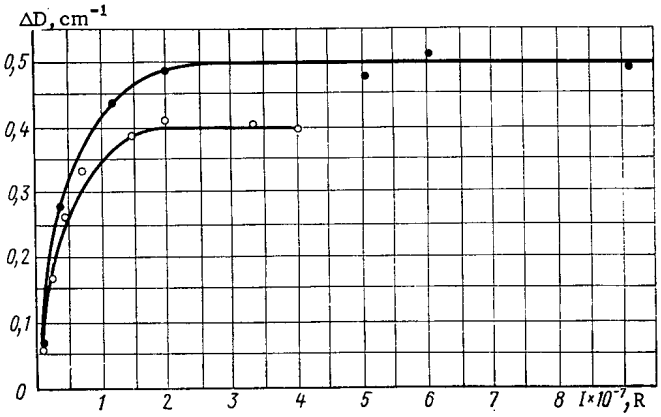

Fig. 3

Fig. 2. Relative variation of the increase in optical density as a function of dose rate for I $\gtrsim 3 \times 10^7$ R: ●) Λ = 360 mμ; ○) Λ = 1000 mμ; $\Delta D_{max} = \Delta D_{(P = 130\ R/sec)}$.

Fig. 3. Increase in optical density as a function of irradiation dose for Λ = 550 mμ: ●) (= 130 R/sec; ○) P = 40 R/sec.

Translated from Atomnaya Energiya, Vol. 33, No. 1, pp. 595-596, July, 1972. Original article submitted October 21, 1971.

where K is the transmission factor, and D_f and D_i are the final and initial optical densities of the sample respectively.

The change in optical density of polymethylmethacrylate can be described by the relation

$$\Delta D = \frac{AP}{\lambda}(1 - e^{-\lambda t}),$$

where A is the coefficient of optical radiation resistance, $cm^{-1}R^{-1}$; λ is the rate constant for thermal decay of color centers which depends only on wavelength at a fixed temperature, sec^{-1}; t is the irradiation time sec; $t = I/P$; I is the irradiation dose, R; P is the irradiation dose rate, R/sec.

Figure 3 shows three characteristic regions of variation in induced optical density as a function of irradiation dose:

1) a region of linear dependence which extends over doses $< 10^6$ R; Eq. (1) then takes the form $\Delta D = AI$;

2) a transition region where ΔD is a function of both I and P; this region extends from 10^6 to (2-5) $\times 10^7$ R;

3) a saturation region at doses $\geq 3 \times 10^7$ R. ΔD has a constant value; Eq. (1) then takes the form $\Delta D = \Delta D_{max} = AP/\lambda$.

Figure 2 shows ΔD_{max} as a function of P, and three similar regions of ΔD_{max} variation are seen. Thus a thin layer of plastic (~ 0.5 cm thick) irradiated to a dose of $\sim 10^7$ R can be used as a filter for ultraviolet radiation (in the wavelength region 320-400 mμ).

INFORMATION

RADIOISOTOPE PROCESS MONITORING AND RESEARCH TECHNIQUES IN THE BUILDING MATERIALS INDUSTRY

I. G. Abramson, E. I. Pavlov,
and V. L. Chebotarev

The all-Union science and engineering seminar on exchange of experience in the use of ionizing radiations for research and monitoring of technological processes in the building materials industry was held in Moscow, March 28-31, 1972.

Representatives of scientific institutions, colleges, and industrial plants (numbering over 70 persons) took part in the deliberations of the seminar; representatives of instrument design organizations were also in attendance. Some 29 reports were heard and discussed.

It was shown that work on applications of ionizing radiations is being carried out along the following lines at the present time.

1) Development of techniques and instruments for monitoring of various parameters for cases where monitoring of these parameters with the aid of instruments based on other (non-radioisotope) techniques would be either impossible altogether, or would fail to meet production requirements.

2) The use of already approved procedures, as well as working out, and realizing in practice, new options for applications of radioactive isotopes as tracers in the investigation of various problems whose solution by other methods would be either impossible or would fail to yield reliable results.

There was considerable interest shown in a report by V. A. Vorob'ev on the results of the development of techniques and equipment for radiation nondestructive testing of concrete products and reinforced concrete products at the Scientific Research Institute for Electronic Introscopy [NIIEI], an affiliate of the Tomsk Polytechnic Institute. Radiation nondestructive testing work in the building industry is confronted with the greatest variety of problems, and three types of betatron flaw detection laboratories have been developed on the basis of betatrons used as radiation sources a stationary variant, a variant featuring a temporary periodically operative control console, and a mobile betatron flaw-detection laboratory mounted on a truck.

A. A. Arkhangel'skii (Leningrad Institute of Railway Transportation Engineers) reported on the capabilities of γ-ray flaw detection in quality control of lumber.

Yu. N. Telkov reported on exploitation of the effect of slowing down of fast neutrons by hydrogen atoms, with subsequent recording of the slow neutrons, in a paper on the development of a device for automatic continuous and contactless monitoring of the moisture content of material in rotary kilns (downstream of a tandem heat exchanger), noting that the device, designed by Giprotsement and VNIIRT institutes, is scheduled to go into large-lot production sometime in 1973.

Also deserving of mention here is a report by E. A. Sokolova on a method of continuous and contactless monitoring of the degree of decarburization of material in rotary kilns now being developed at Giprotsement, and based on the effect of recording neutrons scattered by carbon nuclei in the composition of the limestone.

The effect of attenuation of direct or scattered γ-radiation in the water and in the solid constituents of concrete or sludge (expressed differentially) has been used in the development of instruments for nondestructive and contactless monitoring of the bulk density and water content of a concrete mix laid in the

Translated from Atomnaya Énergiya, Vol. 33, No. 1, pp. 597-598, July, 1972.

foundations of an electric power generating station (Yu. D. Markov, Orgenergostroi State Power Construction Institute). This device is also used in contactless and continuous monitoring of the moisture content of sludge found in cement kilns (E. I. Pavlov, Giprotsement), and for monitoring the bulk density of concrete in products and structures (S. F. Popov, LISI).

Several organizations are using the dependence of the attenuation factor of γ-radiation on the density of lime, which is a function of the degree of calcination, to good advantage in contactless and continuous monitoring of the degree of calcination of lime in shaft furnaces.

Several reports dealt with valuable findings obtained by radioisotope tracer techniques. This method has proved highly efficacious (A. A. Gusev, LISI) in studies of pollution of the atmosphere by industrial plants venting fumes from smokestacks and ventilation systems, and in finding the optimum control devices for industrial ventilation systems.

A novel application of the radioactive tracer technique was found in the development of a procedure for determining the impermeability of building materials to water by recording neutrons generated via the (α, n)-reaction in the interaction between nuclei of the stable tracer isotope B^{10} dissolved in the filtration liquor (water) and α-particles (the source of the latter was situated on the side of the concrete specimen opposite to the solution feed point). The reaction is initiated at the instant when the tracer traverses the entire bulk of the specimen. This development was reported on by L. S. Pavlov (All-Union Scientific Research Institute for Physics and Radio Engineering Measurements, and the All-Union Scientific Research Institute for Hydraulic Engineering and Land Reclamation).

The radioactive tracer method is being used on a broad scale and in fruitful applications in current research on patterns of material flow and dust travel through closed heat power equipment (F. I. Bednyakov, Volgograd branch of SUMNRT, T. E. Eenmaa of the Punane Kunda cement factory, Yu. S. Shlionskii, L. S. Fraiman and V. A. Boikov of Giprotsement), and in optimization of working conditions in construction of pulverizing mills for cement production (M. A. Veridyan, NIItsement).

V. L. Chebotarev (Giprotsement) reported on work aimed at discerning the dependence of the shape of detector curves obtained in radiotracer experiments on the geometrical conditions in recording of γ-emission from the labeled material, and on the parameters of the source and of the radiation detector, and also on the rate of travel of the labeled material relative to the detector.

After the reports had been discussed, recommendations designed to contribute to further progress in the building materials industry were presented and discussed.

It is recommended that the seminar reports be published in order to facilitate a more effective exchange of information.

LEARNED COUNCIL OF THE INTERNATIONAL THEORETICAL PHYSICS CENTER

B. B. Kadomtsev

The ninth session of the Learned Council of the International Theoretical Physics Center was held in Trieste on January 11-12 of the current year. The council heard a report by its director, Abdus Salam, on the activities of the Center during 1971, and placed on the agenda the proposed program of scientific activities of the body during 1972-1973.

The fundamental purpose of the Theoretical Center is to encourage the further development of theoretical physics by preparing research cadres and conducting scientific research. Attention is centered on the needs of the developing countries. Workteams on various narrow topics have been organized to aid the theoretical physicists of those countries in continuing and further developing scientific research. Both youth and more experienced representatives of the older generation are being attracted to the program. The workteams conduct original theoretical research and provide preparation for young researchers. In addition, the Center organizes conferences, symposia, and colloquia on narrow ranges of topics, and also invites outstanding scientists from various countries to lecture at the Center.

Since January 1970 the Center has been under IAEA and UNESCO sponsorship (previously, it had been under IAEA) and this was reflected to a considerable extent in its program: UNESCO is more interested in the development of research on solid state physics and mathematics. At the present time, and in subsequent years, the main topics of interest at the Center will be high-energy physics and solid state physics. Original research and topical colloquia will be held annually on those subjects. In addition, there will be research efforts (but on a lesser scale, and alternating in time) on nuclear physics and plasma physics. Only conferences and topical colloquia are proposed on other sectors of theoretical physics and on mathematics.

Two research workteams on nuclear physics and solid state physics were organized in 1971, as well as two expanded lecture series: "Nuclear physics" and "Mathematics as the language of physics." In addition, research was conducted on elementary particles, and topical conferences were organized on the quantum theory of gravitation, the physics of photons, astrophysics, and marine physics. The Center was visited by about 760 physicists from 64 countries, including the Soviet Union. The "Mathematics as the language of physics" lecture series was well attended: there were 239 scientists from 54 nations (other than those represented in the Center at that time) present.

The principal topic for 1972 is solid state physics. UNESCO and UNODP (United Nations Organization Development Program) are financing the work. The year began with a three-month expanded course on the solid state led by G. Seiman, and later on a research workteam will be working up to July.

The second (monthly) lecture series, also supported by UNODP, proposes to take up applied mathematics (general analysis and its applications to physics), in July, after which a mathematical workteam will be organized on the theory of functions, harmonic analysis, and dynamical systems (note that fundamental results have been obtained by Soviet mathematicians in those areas).

Research on elementary particles, and modest topical conferences on high-energy physics, and on the history of the quantum theory, etc., are also being planned.

Plans for 1973 call for organizing an expanded course on the physics of atomic phenomena (led by A. Kastler). Two workteams, on nuclear physics, and on the solid state, will be organized. Topical colloquia

Translated from Atomnaya Énergiya, Vol. 33, No. 1, p. 598, July, 1972.

on plasma physics and an expanded course on the physics of the sea and atmosphere are being planned, to be followed up by the organization of a research workteam. But the basic research topics at the Center must still continue to be solid state physics and high-energy physics. It has also been proposed that research on mathematics be continued in 1973, but a more detailed program agenda will be decided upon later.

Research on the solid state, mathematics, high-energy physics, and nuclear physics is planned for the 1974-1975 period. An international conference on plasma theory is a possibility for 1975.

The Learned Council approved the report on the activities of the Center for the outgoing year, and approved the work program of the Center for 1972.

DEVELOPMENT OF FAST NEUTRAL ATOM INJECTORS FOR THERMONUCLEAR FACILITIES IN THE USA

N. N. Semashko

In January 1972 representatives of the USSR Government Committee on the Utilization of Atomic Energy (V. V. Alikaev and N. N. Semashko) visited scientific laboratories in the United States at Oak Ridge, Livermore, Berkeley, and Princeton and became acquainted with research on the production of intense, fast ion beams and neutral atom beams in conjunction with the controlled thermonuclear research program. The fast particle injectors are designated for the accumulation of plasma in open traps or for its heating in closed systems. The goal is the creation of focussed beams of tens of amperes at energies from a few kiloelectron volts to tens of kiloelectron volts. At the same time our representatives became acquainted with methods of high-frequency plasma heating in closed systems.

The possibility of additional plasma heating in closed systems by means of fast neutral atom injectors is being studied at Oak Ridge. The ohmic heating employed at present is limited by the fact that the plasma resistance falls with the growth of its temperature, and furthermore a skin effect exists. Evidently this method alone will not permit attainment of high ion temperatures necessary for thermonuclear reactions. Among the methods of additional plasma heating, fast neutral atom injection possesses definite advantages, since one can easily change the energy of the injected particles and it is comparatively simple to join the injector to the magnetic confinement system. The power efficiency of the whole system can be fairly large and the cost comparatively low. This whole discussion is based on the assumption that the injection of particle beams does not cause additional plasma losses from the confinement device.

The energy of the particles is chosen such that their thermalization time is shorter than their lifetime in the trap. The capture of atoms is dependent on their ionization by ions and electrons of the plasma, and the mean free path of the atoms to ionization must be small in comparison to the length along which their capture in the trap can occur. At the same time it is necessary to insure the penetration of the particles to the center of the plasma column. The fraction of the energy shared immediately by the plasma ions decreases with increasing energy of the injected particles, and the fraction of the energy given to the plasma electrons grows. The efficiency of the injection circuit has an optimum with regard to energy.

At Oak Ridge a toroidal trap "Ormak" (G. Kelly) is being constructed with a minor radius of 23 cm and a major radius of 80 cm. The magnetic field at the center of the column is to be 25 kG and the plasma volume 8×10^5 cm^3. A beam of atoms with a diameter 9 cm is to be injected along a tangent to the plasma column and the length of the capture region will be about 150 cm. The energy of the beam must be comparable with the energy obtained in the plasma by ohmic heating, and the introduction of the beam must be accomplished during a time less than the energy loss lifetime of the plasma. To obtain a plasma with a density 2×10^{13} cm^{-3} and ion and electron temperatures on the order of 0.5-1 keV by joule-heating, an energy of 10-20 kJ is expended. During the expected energy lifetime of 20-100 msec the energy given to the plasma from the beam must reach 5-25 kJ. It is planned to install four injectors for introduction of the beams into the trap, each with 8 A (equivalent) at an energy of 20-40 kev.

For this the ion source "duopigatron" (O. Morgan) was developed. It is a modification of the four-electrode Ardenne–Demirkhanov source. The oscillating discharge of the duo-plasmatron source burns in a magnetic field falling almost to zero, where the ion-emission surface with an area of about 20 cm^2 is created. The ion acceleration and beam formation is produced by a system of three copper electrodes (5 cm in diameter) containing tens and hundreds of calibrated apertures with diameters of 2-4 mm. The

Translated from Atomnaya Energiya, Vol. 33, No. 1. pp. 599-600, July, 1972.

transparency of the electrodes reaches 50%. The emission current is approximately 1 A for ion energies of 1.5-5 keV and about 4 A at energies of 20-40 keV. The current pulse duration is about 0.1 sec. Dissociation and charge exchange of the beam containing about 50% H^+ ions and 50% H_2^+ ions occurs in the gas flowing out of the source. The absence of a magnetic lens permits use of both beam components. The source is placed at a distance of 0.8-1 m from the entrance to the plasma confinement chamber. About half of the ion current coming out of the source is within a divergence angle of ±1.2° and corresponds to the entrance aperture of the trap (with a diameter of 9 cm). An ion current of 2.25 A at 35 keV is transformed into a neutral atom beam with an intensity of 1.8 A (equivalent) at an energy of 17.5 keV and an intensity of 0.7 A (equivalent) at an energy of 35 keV. The Ormak injection device is planned to begin operation in 1972.

Work on the creation of a hot electron plasma in a minimum B open trap is being done on the device "Interem" (N. Lazar). Plasma heating is accomplished by means of electron-cyclotron resonance heating at a frequency of 10.6 GHz. The suppression of instabilities connected to anisotropic velocities and the presence of a loss cone is accomplished by electron heating at a non-resonant frequency of 36 GHz. A 20 keV neutral atom beam is injected into a preliminarily-created plasma with hot electrons ($n_e \approx 10^{13}$ cm^{-3}) in order to study the accumulation of a hot ion plasma in the device IMP (open trap with minimum B). This permits studying the efficiency of the plasma target at initial stages of accumulation and the behavior of the plasma when Coulomb scattering plays the determining role.

Study of plasma accumulation in open magnetic traps is conducted at Livermore. Apparently fast neutral atom injection is the only effective method for plasma accumulation in such systems. The research must show if it is possible to obtain plasma with thermonuclear parameters by means of such accumulation, and if such a plasma is obtained, whether its parameters can be maintained by means of external injection. The experiments are conducted on two devices: "Baseball-II" and 2X-II. On the first device, programmed injection of fast atoms with energies of 1-20 keV will be carried out at currents of tens of mA (equivalent); on the second device plasma is created by injection of plasma blobs from a gun and its density is to be maintained by means of injection of intense neutral atom beams.

At present the technology for obtaining high vacuum and strong magnetic fields and the development of injection systems create the prerequisites for studying plasma accumulation at high parameters (10^{11}-10^{13} cm^{-3}), for studying the loss related to charge exchange and instabilities, and also for overcoming the instabilities. One of the methods for suppressing instabilities is to program the injection of atoms so that the accumulation of plasma in the trap occurs under conditions of a very broad distribution function of captured ions in velocity space. The energy of the injected particles is slowly increased simultaneously with the increase of beam intensity. The density and lifetime of the plasma increase and a strong coulomb scattering is maintained. The injection parameters for each moment of time are found from the conditions of plasma stability and of maintaining a vacuum in the system.

The device "Baseball-II" (R. Post, C. Damm) is a magnetic trap with minimum-B, plasma volume 10^4 cm^3, magnetic field strength up to 20 kG at the center and a mirror ratio of two to one. At the present time one injector is operating, which can provide the conditions for plasma research in the beam energy range of 1-3 keV. It is planned to place a second injector perpendicular to the first with a particle energy of 5-15 keV. The possibility of setting up an injector with several sources of the calutron type is being investigated to create beams with various ion energies.

In order to obtain a low energy (1-2 keV) continuous beam, an oscillating discharge ion source has been developed (D. Osher, G. Hamilton). The gas discharge plasma flows out into a falling magnetic field, increasing its cross-section fifty times, and forms an ion emission surface with a diameter of 6.3 cm. The ion beam is formed by means of a system with three carefully-adjusted copper electrodes having up to 331 apertures with a diameter of 2 mm. The fundamental difficulty is maintaining homogeneity of plasma density along the ion emission surface, since inhomogeneities significantly increase beam divergence. The total current reaches 1-2 A at an energy of 1-2.25 keV. A directed flow of nitrogen is used as a neutralizer. The nitrogen is introduced through 0.1 mm diameter capillaries and is condensed on a surface cooled by liquid helium. To decrease the gas flow into the trap along the injection path a directed flow of neon is used as a curtain. The neutralization efficiency of a beam containing 80% H^+ ions is about 70%. A current up to 25 mA (equivalent) is introduced into the trap.

Special attention is given to producing atom beams with energies above 100 kev by the following scheme. Positive deuterium ion beams with an energy 1.5 kev are transformed by a cesium vapor target

into a beam of negative ions with a 25% efficiency. The negative ion beam is then accelerated to the required energy and is transformed on a second target into neutral atoms with an efficiency of approximately 70%.

An ion source without a magnetic field (W. Kunkel, K. Ellers) is being developed at Berkley for the external fast neutral atom injectors for 2X-11. The calculated currents are 10-20 A at an energy of 20 keV.

To create a plasma source with an emission surface of about 10 cm^2, a discharge is ignited in a cylindrical chamber with incandescent filament cathodes placed along the external surface of the chamber. The anode is at the center of one end of the chamber and at the other end is the first electrode of the system for the acceleration and formation of the ion beam, as discussed above, with a multitude of calibrated apertures or narrow gaps. The geometry of the electrodes and the size of the apertures is based on the numerical calculations of the ion trajectories, taking into account the shape of the emission surface, the effect of the space charge, and the electrostatic interaction of neighboring elementary beams. The efficiency of gas utilization in this source is not large (about 10%). The current obtained during a pulse of about 20 msec is 5-7 A at a particle energy up to 14 keV.

At Princeton primary attention is given to the study of closed systems, to high-frequency plasma heating in them and also to external particle injection. On the ST Tokamak, created by reconstruction of the C-1 Stellerator, experiments are being prepared to study ion-cyclotron resonance heating (25 MHz). Initially the Tokamak regime with ohmic heating is practised. Formerly, using this regime, with a magnetic field of 16 kG and plasma current of about 20 kA, a plasma with a density of 1.6×10^{13} cm^{-3}, an electron temperature of 400 ev (at the center), and a lifetime of 2 msec was obtained. It is proposed to heat ions at either the first or second harmonic of the ion-cyclotron frequency by introducing several hundreds of kilowatts of high frequency power into the plasma.

Other high frequency heating methods at the electron cyclotron and lower hybrid frequencies are being developed simultaneously on the Spherator device (a system with a levitating ring).

A new toroidal device with adiabatic plasma compression (ATC), similar to Tokamak T-3 in its dimensions, is being constructed. The system contains no iron. The longitudinal current is created by an air core transformer. On the surface of the chamber, combined coils are placed for the joule heating and for plasma equilibrium. The initial major radius of the plasma column is 90 cm and the minor radius is 17 cm. After compression they will be 38 cm and 10 cm correspondingly. During compression the density should increase by a factor of about ten and the temperature by a factor of about three. It is assumed that the electron temperature will reach 2 keV, the ion temperature 1 keV, and the density 2×10^{14} cm^{-3}. During the first stage (ohmic heating) with a duration of 10-20 msec, the magnetic field is about 20 kG in the region of the plasma; the current in the plasma is about 90 kA. The compression process is accomplished in 1-2 msec, during which the plasma column moves into a magnetic field of about 50 kG. A lifetime of about 6-10 msec is expected.

A careful estimate of the advantages of additional plasma heating during the first stage (before compression) by means of fast neutral atom beam injection is being conducted. With an increase in the initial temperature of the plasma particles, a higher final temperature after compression can be obtained. The injection is assumed to occur along a tangent to the plasma column in the direction of the current. The injection current of about 6 A (equivalent) with a deuterium atom energy of 30 kev insures additional heating above the parameters from ohmic heating.

In conclusion it may be noted that the development of injectors and high frequency heating methods is very important as a promising method for the creation of a dense, high-temperature plasma.

BRIEF COMMUNICATIONS

A conference of Soviet and Czechoslovak specialists on scientific and industrial collaboration between the USSR State Committee on the Peaceful Uses of Atomic Energy and the Czechoslovak Atomic Energy Commission (GKIAÉ SSSR and ČSKJE) was held April 10-14 in Moscow, at the GKIAÉ SSSR premises. The conference agenda covered the status of scientific research and experimental design work governed by the July 23, 1970, agreement. Following the discussion, the specialists of the two parties noted that work contributing to the further development and deepening of collaboration between the two countries in the field of nuclear power development had been accomplished during 1971.

A working plan of scientific and industrial collaboration between GKIAÉ SSSR and ČSKJE was signed on April 14, with terms stipulating joint research to be continued along the following lines: water-cooled water-moderated power reactors, fast reactors, chemistry and metallurgy of nuclear fuel, nuclear instrumentation, work in plasma physics, exchange of experience in the organization of patenting and licensing work. This collaboration includes extensive work in the area of devising types of equipment for nuclear power applications, and comprehensive research on materials and production processes in the field of peaceful uses of atomic energy. A broad range of scientists and specialists was drawn upon to represent GKIAÉ SSSR and ČSKJE in these efforts.

In line with an agreement contracted between the governments of the USSR and Czechoslovakia on collaboration in building two 1700 MW rating nuclear power stations in Czechoslovakia, the V/O Tekhnopromeksport agency and the Skoda-export external commerce enterprise signed contracts on May 5 and September 13, 1971. The first power-generating unit of the first nuclear power station is scheduled to go on line in 1977, the second power unit in 1978; the first power-generating unit of the second nuclear power station is scheduled to start feeding power to the Czech national grid in 1979, the second power unit of the second nuclear power station will be ready in 1980.

In March 1972, on the basis of a design assignment agreed upon by organizations on both sides, V/O Tekhnopromeksport agency turned over to the Skoda-export external commerce enterprise the engineering plans for the first power station. The engineering plans and blueprints for the secondary loop are based on the engineering plans for the basic process equipment developed and delivered to the Czechoslovak organizations. The contract for the working design will be signed after the technical plans have been confirmed. Deliveries of primary-loop equipment and other process equipment, parts, and materials for the power stations are planned for the 1975-1979 period.

* * *

Under the terms of a contract, the Soviet V/O Tekhnopromeksport agency will render the German Democratic Republic technical assistance in building the first echelon of the Nord nuclear power station, which will feature two water-cooled water-moderated power reactors with a total power output rating of 880 MW.

At the present time, work has started on rigging and assembly of the basic technological process equipment for the first power-generating unit. The physical startup of the reactor is scheduled for 1973.

* * *

In March 1972, a seminar was held in Vladivostok on the topic: "Applications of radioactive isotopes and radioisotope devices in the national economy." It was organized under the sponsorship of the Far-Eastern Center of Scientific and Technical Information and the Vladivostok section of the specialized board in charge of installation and adjustment of radiation equipment, in collaboration with the V/O Izotop agency.

The seminar was attended by 120 engineering–technical and scientific research workers. Experience with applications of radioisotope equipment, and the outlook for applications of radioisotope equipment in the maritime provinces were discussed: operating experience with radioisotope instruments at the enterprises of the Primorskugol' coal combine, at the Suchan forestry collective, at fisheries, etc.

Translated from Atomnaya Énergiya, Vol. 33, No. 1, p. 601, July, 1972.

An excursion to the Sudoremont shipbuilding works and the Butoshchebenka factory was organized, to familiarize the participants of the symposium with successful work being done with radioisotope equipment at those factories.

The seminar participants showed great interest in the display "Atoms for peace, science for humanity" organized at that time by the USSR State Committee on the Peaceful Uses of Atomic Energy in Vladivostok.

* * *

A scientific–technical conference on the present status and future outlook of applications of radioisotope equipment at enterprises and organizations of the Moscow district of Kiev was held in Kiev in March 1972. The purpose of the conference was to acquaint managers of enterprises and services with the radioisotope instrumentation being manufactured in quantity lots by Soviet industry for monitoring and automatic control of manufacturing processes, and with experience in the use of such devices at industrial plants.

It was pointed out that radioisotope instruments are being used with success at several enterprises, but that most industrial plants of the district are paying insufficient attention to the job of putting such instrumentation into production service, even though they have every reasonable opportunity for doing so. A branch of the V/O Izotop All-Union agency is located at Kiev, and has been making radioisotope equipment and know-how available to interested organizations in the region (this includes radioactive and stable isotopes, dosimetric and radiometric monitoring devices, radioisotope devices and radiation facilities, shielding equipment and shielding materials for handling radioactive devices). Kiev even boasts an organization responsible for the installation and adjustment of radioisotope devices (the installation and adjustment sector No. 3 of the Specialized Board on installation and adjustment of radioisotope equipment). These organizations are currently making a study of local industrial plants (to ascertain the possibilities of incorporating radioisotope equipment into the production processes at those plants), and are making recommendations and finding practical solutions to problems involving applications of radioisotope devices in technological processes.

The managers of local enterprises and services were recommended the GR-6, GR-7, and GR-8 gamma-relay switches, the UR-8 and Udar-5 level gages, the PR-1024V, PGP-2, and GGP-2 density gages, the Neitron-3 and NIV-2 moisture content gages, the TOR-1 thickness gage, and the RSP-12M counters, for process monitoring and automatic process control applications, as well as a variety of gamma-ray nondestructive testing equipment, and neutralizers of static electricity.

Recommendations were presented to scientific research institutes, design and planning institutes, and specialized design offices (SKB) to reflect utilization of radioisotope equipment in the plans and designs of enterprises now under construction or slated for modernization.

BOOK REVIEWS

NEW BOOKS

G. A. Bat', A. S. Kochenov, and L. P. Kabanov

NUCLEAR RESEARCH REACTORS*

Nuclear research reactors are discussed as a specific and extensive class of nuclear facilities. The history of the design and development of research reactors is reviewed for the first time, and special features of the physics and engineering of research reactors, the physical fundamentals of the design of research reactors, their design and technological systems, and trends in further development of research reactors, are discussed.

The book is written for students in physics and engineering colleges. It will be of interest to a broad range of specialists directly involved in the design and operation of research reactor facilities.

J. Mathews and R. Walker

MATHEMATICAL METHODS IN PHYSICS*

This book comprises a lecture course delivered by Prof. R. Feynmann at the California Technological Institute. It offers a rather original approach to most of the standard topics in mathematical physics. An analysis is given of the normal oscillations of specific symmetrical configurations using the methods of group theory, with a diagrammatic presentation of the Fredholm solution of linear integral equations, and dispersion relations and some related integral equations are discussed, along with detailed applications of probability theory in the processing of experimental data.

The book can be used as a textbook for students studying techniques in mathematical physics. Attention is centered on solution of problems and on the discussion of such important topics as numerical methods, group theory, and probability theory, so that the book will prove useful to both scientists and students studying these topics independently.

V. V. Matveev and B. I. Khazanov

INSTRUMENTS FOR MEASURING IONIZING RADIATIONS*

This the second and revised edition of a textbook which originally appeared in 1967.

The fundamentals of the theory and design of instruments for measuring ionizing radiations are presented here. Both general topics relevant to instrument and equipment design, and methods for designing the principal modules and units in such systems, are discussed.

Structural layouts of instruments and semiconductor detectors are dealt with more extensively than in the first edition. Sections on integrated microcircuitry have been added.

The book is a text for students in engineering and physics departments specializing in the design and applications of instruments devised for measuring ionizing radiations. It may also prove useful to engineers, research scientists working in applied nuclear physics and on applications of radioactive isotopes in industry, and also to graduate students specializing in these topics.

*Atomizdat, Moscow (1972).

Translated from Atomnaya Énergiya, Vol. 33, No. 1, pp. 602-606, July, 1972.

N. G. Rassokhin

STEAM GENERATOR PLANTS FOR NUCLEAR ELECTRIC POWER GENERATING STATIONS*

Designs of steam generator units for nuclear electric power generating stations are described, with attention given to validation of the selection of optimized design solutions on the basis of studies of the properties of coolants, and engineering cost considerations. Heat-transfer and physicochemical processes occurring in primary-loop and secondary-loop coolants are discussed, a theoretical basis is laid, and the results of the latest experimental research performed in the areas of the hydrodynamics, heat transfer, and water managements of steam systems are presented. Design calculations for components of the steam generator plants of nuclear power stations are also presented.

The required close attention to the validation of off-design initial data (to be assigned) is given in the presentation of the design procedure. The material in this section is based on new design calculation standards. Engineering cost procedures relevant to steam generators are dealt with in a special chapter.

The book may be useful to senior students on the collegiate level, and also to engineers engaged in the design, operation, and investigation of heat-transfer equipment.

A. G. Sitenko and V. K. Tartakovskii

LECTURES ON THE THEORY OF THE NUCLEUS*

This book comprises a lecture course on the theory of the nucleus given by the authors over the course of several years at Kiev State University. The fundamentals of modern concepts of the structure of the atomic nucleus are presented. The book contains five chapters: 1. Nuclear forces. 2. Nuclear matter. 3. The shell structure of nuclei. 4. Rotations and vibrations of nuclei. 5. Pair correlations in nuclei. Various nuclear models and their interrelations are discussed in detail. Even though attention is centered on the presentation of fundamentals, the latest achievements in the theory of the nucleus are reflected quite amply. Some of the questions discussed have only begun to appear in the periodical literature and have never been presented at the textbook level.

The book is written as a textbook for undergraduate and graduate physics majors in universities and engineering and physics colleges. It may also be useful to instructors and research scientists working in theoretical nuclear physics.

N. P. Galkin, Yu. N. Tumanov, and Yu. P. Butylkin

THERMODYNAMIC PROPERTIES OF INORGANIC FLUORIDES*

Results of calculations of the thermodynamic properties of many-atom fluorides of elements belonging to groups V-VII in the periodic table are discussed.

The methods of statistical thermodynamics applied in computer work over the temperature range from 298° to 5000°K were used to calculate the thermodynamic properties of hexafluorides, pentafluorides, trifluorides, difluorides, and monofluorides of the elements belonging to those groups in the periodic table. Equivalent and reduced molecular constants of the possible models of molecules when the true structure and the geometric and energy constants of the molecule are unknown lie at the basis of the calculations of the thermodynamical properties. It is shown that the accuracy of calculations performed by this method is not inferior to the accuracy attainable in calculations using the true molecular constants.

The reference text can be useful to a broad range of technicians and chemists working at scientific research institutes, in industrial plants, and in design agencies specializing in chemical thermodynamics.

*Atomizdat, Moscow (1972).

V. G. Zolotukhin, I. B. Keirim-Markus, O. A. Kochetkov, et al.,

TISSUE DOSES OF NEUTRONS IN THE HUMAN BODY*

This is a reference manual on the distribution of tissue doses of monoenergetic neutrons in the human body. Procedures for calculating tissue doses are presented, with discussions of the distribution of absorbed dose equivalent at different directions of incidence of neutrons, with the geometry of the human body taken into account.

The book contains some original graphical material and will be of great interest to specialists working in the field of radiation hygiene [health physics] and medicine, dosimetry and shielding, and will also be useful to graduate and senior undergraduate students majoring in related fields.

V. S. Galishev

PROBLEMS IN THE THEORY OF MULTIPLE SCATTERING OF PARTICLES*

This book deals with the theory of the passage of charged particles through matter, with multiple scattering and energy losses taken into account. Considerable space is reserved for the author's original work on investigation of boundary problems referable to γ-photons, electrons, and protons. In that research, the author made use of the most general approximate methods for solving kinetic equations suitable for applications of numerical computational techniques and computer techniques at the present stage.

The book is written for research scientists, senior undergraduate and graduate students specializing in applied nuclear physics.

J. J. Sakurai

CURRENTS AND MESONS*

The book comprises a lecture course presented by J. J. Sakurai to undergraduate and graduate students at the University of Chicago, on the basis of the widely accepted model of vector dominance in the theory of elementary particles, a model of which Sakurai is the author.

The lectures are typified by an original style, liveliness, simplicity, and directness of presentation.

The book is written for senior undergraduate and graduate students and research scientists specializing in the theory of elementary particles.

M. A. Leontovich (editor)

PROBLEMS IN PLASMA THEORY*

Some new and interesting material of practical importance has been accumulated in the realm of plasma theory since the appearance of the fifth, most recent, issue in this series (1967).

This collection of articles contains four review articles: "Quasilinear effects in two-stream instabilities" (A. A. Vedenov, D. D. Ryutov); "Electromagnetic instabilities of a non-Maxwellian plasma" (A. B. Mikhailovskii): "Interaction between radio-frequency fields and plasma" (A. A. Ivanov); "Hydromagnetic stability of closed plasma configurations" (L. S. Solov'ev).

The book is written not only for specialists in plasma physics, but for any readers interested in topics of modern physics. It will be of interest to senior undergraduates, graduate students, and instructors in physics and engineering colleges.

*Atomizdat, Moscow (1972).

V. Hess

RADIATION BELTS AND THE MAGNETOSPHERE*

This book was written by a famous American specialist on outer space, and illustrates the basic results of studies of the magnetosphere and of the interplanetary medium. It contains a review of the basic tenets of plasma physics needed to understand phenomena detected by artificial Earth satellites.

The book will be useful not only to specialists in space physics, but also to a broad range of research scientists interested in the physics of the interplanetary plasma and the geomagnetosphere, as well as to senior undergraduates and graduate students majoring in the related fields.

D. D. Kalafati and V. B. Kozlov,

THERMODYNAMICS OF LIQUID-METAL MHD CONVERTERS*

This book is devoted to the thermodynamics of the magnetohydrodynamic method of direct conversion of thermal energy to electrical energy with the aid of a liquid-metal working fluid. This method holds excellent promise, and has met with wide applications in transportation and stationary power plants based on nuclear sources of heat. Various possible thermal circuits and cycles of liquid-metal MHD direct converters are discussed, along with their ranges of application and special features and configurations. The thermodynamical analysis of possible cycles of liquid-metal MHD direct converters has made it possible to single out the best way of enhancing their effectiveness and optimizing their parameters. A special section of the book is devoted to the outlook for the use of liquid-metal MHD direct converters as the superstructure in a steam turbine cycle in a binary power plant for stationary nuclear power stations.

The book is written for engineers and research scientists engaged in research and design work on facilities for direct conversion of heat power to electric power, and also for students enrolled in power and general engineering colleges.

Yu. I. Gal'perin, L. S. Gorn, and B. I. Khazanov,

RADIATION MEASUREMENTS IN OUTER SPACE*

The features of the object measured and the measurement conditions in outer space determine the specific features and behavior of radiometric instruments used for such measurements, and have led to the design of many forms of specialized equipment for the purpose. The book reviews the basic topics related to measurement of ionizing radiations in outer space: modes of radiation as objects of measurement, and their characteristics, the most characteristic problems to be solved by the equipment; methods for detecting the principal modes of radiation and attaining the required parameters, viz. sensitivity, selectivity with respect to perturbing radiations, etc. Of the available electronic measuring devices, only those specific to space research electronics are dealt with; data processing on board artificial Earth satellites is discussed.

The book is written for research scientists and engineers responsible for measurements on outer-space objects, or for the preparation of the requisite equipment, and also for persons working in the field of nuclear instrument design.

R. I. Alekseev and Yu. P. Korovin

MANUAL FOR COMPUTATION AND PROCESSING OF QUANTITATIVE ANALYSIS RESULTS*

The basic problems confronting workers in analytical laboratories in the computation and statistical processing of results of quantitative analysis of the composition of different substances are discussed.

Methods for calculating and processing the results are presented in handbook form, with appended numerical examples, so that the readers (analytical chemists) can use them directly without formal preparation in mathematical statistics.

*Atomizdat, Moscow (1972).

The book is written for a broad range of analytical chemists working in all fields of the national economy.

V. I. Levin

PRODUCTION OF RADIOACTIVE ISOTOPES*

The book deals with the isolation or production of the radioactive isotopes widely used in the national economy. The methods (or technology) relied upon in the production of the isotopes, and the science and engineering fundamentals of isotope production, are described. The properties of the radioactive isotopes, nuclear reactions occurring in their production, and methods for chemical isolation of the desired material from targets and from nuclear fuel reprocessing wastes are considered.

The book will be of interest to specialists engaged in the production of isotopes and radioactive preparations, and also to research scientists and engineers using isotopes in their work.

M. S. Chupakhin, O. I. Kryuchkova, and G. I. Ramendik

ANALYTICAL CAPABILITIES OF SPARK MASS SPECTROMETRY*

The book deals with one of the most highly sensitive methods of analysis available. Mass spectrometry using a mass spectrometer with a spark ion source can be used to solve such problems as high-sensitivity analysis of materials in common use in nuclear industry and in the space industry for any impurities, analysis of semiconducting materials at any stages in production, investigation of metallic, semiconducting, and insulating thin films layer by layer, determination of the composition of geological and biological specimens and different liquids.

The book is written for a broad range of scientific and engineering–technical workers, physicists, chemists, metallurgists, and instructors and students in colleges.

V. A. Dobromyslov and S. V. Rumyantsev

RADIATION INTROSCOPY*

The physics and engineering fundamentals of radiation introscopic methods of nondestructive testing; "seeing into" opaque objects to detect flaws (inhomogeneities), are presented. The methods are based on transmitting penetrating ionizing radiations through the objects to be inspected, and using electronic image converters and image amplifiers backed up by a television system. The sensitivity and productivity of the methods, and their applications to quality control of materials, billets and ingots, castings, welded and soldered joints, assembly, and other manufacturing processes, are discussed. Data on industrial equipment, on inspection procedures and equipment, on engineering costs, and on labor safety in production are cited.

The book is intended for engineers and technicians engaged in nondestructive testing of products. It may also be useful to research scientists, graduate students and undergraduates in technical colleges, and to persons taking skill-upgrading courses, who are specializing in nondestructive testing methods.

E. Rogers

AUTORADIOGRAPHY*

The method of autoradiography (determining radioactivity with the aid of photographic emulsions) has met with widespread application in various branches of science and industry, and is undergoing rapid improvement. Following a presentation of the principles underlying autoradiographic investigation, the book launches into a detailed description of various techniques currently in use in biology and medicine, enabling the reader to select the appropriate modification of the autoradiographical method for each specific case in his work.

*Atomizdat, Moscow (1972).

The book will be of great interest to a broad range of specialists working with radioisotopes in different branches of biology and medicine, and also to those utilizing radioisotope techniques in different branches of science and industry.

N. P. Belous and P. M. Maiboroda

SPECIALIZED SEWERAGE*

This book is a generalization of production experience on the construction, installation, and geodetic servicing of individual specialization networks for conveying radioactive effluents at plants utilizing nuclear power for peaceful purposes. Specialization sewerage equipment and the special features of the design, fabrication, installation, and safe handling of sewerage devices in construction work are discussed. Experience in the building, installation, maintenance, and geodetic servicing of specialized sewerage is discussed to the fullest extent.

The book is intended for production personnel and technicians, construction workers, and rigging and maintenance men engaged in laying down specialized sewerage networks.

I. K. Sokolova

CHEMICAL METHODS OF DOSIMETRY IN RADIOBIOLOGY* (I. B. Keirim-Markus (editor))

Chemical methods used in the dosimetry of diverse modes of radiation are described. The theoretical fundamentals of chemical dosimetry, the basic types of chemical dosimeters, and methods for analyzing radiation–chemical effects are discussed. Specific problems confronting dosimetry in radiobiology are described, along with ways of solving those problems with the aid of chemical dosimeters.

The book is written for specialists dealing with measurements of absorbed energy in radiobiology, as well as in other branches of radiation engineering.

N. N. Klemparskaya (editor)

AUTOANTIBODIES OF THE IRRADIATED ORGANISM*

Literature data and results of the authors' own researches in the study of the features of the dynamics of autoantibody formation in irradiated organisms, and also in persons undergoing x-ray therapy, are reviewed in this text. Procedures for isolating and purifying preparations of autoantibodies from blood serum and internal-organ tissues of irradiated animals are presented, and the results of using those preparations in the treatment of radiation sickness are discussed. The role of autoantibodies in the pathology of the progeny of irradiated animals, and autoimpulse responses in vaccinated animals, were also studied. Material on counts and determinations of cells forming autoantibodies in human blood and in the blood and organs of exposed animals are reviewed. The relationship between the autoimpulse response and the radiation dose rate is studied.

The book contains not only new theoretical data in radiobiology, but practical recommendations as well. It will be of interest to a broad range of specialists such as radiobiologists, immunologists, research workers, and medical practitioners.

I. A. Zakharov and A. S. Kriviskii

RADIATION GENETICS OF MICROORGANISMS*

The radiation genetics of microorganisms is presented for the first time in the worldwide literature in systematized review form as an independent branch of genetics and radiobiology. Data on the lethal and mutagenic effects of different modes of ionizing radiations on fungi, microscopic algae, bacteria, and viruses are presented. Special attention is given to methods of biophysical analysis of the results of radiation-genetic experiments, the dose dependence of radiation exposure effects, genetic monitoring of radiostability

*Atomizdat, Moscow (1972).

and recovery of microorganisms subjected to lethal and mutagenic injuries. The genetic fundamentals of radiation selection of microorganisms are discussed, and the development of the radiation genetics of microorganisms is summarized.

The book is written for geneticists, radiobiologists, and microbiologists. It can also be useful to instructors and graduate students at the collegiate level.

Yu. F. Koval'

ACCELERATED REMOVAL OF RADIOACTIVE ISOTOPES FROM THE ORGANISM*

The book deals with one of the most pressing problems in modern radiobiology: how to speed up the removal of radioactive materials from an exposed organism. The total characteristics of the methods employed to that purpose are presented. The basic principles and recommendations on lowering the intake of radioisotopes by the animal or human organism are cited, side effects observed in the accelerated removal of radioactive materials from the organism are described (effect of osmotic diuresis, DTPA, etc.).

The book is intended for radiobiologists, biophysicists, physiologists, toxicologists, public health experts, and physicians interested in the problem.

M. A. Nevstrueva, V. M. Shubik, and I. B. Tokin

EFFECT OF INCORPORATED RADIOISOTOPES ON IMMUNOLOGICAL PROCESSES*

This monograph discusses the effects of the most important radioisotopes encountered in practical work (Sr^{90}, Cs^{137}, Ce^{144}, I^{131}, and mixtures of fission products) on the immunological response of the animal organism. Both antimicrobe resistance and formation of autoantibodies in the exposed organism were studied. The authors applied investigations at different levels (the whole organism, cellular and subcellular levels) using modern techniques to uncover some of the mechanisms behind changes in immunity in response to incorporated radioactive isotopes.

The book is written for radiobiologists, immunologists, health physicists, and students studying in biological departments and medical colleges.

I. Ya. Pomeranchuk

COLLECTED WORKS: 1. LOW-TEMPERATURE PHYSICS. NEUTRON PHYSICS†

The present three-volume edition of the works of the renowned Soviet theoretical physicist I. Ya. Pomeranchuk (1913-1966) covers virtually all of his scientific output.

The first volume contains the following sections: theory of metals and dielectrics, theory of neutron scattering and absorption, and contributions on low-temperature physics.

The edition is intended for theoretical physicists.

THEORY OF COHERENT PARTICLE ACCELERATION, AND STUDIES OF RELATIVISTIC BEAMS‡

A new collective method of accelerating particles proposed by V. I. Veksler has been attracting general attention of late.

*Atomizdat, Moscow (1972).
†Nauka, Moscow (1972).
‡Proceedings of the P. N. Lebedev Institute of Physics (FIAN), Vol. 66, Nauka, Moscow (1972).

This collection includes theoretical contributions reviewing several variants of the collective method of acceleration, and offers a detailed investigation of related problems. Theoretical investigations of radiation and of the stability of high-current relativistic electron beams are described.

This collection of articles is intended for research scientists involved with problems of plasma physics, charged-particle accelerators, and nuclear physics.

R. Sh. Shafeev, V. A. Chanturiya, and V. P. Yakushkin

EFFECT OF IONIZING RADIATIONS ON THE FLOTATION PROCESS*

Results of an experimental investigation of the effect of ionizing radiations on flotation of apatite, antimonite, pyrochlore, zircon, ilmenite, and several other minerals, and also on the microhardness and electrochemical and electrophysical properties of minerals, and on the physicochemical properties of the aqueous phase of pulp, are presented in this text. The research findings confirm the feasibility of using ionizing radiations in order to intensify flotation of ores and other mined products.

This edition is intended for engineering and technical personnel in mining enterprises, and for research scientists, graduate and undergraduate students of technical colleges studying the physical chemistry of surface phenomena, and working in the field of beneficiation of ores and other mined products by flotation.

CONSTITUTIONAL DIAGRAMS AND PHASE TRANSFORMATIONS OF URANIUM ALLOYS*

The monograph included a critical review of data in the literature (up to 1969 inclusive) on the phase diagrams of binary, ternary, and quaternary systems of uranium, and on the phase transformations of uranium alloys.

Regular patterns of variation in the shape of the constitutional diagrams are discussed in their relationship to the physicochemical characteristics of the constituents. Crystallochemical characteristics of phases existing in the systems are given. Close attention is given to nonequilibrium states of uranium and of uranium alloys, the kinetics and mechanisms of their transformations, and their structure. The general patterns of transformations of uranium alloys playing a major role in the development of the general theory of phase transformations are discussed.

This edition is intended for specialists engaged in the search for, study of, and utilization of uranium alloys, and for research scientists working in the field of the theory of alloys.

NUCLEAR GEOPHYSICAL TECHNIQUES†

This collection of articles centers around applications of nuclear physics techniques to the solution of some problems in geology and geophysics. The present state and the developmental outlook of those methods is discussed, the methods are classified, and a description is given of scintillators and radioactive isotopes manufactured by industry. Applications of nuclear geophysics techniques to prospecting and exploration of minerals in Siberia and in the Far East are discussed. A description is given of new developments in equipment, including a portable gamma-ray spectrometer, a neutron-logging radiometer, borehole neutron generators, etc. Results of applications of charge-particle accelerators in nuclear geophysical analysis are presented.

The book is intended for a broad range of specialists engaged in the development and regular use in production of new nuclear geophysical techniques and also for instructors and students in geological–geophysical and mining engineering departments.

*Nauka, Moscow (1972).

†Proceedings of a symposium (Institute of Geology and Geophysics of the Siberian Branch of the Academy of Sciences of the USSR, Nauka, Novosibirsk (1972)).

V. M. Case

CONVECTIVE HEAT- AND MASS-TRANSFER*

The theory of convective heat transfer and mass transfer is presented consistently and rigorously. A range of fundamental analytical problems relating to convection often confronting heat transfer engineers is outlined. Close attention is given to engineering applications of the theory of convective transfer. The solutions of individual problems are constructed for computerized work.

The book is based on a course of lectures delivered by the author to students majoring in heat transfer engineering. It can also be used as a textbook for students in colleges, or as a reference book for engineers.

A. Rose-Innes and E. Rhoderick

INTRODUCTION TO SUPERCONDUCTIVITY PHYSICS†

This book, written by famous British physicists, encompasses, despite its slender volume, all of the major topics in the physics of superconductors of the first and second kinds. Superconductors are not only of current scientific interest, but also of broad practical importance in applications, particularly for generating strong magnetic fields, in computer engineering, etc. Familiarity with the fundamentals of superconductivity theory is consequently a must for a broad range of engineers and specialists in allied fields. The book will prove highly useful to such people, since the material it contains is presented in a very simple manner, with almost no reliance on mathematics, but with numerous illustrations. It will also be useful to senior undergraduate and graduate students.

D. Ingram

BIOLOGICAL AND BIOCHEMICAL APPLICATIONS OF ELECTRON SPIN RESONANCE‡

The book deals with applications of the electron spin resonance method to the study of biological and biochemical processes. The author's name is quite familiar to Soviet readers from his other books that have been translated into Russian: Radiofrequency and Microwave Spectroscopy, and Electron Spin Resonance in Free Radicals. Ingram is one of the founders of the ESR method, and was one of the first to use the method in biological research. One special merit of the book for biologists is the very accessible presentation of the physics sections of the book; excellent illustrations aid in assimilating this portion of the text.

The book is intended for biophysicists, biochemists, physiologists, radiobiologists, and also biologists and medical physicians in various special lines of activity utilizing the ESR method, and for chemists and physicists working in the field of biology.

A. Gosman, W. Pun, A. Runchal, D. Spalding, and M. Wolfstein

HEAT AND MASS TRANSFER IN RECIRCULATING FLOWS‡

A numerical technique for calculating stationary two-dimensional single-phase, laminar, and turbulent flows, with inhomogeneities of the properties of the media taken into account, is presented. This method is used as a basis in the discussion of eleven specific problems: flow patterns in a steam superheater unit, flow downstream of a flame stabilizer in a ramjet engine, flow patterns in the air cushion in the case of ground-effect machines, etc. The book is written on a high theoretical level, but is entirely accessible to practising engineers. Actual programs for computing flow patterns, written in FORTRAN-4 language, are appended at the end of the book.

*Énergiya, Moscow (1972).
†Mir, Moscow (1972); English edition: Oxford (1969).
‡Mir, Moscow (1972); English edition: London (1969).

This volume will be of great interest to mechanical engineers, power engineers, computer mathematicians concerned with computations in intricate gas-dynamics problems, and also to graduate and undergraduate students majoring in related fields.

breaking the language barrier

WITH COVER-TO-COVER ENGLISH TRANSLATIONS OF SOVIET JOURNALS

in mathematics and information science

Title	# of Issues	Subscription Price
Algebra and Logic *Algebra i logika*	6	$110.00
Automation and Remote Control *Avtomatika i telemekhanika*	24	$185.00
Cybernetics *Kibernetika*	6	$125.00
Differential Equations *Differentsial'nye uravneniya*	12	$150.00
Functional Analysis and Its Applications *Funktsional'nyi analiz i ego prilozheniya*	4	$ 95.00
Journal of Soviet Mathematics	6	$135.00
Mathematical Notes *Matematicheskie zametki*	12 (2 vols./yr. 6 issues ea.)	$175.00
Problems of Information Transmission *Problemy peredachi informatsii*	4	$100.00
Siberian Mathematical Journal of the Academy of Sciences of the USSR Novosibirski *Sibirskii matematicheskii zhurnal*	6	$185.00
Theoretical and Mathematical Physics *Teoreticheskaya i matematicheskaya fizika*	12 (4 vols./yr. 3 issues ea.)	$125.00
Ukrainian Mathematical Journal *Ukrainskii matematicheskii zhurnal*	6	$135.00

Back volumes are available.
For further information, please contact the Publishers.

SEND FOR YOUR FREE EXAMINATION COPIES

PLENUM PUBLISHING CORPORATION
Plenum Press • Consultants Bureau
• IFI/Plenum Data Corporation
227 WEST 17th STREET
NEW YORK, N. Y. 10011

In United Kingdom
Plenum Publishing Co Ltd., Davis House (4th Floor)
8 Scrubs Lane, Harlesden, NW10 6SE, England

breaking the language barrier

WITH COVER-TO-COVER ENGLISH TRANSLATIONS OF SOVIET JOURNALS

in physics

Title	# of Issues	Subscription Price
Astrophysics *Astrofizika*	4	$100.00
Fluid Dynamics *Izvestiya Akademii Nauk SSSR mekhanika zhidkosti i gaza*	6	$160.00
High-Energy Chemistry *Khimiya vysokikh énergii*	6	$135.00
High Temperature *Teplofizika vysokikh temperatur*	6	$125.00
Journal of Applied Mechanics and Technical Physics *Zhurnal prikladnoi mekhaniki i tekhnicheskoi fiziki*	6	$150.00
Journal of Engineering Physics *Inzhenerno-fizicheskii zhurnal*	12 (2 vols./yr. 6 issues ea.)	$150.00
Magnetohydrodynamics *Magnitnaya gidrodinamika*	4	$100.00
Mathematical Notes *Matematicheskie zametki*	12 (2 vols./yr. 6 issues ea.)	$175.00
Polymer Mechanics *Mekhanika polimerov*	6	$120.00
Radiophysics and Quantum Electronics (Formerly Soviet Radiophysics) *Izvestiya VUZ. radiofizika*	12	$160.00
Solar System Research *Astronomicheskii vestnik*	4	$ 75.00
Soviet Applied Mechanics *Prikladnaya mekhanika*	12	$160.00
Soviet Atomic Energy *Atomnaya énergiya*	12 (2 vols./yr. 6 issues ea.)	$150.00
Soviet Physics Journal *Izvestiya VUZ. fizika*	12	$160.00
Soviet Radiochemistry *Radiokhimiya*	6	$145.00
Theoretical and Mathematical Physics *Teoreticheskaya i matematicheskaya fizika*	12 (4 vols./yr. 3 issues ea.)	$125.00

Back volumes are available. For further information, please contact the Publishers.

SEND FOR YOUR FREE EXAMINATION COPIES

PLENUM PUBLISHING CORPORATION
227 WEST 17th STREET
NEW YORK, N. Y. 10011
Plenum Press • Consultants Bureau
• IFI/Plenum Data Corporation

In United Kingdom,
Plenum Publishing Co. Ltd., Davis House (4th Floor)
8 Scrubs Lane, Harlesden, NW10 6SE, England